Nigerian Journal of Renewable Energy Research

Volume 1, Number 1, 2023: ISSN _____

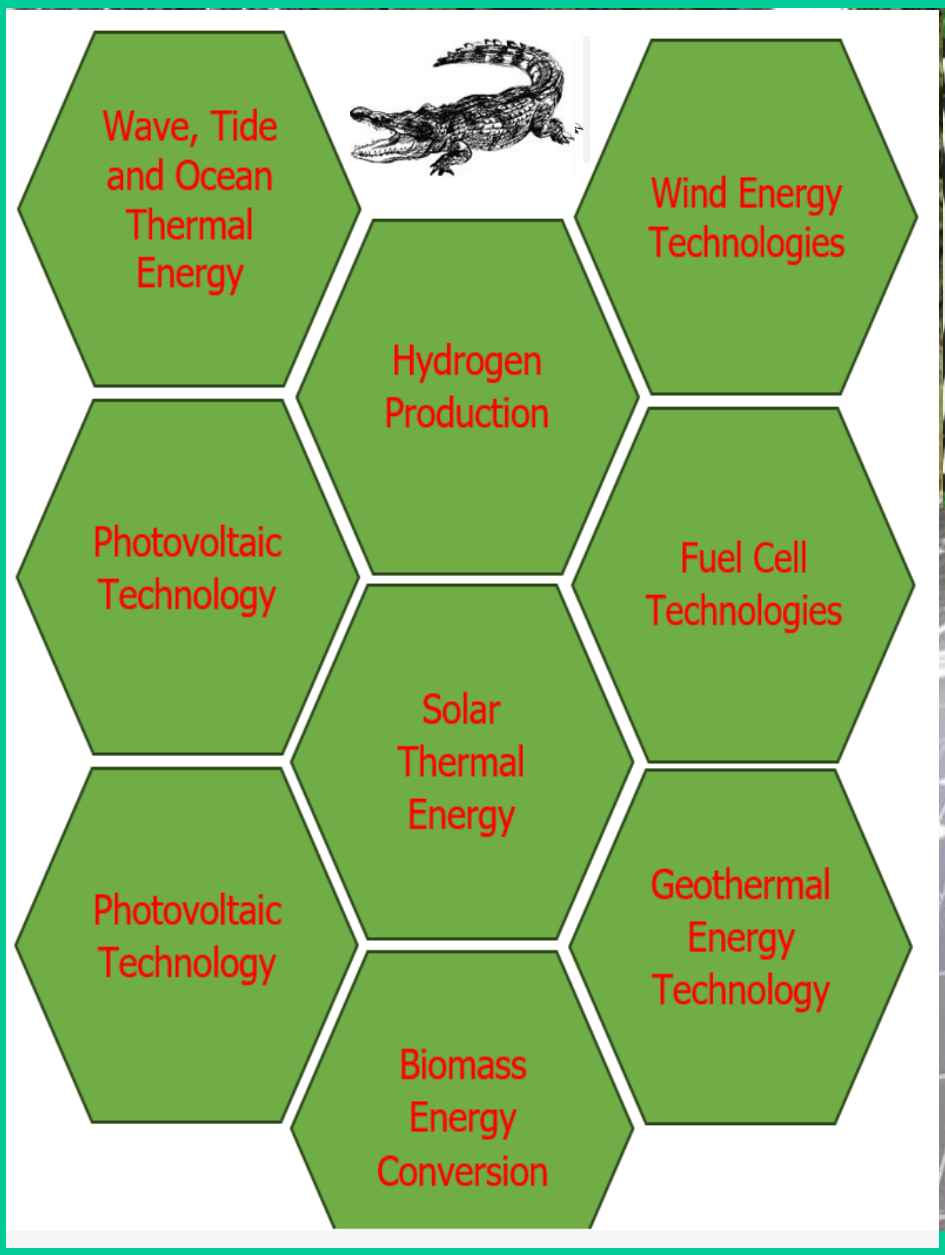

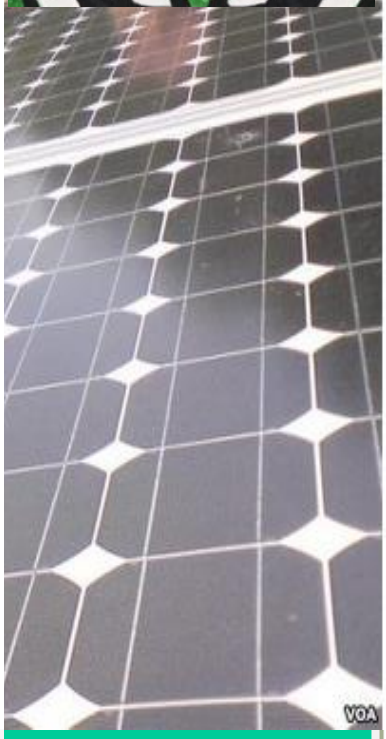

Published by the TETFund Centre of Excellence for Renewable Energy, Kaduna Polytechnic, Kaduna, Nigeria ©2024

This volume was published with funds provided by Tertiary Education Trust Fund.

Nigerian Journal of Renewable Energy Research (NJRER)
Volume 1, Number 1, 2024 ISSN _____

About Nigerian Journal of Renewable Energy Research (NJRER)

The **Nigerian Journal of Renewable Energy Research** (NJRER) is a freely accessible publication covering all facets of the topic. NJRER invites submissions that uphold high scientific standards and importance. Once accepted, articles typically appear within half a year. All entries in NJRER undergo a peer review process.

The Nigerian Journal of Renewable Energy Research is published once a year.

Types of paper

Regular articles: Such pieces should outline fresh and thoroughly validated discoveries. The experimental methods must be detailed enough to allow others to replicate the study. The article's length should be concise, only as long as necessary to clearly convey and explain the research.

Short Communications: A Short Communication is apt for documenting outcomes of minor yet complete studies, or for sharing new concepts, pioneering techniques, or equipment. The structure doesn't have to mirror that of longer articles. These notes span 2 to 4 printed pages, equivalent to roughly 6 to 14 handwritten pages.

Reviews: Contributions offering reviews and insights on contemporary subjects are appreciated and encouraged. Reviews ought to be succinct, spanning between 4-6 printed pages (equivalent to 12 to 18 written pages). Nonetheless, reviews analysing methods and designs might extend to a maximum of 30 printed pages. All review articles undergo a peer review process.

For further information, please contact
The Editor in Chief; Nigerian Journal of Renewable Energy Research
email: editor_njrer@tetfundkadpolycoex.org.ng*; Phone: +234-8037619719*
Website: www.tetfundkadpolycoex.org.ng

Editorial Policy

Any paper presented to the Nigerian Journal of Renewable Energy Research must assert that the research detailed hasn't been previously published (barring its presence as an abstract, a part of a public lecture, academic dissertation, or conference notes). Furthermore, it shouldn't be under review elsewhere. Every author must endorse its publication, and it must also receive either implicit or explicit approval from the pertinent institutions where the research took place. Upon acceptance, the content mustn't be republished elsewhere, digitally or otherwise, in its current format, whether in English or any other language, without the explicit permission of the rights owner.

Copyright Notice

Authors who publish in this Journal agree to the following legal terms:

1. Authors maintain their copyright but give the Journal the privilege of first-time publication. Concurrently, the work is licensed under a Creative Commons Attribution License. This allows others to distribute the work, provided they credit the original authorship and its first publication in any journal overseen by the Centre for Renewable Energy Research and Development.
2. Authors have the flexibility to engage in separate, supplementary agreements for the non-exclusive dissemination of the version of the work published by the Journal, always acknowledging its first appearance in this Journal.
3. Once their manuscript is accepted, authors are both allowed and advised to upload their work online and supply (in print form) to local libraries. This is to promote fruitful discussion and broader referencing of the published material.

NIGERIAN JOURNAL OF RENEWABLE ENERGY RESEARCH
Volume 1, Number 1, 2023 ISSN _____

SCOPE

The **Nigerian Journal of Renewable Energy** Research delivers intricate papers to the research community, aimed at sparking additional studies or advancements. This publication is annual. Within its pages, the Journal presents original articles, detailed reports, and critical reviews. Authors are urged to contribute manuscripts that address essential voids in the field of Renewable Energy research and evolution.

The Nigerian Journal of Renewable Energy Research is dedicated to advancing and sharing knowledge on the diverse topics and technologies related to renewable energy systems and components. Its objective is to assist professionals such as researchers, engineers, economists, manufacturers, NGOs, associations, and societies to stay updated with the latest advancements in their respective areas, ensuring the integration of sustainable energy alternatives into existing practices.

This multi-disciplinary journal focuses on renewable energy science, engineering, technology, and research. It aspires to establish itself as a top-tier, peer-reviewed medium, providing authoritative insights and findings in the renewable energy domain.

The research scope of the Nigerian Journal of Renewable Energy Research includes:

- Photovoltaic Technology Transformation
- Applications of Solar Thermal Energy
- Advancements in Geothermal Technology
- Wave, Tide and Ocean Thermal Energy Innovations
- Advancements in Hydro Power
- Biomass Energy Conversion
- Wind Energy Technologies
- Water Desalination Techniques
- Innovations in Solar and Low-Energy Building Designs
- Studies in Climatology and Meteorology
- Developments in Hydrogen Production and Fuel Cell Technologies
- Socio-economic Aspects and Policy Discussions on Renewable Energy

Additionally, while the Journal is open to topics related to renewable energy, it emphasises the necessity of the papers being focused on power generation via renewable or sustainable means. As an illustration, studies on materials designed for renewable energy systems that don't evaluate the energy they'll produce are not considered relevant.

Original research articles and review papers are accepted by the **Nigerian Journal of Renewable Energy Research**. However, review papers are by the Editor-in-Chief's invitation only. Prospective authors for review papers are advised to submit an outline of their proposed paper along with a brief CV of the main author/s to the Editor-in-Chief for prior approval.

Contributions aligning with the United Nations' sustainable development goals, especially SDG 7 (Affordable and Clean Energy) and SDG 13 (Climate Action), are particularly welcomed.

NIGERIAN JOURNAL OF RENEWABLE ENERGY RESEARCH
Volume 1, Number 1, 2023 ISSN _____

Acknowledgement

The Centre of Excellence for Renewable Energy wishes to thank the Tertiary Education Trust Fund (TETfund) for sponsoring this publication.

NIGERIAN JOURNAL OF RENEWABLE ENERGY RESEARCH
Volume 1, Number 1, 2023 ISSN _____

FOREWORD

Renewable energy is derived from sources that naturally replenish within a short span. This includes solar, wind, water, biomass, and geothermal energy. Although 'green energy' aligns closely with renewable energy, it is a specific category that offers maximum environmental advantages. Clean energy sources, which produce minimal carbon emissions, comprise renewable energies as well as nuclear power.

Historically, renewable energy has been employed for heating and power, and in more modern contexts, electricity generation. In Nigeria, like many developing nations, renewable energy hasn't made a significant mark in primary energy utilization. Despite a heavy reliance on fossil fuels for heating, electricity, and transport, events like the 1970s oil crises urged investments in alternative energies. Likewise, the adverse impacts of climate change have amplified the public's call for energy not derived from fossil fuels, with this call being further bolstered by governmental incentives and standards.

The **Nigerian Journal of Renewable Energy Research** is committed to providing essential resources centered on the commerce of renewable energy production and distribution. Augmenting renewable energy's role in sustainable development encompasses:

a. Backing initiatives that address the environmental, economic, health, and social repercussions and advantages of renewable energy, promoting transparency, and ensuring sustainability in energy development through collaborations at various levels.
b. Amplifying stakeholder involvement, including that of local, indigenous communities and women, to actively partake in renewable energy projects, including post-operational mine closures and site rehabilitation.
c. Encouraging sustainable practices in renewable energy utilization by offering financial, technical, and capacity-building support to developing nations, promoting value-added processing, and focusing on site restoration.

Renewable energy is crucial for every nation, especially the developing ones, given its pivotal contributions to the global economy and contemporary societies. To capitalize on this sector, judicious investments are essential. In Nigeria, the sector's potential remains untapped. Effective management of renewable energy can propel comprehensive economic growth, alleviate poverty, and help nations achieve global developmental milestones, such as the Sustainable Development Goals.

For Nigeria to benefit from the renewable energy sector, it must invest rightly, instate robust legal frameworks, ensure economic and social benefits, minimize adverse impacts, uphold biodiversity, and counter illegal financial outflows from mining operations. Despite the significance of the sector, Nigeria has faced hurdles in drawing investments from domestic and international renewable energy firms. This hesitancy stems from the unpredictability of this sector's investments in the country. To counter this, a cohesive

effort involving the national and local governments, industry stakeholders, and the public is needed to ensure a stable investment landscape.

A thriving renewable energy industry is paramount for Nigeria's vision of a well-rounded and robust economy, offering opportunities to all. The nation should consistently bolster the renewable energy sector, focusing on research, clean energy utilization, and environmental safeguards. The right research can spur economic growth by luring investments and initiating auxiliary projects, which, in turn, can provide job and business prospects for its citizens.

This Journal is dedicated to advancing research endeavors in renewable energy. We see this publication as a testament to our commitment to a pivotal economic sector and our allegiance to environmental conservation.

S.N. Mumah, *PhD, FNSChE*
Director, TETFund Centre of Excellence for Renewable Energy,
Kaduna Polytechnic, Kaduna, Nigeria.

NIGERIAN JOURNAL OF RENEWABLE ENERGY RESEARCH
Volume 1, Number 1, 2023 ISSN _____

TABLE OF CONTENTS

		Page
	About The Nigerian Journal of Renewable Energy Research (NJRER)	ii
	Acknowledgement	v
	Foreword	vi
	Papers	
1	Assessment of Kalambaina Limestone for Quicklime Production: by Akande, H. F, Saka, A. S., Kovo, A. S., Azeez, O. S., Mumah, S. N. and Onifade, K. R.	1 – 10
2	Review of the Selection and Performance Evaluation Procedures for Jaw Crushers; by Mumah, S.N., Kuye, A.O, Okpara, K.O. and Chukwuma, F.O.	11 – 38
3	Application of the Novel Proportional Nodes Curve Fitting Method to develop Correlations for the Dynamic Viscosity of Ammonia-Water Solution; S. N. Mumah, H.F. Akande, S. Alexander, K.Y. Mudi[1] and F. Samuel	39 - 49
4	Safety Requirements in Blasting at Edile Rock Nigeria Ltd. Quarry, Talata Mafara, Zamfara State, Nigeria: by Salawu, O.M, Bida, A.D and Godiya, Z.M.	50 – 61
5	Characterisation of Mica from Bukkuyum Area of Zamfara State, Nigeria: by Abubakar G. Salisu, Hadiza A. Isa, Hamisu Adamu and Zalihatu M. Idris	62 – 68
6	Performance Prediction of Xanthogenate Collectors Using Flotation Kinetic Equation: by Damisa, E.O.A.	69 – 79
7	Determination of Liberation Size of Agwada Chalcopyrite Ore, Nasarawa State, Nigeria: by Ali M, Aye, A.E. and Akindele. U.M.	80 – 83
8	Performance Evaluation of an Active Solar Still under Forced Circulation Mode; by S. N. Mumah, Tanimu Garba Ibrahim, H.F. Akande and Abdullahi Ismail Belli	84 - 99
10	Instructions for Authors	100– 106

"With the pace of technological innovation today, we can't afford to stand still for a year or two years or three years. We've got to seize every opportunity we have to stay ahead. And we can't let other countries win the race for ideas and technology of the future. And I say that, by the way, not out of just any nationalistic pride — although, obviously, that's part of it — but it's also because nobody does it better than we do when it's adequately funded, when it's adequately supported. And what we produce here ends up having benefits worldwide. We should be reaching for a level of private and public research and development investment that we haven't seen since the height of the Space Race. That's my goal".

President Barack Obama's Speech to the National Academy of Sciences 150th Anniversary (30/04/2013)

Nigerian Journal of Renewable Energy Research
Volume 1, Number 1, pp 1-10, 2023

Assessment of Kalambaina Limestone for Quicklime Production

Akande, H. F[+]*, Saka, A. S., Kovo, A. S.**, Azeez, O. S.**,**
Mumah, S. N.* and Onifade, K. R.**

*Department of Chemical Engineering, Kaduna Polytechnic, Kaduna, Nigeria
**Department of Chemical Engineering, Federal University of Technology, Minna, Nigeria
[+] Corresponding author: hassan.akande@kadunapolytechnic.edu.ng

https://www.tetfundkadpolycoex.org.ng

ARTICLE INFORMATION

Article history:
Received 21 May, 2023
Revised 22 Jul, 2023
Accepted 08 Oct, 2023
Available online 30 Dec, 2023

Keywords:
Kalambaina
limestone
characterization, quicklime
ICP-OES, XRD, SEM, ASAP BET

Abstract

Quicklime of high quality is an important mineral for many industries (such as building, agriculture, water treatment, sugar refining, tannery, paper, glass, etc) all over the world. In Nigeria most of the demand for this chemical product is met through importation of quicklime. The Nigerian Kalambaina limestone was subjected to physical, chemical, mineralogical and thermal characterization to determine its suitability for direct use in quicklime production. The physical, chemical, mineralogical and thermal characterization were carried out using Accelerated Surface Area Porosimeter Braunner-Emmet-Teller (ASAP-BET) and Scanning Electron Microscope (SEM), Inductively Coupled Plasma Optical Emission Spectrometer (ICP-OES) and X-Ray Diffractometer (XRD) respectively. The results of the chemical analysis showed that the limestone contains 99.04, 0.894, 0.0414, 0.0085 and 0.006 percents of calcium, magnesium, silicon, iron and aluminum respectively. The XRD result shows that Kalambaina limestone is composed of calcite mineral with small amount of silica. The result of SEM shows that Kalambaina limestone has fine grain of crystals with homogeneous texture. Thermal characterization using TGA shows that weight loss due to release of carbon dioxide from Kalambaina limestone sample is 44.6% and optimum calcination temperature for obtaining quicklime of highest yield in nitrogen atmosphere is 800^{o}C. Also, the physical characterization using ASAP BET method shows that Kalambaina limestone has a surface area of 2.7764 m^{2}/g. The results of physical, chemical, mineralogical and thermal characterization shows that Kalambaina limestone is highly suitable for the production of quicklime making beneficiation treatment little or unnecessary.

1.0 Introduction

Limestone is a naturally occurring mineral that consists principally of calcium carbonate. It generally contains some magnesium carbonate as a secondary component. Limestone is found in many forms and is classified in terms of its origin, chemical composition, structure, and geological formation (Oates, 1998). Thus, limestone may be pure calcite, a mixture of calcite and dolomite or pure dolomite (Benton, 1973).

Large limestone and dolomite occurrences have been reported by Bell (1963), Ola (1977), Gwosdz et al (1996), RMRDC (2010) and Akande (2015). They are widespread in the sedimentary basin of Nigeria. Nigeria Ministry of Mines and Steel Development reported that Nigeria has an estimated reserve of about 3 trillion tonnes of limestone which are scattered in different states of the country. Those states include Abia, Anambra, Benue, Cross River, Ebonyi, Enugu, Ogun, Sokoto, Gombe, Nassarawa, Edo, Borno, Yobe, Adamawa and Kebbi (RMRDC, 2010).

Kalambaina limestone quarry belongs to the Paleocene marine sediments deposited in the Sokoto Basin during the second phase of sediment deposition when the Tethys Sea moved southwards through the Sahara (Nyong, 1995). The exposed section measured ca.19.5m in thickness. The lower part of the section consists of limestone-shale inter-beds while the upper part is phosphatised shale (Adekeye and Akande, 2002).

Quicklime is a solid material that is produced from thermal decomposition of limestone from which carbon dioxide gas is evolved and upon hydration, forms white powder and releases large amount of heat to form hydrated lime. Hydrated lime is an important industrial mineral because of its physical, chemical and mineralogical properties, as well as its commercial importance and ease of production. Foraminifera (2012) reported that Nigeria has high demand for quicklime based on its wide range of uses. The industries that use quicklime include building, agriculture, water treatment, sugar refining, tannery, paper and glass. The bulk demand for quicklime in Nigeria is for water treatment, soft drink bottling, tannery, breweries and food processing (Foraminifera, 2012).

Quicklime is produced from limestone that varies in properties from one location to another. Dogu (2000) reported that limestone can be obtained from a huge variety of sources and various limestones differ considerably in their chemical composition and physical structure. The chemical reactivity of different limestones shows a large variation due to their differences in crystalline structure and also because of the nature of impurities such as silicon, iron, magnesium, manganese, sodium and potassium present in them (Antonia et al, 2000). There are several references in literature concerning factors that may affect the quality of quicklime. Antonia et al (2000) reported these factors as characteristics of the limestone, calcination temperature, pressure acquired in kilns, rate of calcination, and fuel quality. The effect of calcination parameters on quicklime produced from various limestone deposits have been reported by the following authors (Khraisha and Dugwell (1989); Rao et al (1989); Khinast et al (1996); Dogu and Irfan (2001); Demir et al (2004); Muaazu et al (2011); Okonkwo and Adefila (2012) and Rashidi et al (2012)). Nevertheless, no studies have been reported, to the best of our knowledge, about the suitability of Kalambaina limestone for producing commercial quicklime. Hence, in this study, the characterization of Kalambaina limestone was carried out to determine its suitability for producing commercial quicklime.

2.0 Experimental

2.1 Materials and Procedure

Quicklime was produced from limestone obtained from Kalambaina quarry found in Northern part of Nigeria.

2.2 Analytical methods and techniques

The analytical procedures described below shows the techniques used in characterizing Kalambaina limestone.

2.2.1 Chemical Analysis

ICP-OES was used to determine the metals present in Kalambaina limestone in their elemental form. A mass of 50 g of Kalambaina limestone was dried at temperature of 105^{o}C. 0.5 g subsample of the dried limestone was subsequently digested in 10 ml aqua regia for a period of 1 hr and temperature of 140^{o}C. The digested limestone sample was further heated to temperature of 200^{o}C until the mixture produced a residue. The residue was subsequently dissolved in 2.5 M HNO_3 to form a solution. The solution was filtered and diluted to 50 ml solution. The diluted solution elemental composition was then analyzed using ICP-OES.

2.2.2 XRD Analysis

Kalambaina limestone mineral phases were determined using XRD. The diffractometer was put on and set to a voltage and current of 40kV and 30 mA respectively. The XRD fitted with was also operated at a wavelength of 1.5406. The XRD was scanned at a 2θ range from 20° to 60°. The diffractogram was also scanned at a rate of 3°/min.

2.2.3 Thermal Analysis

Differential thermal and thermogravimetric analyses (simultaneous DTA/TG) were carried out on Kalambaina limestone using Mettler Toledo, TGA/SDTA851 model. 50 mg of the limestone the limestone sample placed in an alumina crucible was weighed. The weighed limestone sample was heated from room temperature to 900°C at a heating rate of 10°C/min and nitrogen flow of 100 mL/min.

2.2.4 SEM Analysis

The texture, shape, and size of the limestone sample was determined using a SEM instrument model, HITACHI, S-3400N. The limestone powder was mounted onto the SEM stubs (layered with sticky carbon tape). 50 mg of the limestone the limestone sample was mounted on SEM stub and placed in a sputter coater (EMITECH, K550X) for five minutes. This is to provide coating with gold so that high reflectivity of the limestone sample during the scanning process. The samples were further heated to temperature of 40°C in an oven before SEM analysis.

2.2.5 Physical Properties Analysis (ASAP-BET-BJH)

Adsorption of nitrogen was performed on the limestone sample to evaluate the specific surface area, total pore volume, and pore size distribution, using a Quantachrome instrument (model Autosorb-1). The physical characterization consisted of three steps, including dehydration, degassing under low vacuum pressure, and nitrogen gas adsorption at 77 K. The isotherm obtained was analyzed using the BET and Barrett-Joyner-Halenda (BJH) methods.

3.0 Results and Discussion

The metals present in Kalambaina limestone sample determined using ICP-OES method is shown in Table 1. The main elements found in it are Ca and Mg, with low levels of Mg and other impurities, such as Fe, Si, K, Na, Al and others. Those impurities either are found in the matrix of the crevices and other strata excavated along with the limestone (Chan et al, 1970).Table 1 shows Kalambaina limestone has Ca content of 99.04%. The 99.04% calcium content of Kalambaina limestone is higher than 98.5% required for limestone used for commercial quicklime production

(Oates, 1998). Kalambaina limestone is a higher purity limestone, since it is higher than 98.5% required for higher purity limestone (Cox et al, 1977). The CaO content, i.e., the Ca content (Table 1) less the LOI content (Table 2) for Kalambaina limestone is 54.44%. The 54.44% calcium oxide content of Kalambaina limestone falls within the range of 50% to 65% required for limestone for quicklime production (Plumpton, 1984). The CaO content is also very close to 54.1% determined for limestone to be used for pilot scale iron-making in India. The CaO content of the raw Kalambaina limestone is higher than 43.05% for Indian Salem Madras deposit and is only slightly lower than the flotation concentrate of Salem limestone with 52.9% CaO (Ryemshak et al, 2012). The Kalambaina CaO content is also far higher than 43.44% and 38.68% for low grade raw limestone under consideration for upgrading by Indian Tata Iron and Steel Ltd. and Rhotas Industries, respectively (Ryemshak, 2012).

Table 1: Elemental Chemical Composition of Kalambaina Limestone using ICP-OES

Chemical Compound	Ca	Mg	Si	Fe	Al	Other Oxides
Kalambaina Limestone (% ppm)	99.040	0.8938	0.0414	0.0085	0.006	0.0157
Commercial limestone (% ppm)	98.5	0.5	0.35	0.6	0.2	0.050

The Mg content of 0.474% in the raw Kalambaina limestone is slightly higher than 0.5% standard specified for commercial quicklime production (Oates, 1998). The Mg content which is a function of MgO present in Kalambaina limestone is lower than minimum of 2.48% standard specified for limestone for direct quicklime production (Plumpton, 1984). The MgO content of Kalambaina limestone is lower than 1.0% MgO content for a limestone for pilot scale iron-making in India (Ghandy, 1966). MgO forms the low melting point magnesium silicate with silica during iron-making. These results strongly suggest that the Kalambaina limestone with low Mg content is a high-grade limestone suitable for use in quicklime production as the Mg content which is present as $MgCO_3$ in limestone produces MgO at high calcination temperature and make the quicklime to sinter (Gunasekaran and Anbalagan, 2008). This sintering effect reduces the yield and reactivity of quicklime and this occur because MgO is produced from dolomite at a lower temperature than CaO and so crystallites tend to grow larger and less reactive (Harrison et al, 1998).

The iron content of 0.004% in Kalambaina limestone is lower than 0.6% standard specified for commercial quicklime production (Oates, 1998). The iron oxide content of 0.004% suggest that Kalambaina limestone will produce quicklime of high yield and reactivity as iron present as Fe_2O_3 reacts with produced quicklime at high temperature to form bellite which reduces the yield and reactivity of quicklime.

The 0.006% aluminum content in Kalambaina limestone is lower than 0.6% standard specified for commercial quicklime production (Oates, 1998). Since aluminum present as alumina is a highly refractory oxide, its low content in Kalambaina limestone strongly indicate Kalambaina limestone as a high-grade limestone. Alumina acts as a base or as an acid depending on the conditions imposed. For example, at high temperature, it may form alumina silicates, while in the presence of a strong base like quicklime it may form undesired calcium aluminate that reduces the porosity of quicklime (Ryemshak et al, 2012).

3.1 Thermal analysis

The TG and DTA curves of Kalambaina limestone obtained in nitrogen atmosphere is shown in Figure 1. The trend of the TG curves obtained for Kalambaina limestone sample shown in Figure 1 represents standard TG curves of calcite (Wagner, 2009). It shows that thermal decomposition with the formation of volatile reaction product (CO_2) occurred. Further examination of the TG curves (Figure 1), shows absence of multi-step decomposition which confirms calcite as the predominant mineral phase present in Kalambaina limestone (Wagner, 2009). This result is also in agreement with XRD, ICP and SEM analysis of the limestone samples. The DTA curve of Kalambaina limestone, shown in Figure 1, presents one endothermic peak at temperature above 750 °C. This confirms calcite as the predominant mineral phase present in the limestone. The typical TG curves of Figure 1 show that Kalambaina limestone presented a weight loss of 2.5% below temperature of 300°C. The weight loss detected in the temperature range of 100–300°C can be attributed to the chemically bound water (Gunasekaran and Anbalagan, 2008). This was followed by a weight loss attributed to the decomposition of carbonates. The thermal curves representing the carbonate mineral are characterized by endothermic peaks caused by the evolution of carbon dioxide. DTA curve of calcite shows one endothermic peak (Harrison et al, 1998).

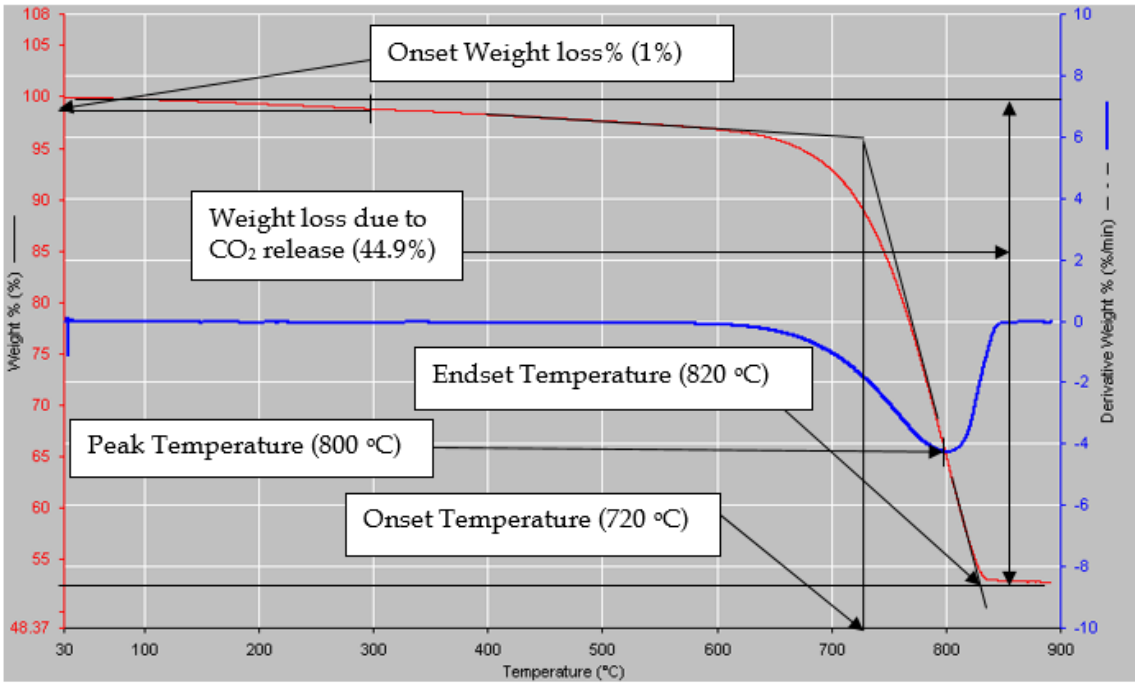

Figure 1: Thermogravimetry and Differential Thermal Analysis of Kalambaina limestone at heating rate of 20ºC/minutes from 30ºC to 900ºC.

The calcination of Kalambaina limestone as shown in Figure 1 and Table 2 begins at 720ºC, reaches a peak at 800ºC and ends at 820ºC. The presence of one peak temperature and absence of peak at lower temperature represents the decomposition of calcite and absence or non-significant yield of dolomite (Anthony et al (2001); Gunasekaran and Anbalagan, (2008); Chan et al (1970); Harrison et al (1998) and Kilic and Mesut (2006)). The result of the TGA shows that optimum temperature for obtaining quicklime of highest yield in nitrogen atmosphere is 800ºCas indicated in the peak temperature obtained in TGA plot of Figure 1.

Table 2: Thermogravimetric Analysis Parameters of Kalambaina Limestone

Limestone Type	Onset Temperature (°C)	Peak Temperature (°C)	Endset Temperature (°C)	Onset Weight (%)	Weight Loss due to CO_2 release (wt%)
Kalambaina	720	800	820	99	44.6

Table 2 and Figure 1 show that weight loss due to release of carbon dioxide from Kalambaina limestone samples is 44.6%. Furthermore, it is observed that the percentage of carbon dioxide of Kalambaina limestone is higher than the theoretical one (44%). This fact might be ascribed to the presence of a high content of dolomite in Kalambaina limestone (Antonia et al, 2000). Gunasekaran and Anbalagan (2008) also reported that the weight loss of calcite is attributed to the decomposition of carbonates. For pure calcite, the expected mass decrease in one step (at 900 °C) is 44.6% (Gunasekaran and Anbalagan, 2008). A value of LOI higher than 44%, are indications for the presence of metallic impurities in the limestone sample which is higher in Kalambaina (44.6%) limestone sample (Gunasekaran and Anbalagan, 2008). Additionally, the case of presence of low quartz (silica) present in Kalambaina limestone, as observed in XRD result (Figure 3) and ICP result (Table 1) leads to no fluctuation in Kalambaina DTA curve, at temperature of 360 - 680 °C (Gunasekaran and Anbalagan, 2008).

3.2 SEM analysis

The scanning electron microscopy (SEM) image of Kalambaina limestone is presented in Figure 2. The SEM image also show there may be presence of Oolites cemented by different types of calcites as observed in Kalambaina and Kalambaina limestones. The SEM analysis confirmed the granulometric characteristic of the calcite as microcalcite and syntaxial calcite in the core of the oolites. The SEM images also show that the crystal shapes of Kalambaina limestone are distributed homogeneously throughout the mass and the crystal size are fine grain, compact and homogeneous texture (Akande, 2015).

SEM image of Figure 2 shows that Kalambaina limestone with fine grain and homogeneous texture of crystals will produce quicklime with bigger surface area and high reactivity due to a fine-grained rock is relatively quick-burning as carbon dioxide diffuses rapidly through the large number of internal pores between small limestone crystals (Harrison, 1993). Kalambaina limestone with fine grain and homogeneous texture of crystals when decomposed, the limestone front will reach the core of the chippings faster and a quicklime product containing burnt carbonate as well as high reactive quicklime will be produced (Harrison et al, 1998).

3.3 XRD analysis

The XRD spectrum of Kalambaina limestone is shown in Figure 3. The horizontal axis caption, 2θ in the figures is doubled Bragg angle in XRD analysis while the vertical axis shows the peak intensity. Analyzing the diffractograms (Figure 3) and peak matching with JCPDS (Joint Committee for Powder Diffraction Standards) data, the crystal phase predominant on the samples was calcite. As can be seen from Figure 3, the main peak of the XRD spectrum appears for calcite at $2\theta = 29.5^{o}$and minor peaks appear at $2\theta = 26.6^{o}$, 29.5^{o}, 31.4^{o}, 36.0^{o}, 39.4^{o}, 43.2^{o}, 47.2^{o}, 47.5^{o} and 48.5^{o}, respectively. The mineral phase of limestone identified in Kalambaina limestone is similar to that obtained by the following authors (Navarro et al, 2009; Soares et al, 2008)

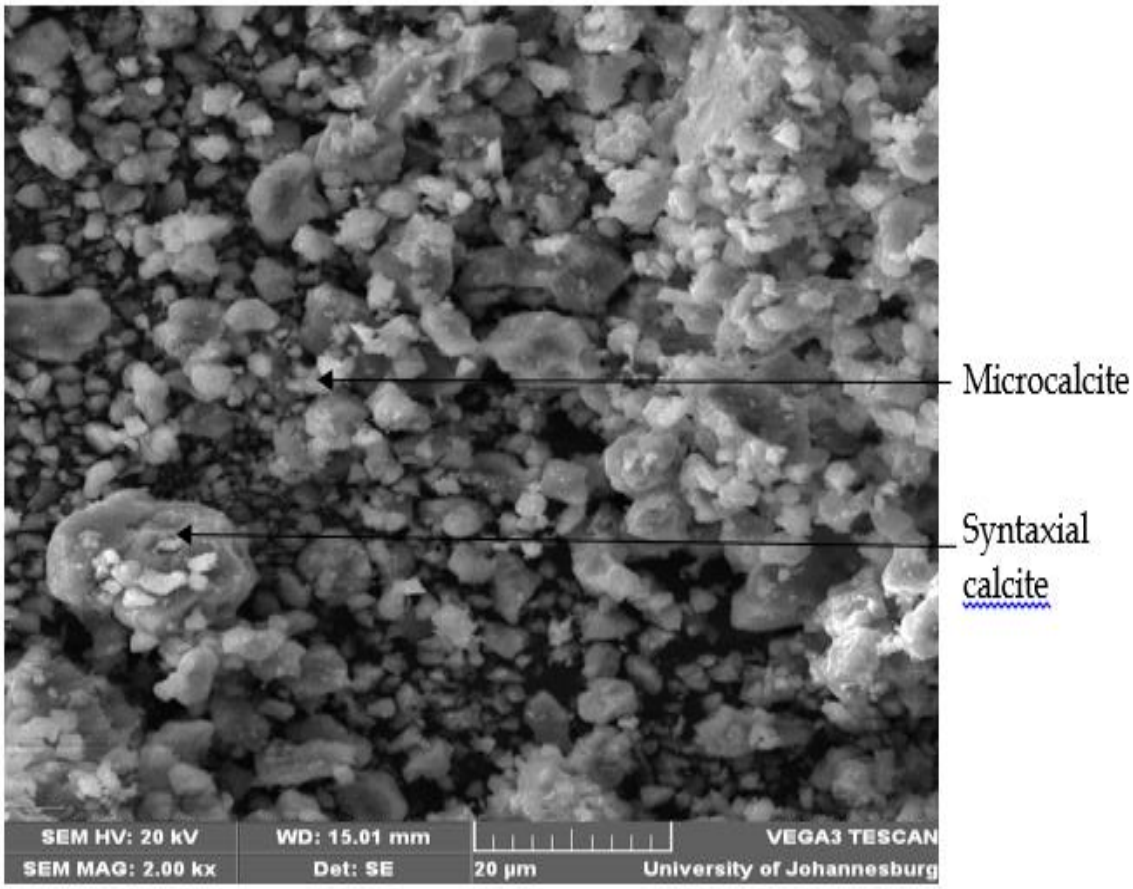

Figure 2: Scanning Electron Microscopic (SEM) Image of Kalambaina Limestone

Table 3 present the crystallinity parameters of limestone samples obtained from XRD analysis. By XRD examination using d-values spacing of $^{o}2\theta$values obtained above, the main constituent of the limestone samples is calcite. The XRD result shown in Figure 3 shows that Kalambaina limestone sample has small yield of quartz. This is corroborated by the silica level determined by ICP-OES (Table 1).

Table 3 shows that Kalambaina limestone has variable grain size of 428.19 *nm* respectively. This shows that Kalambaina has a high coherent scattering domain with perfect arrangement of unit cells at d-spacing (2θ) of 29.5^{o} (Chen et al, 2007). Further examination of the diffractograms of Kalambaina shows that it has a calcitic strain of 0.18%. This shows that Kalambaina limestone is crystalline. The results of crystallite strain show that Kalambaina will produce quicklime of highreactivity and tendency to decrepitate during calcination is low (Harrison et al, 1998). Decrepitation decreases the porosity of the bed, retarding the flow of heat and reducing efficiency of the calciner (Harrison et al, 1998). Also, Kalambaina fine-grained rock is relatively quick-burning as carbon dioxide diffuses rapidly through the large number of pores between small lime crystals (Harrison et al, 1998).

Table 3: Crystallinity Parameters of Limestone Samples Analyzed Using XRD

LimestoneType	Crystallite Size		Strain (%)	
	Calcite	Quartz	Calcite	Quartz
Kalambaina	428.9	-	0.16	-

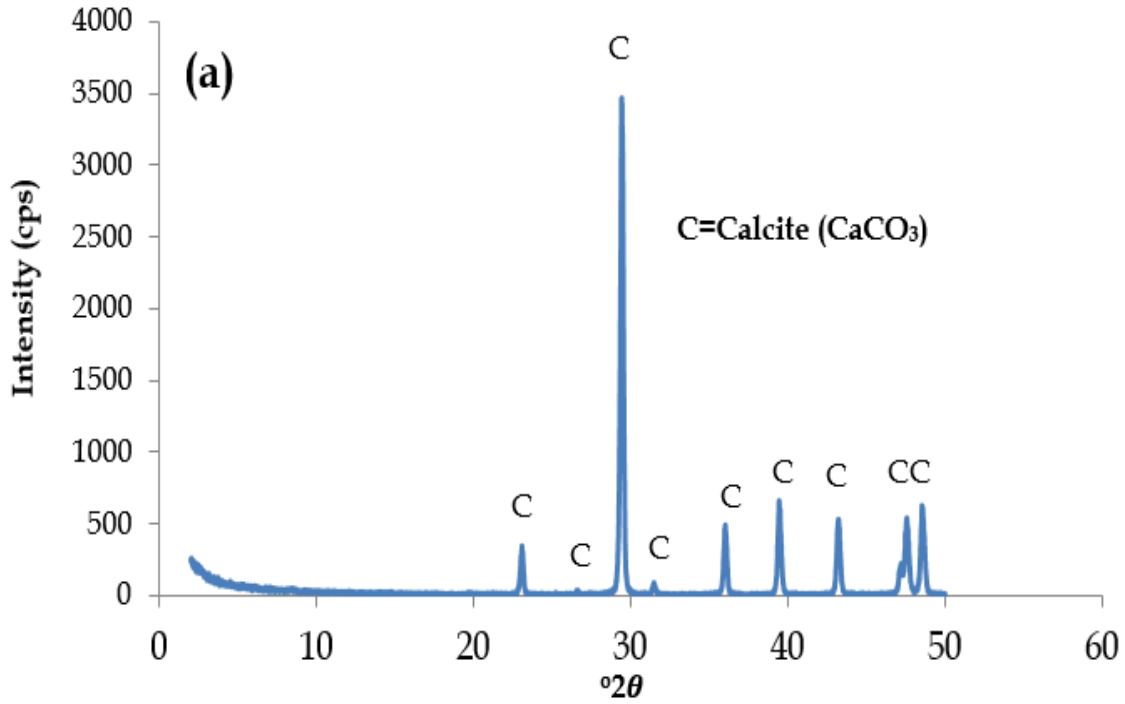

Figure 3: XRD pattern of Kalambaina Limestone

3.4 Surface area analysis using BET

The BET surface area, BJH adsorption cumulative surface area of pores, BJH desorption cumulative surface area of pores and pore volume are 2.7764m^2/g, 3.095m^2/g and 3.424m^2/g and 0.011328 cm^3/g respectively. The BET surface area of 2.7764 m^2/g in the raw Kalambaina limestone is higher than minimum of 1 m^2/g standard specified for limestone (Stanmore and Gilot, 2005). This high surface area greater than minimum shows that Kalambaina will produce more reactive quicklime as the calcination process is under the kinetics reaction control and therefore, the reaction rate is proportional to the BET surface area (Borgwardt, 1985). In addition, the high surface area of the sample will significantly improve the heat distribution within them and thus, accelerates better decomposition process (Mustakimah et al, 2012).

Table 4: Surface Area, BJH Adsorption cumulative surface area of pores, BJH Desorption cumulative surface Area of pores and Pore Volume of Kalambaina limestone

BET Surface Area (m^2/g)	BJH Adsorption Cumulative Surface Area of Pores (m^2/g)	BJH Desorption Cumulative Surface Area of Pores (m^2/g)	Pore Volume (cm^3/g)
2.7764	3.095	3.424	0.011328

4.0 Conclusion

This work has demonstrated the characterization of Kalambaina limestone using analytical techniques in order to determine its suitability for production of commercial quicklime. The following conclusions were obtained:

1. Kalambaina limestone has a calcitic mineral with fine grain homogeneous texture of crystals.
2. Kalambaina limestone is suitable for production of quicklime from limestone.
3. The optimum temperature for producing quicklime of highest yield in nitrogen atmosphere is 800^{o}C.
4. Kalambaina limestone has LOI due to release of carbon dioxide of44.6%.

References

Adekeye, O. A. and Akande, S. O. (2002). Depositional Environment of the Albian Asu River Group around Yandev, Middle Benue Trough, Nigeria. Journal of Mining and Geology, 38, 2, pp 91 – 101.

Akande, H. F. (2015). Multiple Response Optimization of Quicklime Production from Limestone Using Design of Experiment: PhD Thesis Federal University of Technology Minna, Nigeria.

Antonia, M., Bakolas, A., and Aggelakopoulou, E. (2000). The effects of limestone characteristics and calcination temperature to the reactivity of the quicklime. *Cement and Concrete Research*, 3-5.

Bell, J. P. (1963). A Summary of the Principal Limestone and Marble Deposits of Nigeria. *Geological Survey, 11*, 92.

Borgwardt, R. H. (1985). Calcination Kinetics and Surface Area of Dispersed Limestone Particles. *AIChE Journal*, 31 (1), 103-111.

Benton, W. (1973). Encyclopedia Britannica, 15th Edition, 10: 980-982

Chan, R. K., Murthi, K. S., and Harrison, D. (1970). Thermogravimetric Analysis of Ontario Limestones and dolomites I. Calcination, surface area, and porosity. *Canadian Journal of Chemistry*, 48, 2972-2978.

Chen, C., Zhao, C., Liang, C., and Pang, K. (2007). Calcination and Sintering Characteristics of Limestone under O_2/CO_2 Combustion Atmosphere. *Fuel Processing Technology 88*, 171–178.

Cox, F C, McC Bridge, D and Hull, J H, (1977). Procedures for the assessment of limestone resources. Miner Assess Rep Znst *GeolSci*, No 30.

Demir, F., Donmez, B., Okur, H., and Sevim, F. (2004). Calcination Kinetic of Magnesite from Thermogravimetric Data. *Trans IChemE, Vol 81*, 618-622.

Dogu, G. and Irfan, A. (2000). Calcination Kinetics of High Purity Limestones. *Chemical Engineering Journal*, 1-2.

Foraminifera (2012). Hydrated Lime Production from Limestone in Nigeria How Viable. Retrieved from http://www.foramfera.com/index.php/investment-opportunities-in-nigeria/item/420.

Ghandy, J.J. (1966). "*Annual Report*". National Metallurgical Laboratory: Delhi, India. 1965-1966. 32-33, 152-153.

Gwosdz, W., Lorenz, J., Markwich, R. W., and Wolf, F. (1996). Limestone and Dolomite Resources of Africa. *Geology*, 102:326-327.

Gunasekaran, S., and Anbalagan, G. (2008). Thermal Decomposition of Natural Dolomite. *Indian Academy of Sciences*, 30 (4), 339-344.

Harrison, D J, (1993). Industrial minerals laboratory manual: Limestone. *British Geological Survey Technical Report* WG/92/29.

Harrison, D J, Hudson, J M and Cannell, B, (1998). Appraisal of high purity limestones in England and Wales. A study of resources, needs, uses and demands. Part 1 Resources. British Geological Survey Technical Report WF/90/10.

Khinast, J., Krammer, G. F., Brunner, C., and Staudinger, G. (1996). Decomposition of Limestone; The Influence of $CO_2$and Particle Size on the Reaction Rate. *Chem. Eng. Sci. 51*, 623–634.

Khraisha, Y. H., and Dugwell, D. R. (1989). Thermal Decomposition of Couldon Limestone In A Thermogravimetric Analyser. *Chem. Eng. Res. Des. 67*, 48–51.

Kilic, O., and Mesut, A. (2006). Effects of Limestone Characteristics Properties and Calcination Temperature on Lime Quality. *Asian Journal of Chemistry*, 18(1), 655-666.

Muaazu, K., Abdullahi, M., and Akuso, A. S., (2011). Kinetic Studies of Jakura Limestone using Power Rate Law Model. NIgerian *Journal of Basic and Applied Science Vol. 19, No. 1.*, 116-120.

Mustakimah, M., Nor-Adilla, R, Suzana, Y., Lee, K. T., Umer, R., Razol M. A. (2012). Effects of experimental variables on conversion of cockle shell to calcium oxide using thermal gravimetric analysis. *Australian Journal of Basic and Applied Sciences*, 5(9): 1566-1577.

Navarro, R., Ruiz-Agudo, E., Luque, A., Navarro, A.B., and Ortega-Huertas, M. (2009). Thermal Decomposition of Calcite: mechanism of Formation and Textural Evolution of CaO nanocrystal. *Am Mineral.* 94, 578-593.

Nyong, E. E. (1995). *Geological Excursion Guide book to Calabar Flank and Oban Massif*. In the 31st Annual conference of the Nigerian Mining and Geosciences Society, Calabar, March 12 -16.

Oates, J. H. (1998). *Lime and Limestone: Chemistry and Technology, Production and Uses.* Weinheim: Wiley-VCH.

Okonkwo, P. C., and Adefila, S. S. (2012). The Kinetics of Calcination of High Calcium Limestone. *International Journal of Engineering Science and Technology*, 391-400.

Ola, S. A. (1977). Limestone Deposits and Small Scale Production of Lime in Nigeria. *Engineering Geology, 11*, 128.

Plumpton, A.J. (1984). *Production and Processing of Fine Particles.* Third Edition. Pergamon Press: New York, NY.605.

Rashidi, N. A., Mohamed, M., and Yusup, S. (2012). The Kinetic Model of Calcination and Carbonation of Anadara Granosa. *International Journal of Renewable Energy Research*, 2 (3), 497-503.

Ryemshak, S. A., Adeleke, A. A., andSalami, S. (2012). Characterization of Ubo Limestone for Direct Burnt Lime Production. *The Pacific Journal of Science and Technology, 13*(1), 661-668.

RMDC. (2010). *Multi-Disciplinary Committee Report of the Techno- Economic Survey on Non Metallic Minerals Sector.* Abuja: RMDC.

Soares, B. D., Hori, C. E., Batista, E. A., and Henrique, H. M. (2008). Optimization of the Production of Quicklime by Calcination in Rotary. *Materials Science Forum*, 1-5.

Stanmore, B. R., and Gilot, P. (2005). Review-Calcination and Carbonation of Limestone during Thermal Cycling for CO_2 Sequestration. *Fuel Processing Technology 86*, 1707-1743.

Wagner, M. (2009). *Thermal Analysis in Practice*. Mettler Toledo, Usercom.

Nigerian Journal of Renewable Energy Research
Volume 1, Number 1, pp 11-38, 2023
 ISSN _____

Review of the Selection and Performance Evaluation Procedures for Jaw Crushers

Mumah, S.N.*[1], Kuye, A.O[2], Okpara, K.O.[3] and Chukwuma, F.O.[2]

[1]Department of Chemical Engineering, Kaduna Polytechnic, Kaduna, Nigeria
[2]Department of Chemical Engineering, University of Port Harcourt, P.M.B 5323, Port Harcourt, Nigeria
[3]Department of Chemical Engineering, Federal University of Technology, PMB 1526, Owerri, Nigeria
*Corresponding author: mumahsndoyi@kadunapolytechnic.edu.ng

https://www.tetfundkadpolycoex.org.ng

ARTICLE INFORMATION

Article history:
Received 13 Apr, 2023
Revised 23 Aug, 2023
Accepted 07 Oct, 2023
Available online 30 Dec, 2023

Keywords:
crushing
jaw crushers
Selection
performance
design

Abstract

Crushing and grinding of rocks and other particles has many important applications, including coarse crushing mined ore and quarry rock, fine grinding of coal for power station boilers, and for production of paint, ceramics, cement and other materials. Crushing and grinding of rocks and other particles are governed by the laws of physics involving mass, velocity, kinetic energy, gravity, etc. As crushing and grinding activities evolves in the mining industry, the issue of optimization becomes paramount. Crushing plants operate under very harsh conditions and in most cases involve very abrasive materials. Multiple factors therefore influence the performance of crushers.

This paper examines the procedure for selecting and evaluating the performance of jaw crushers. It is however important to note that it is impractical to reduce the process of selecting and sizing a crusher to a series of formulas. The selection process is largely based on experience and testing with actual field applications and laboratory tests that show how a given material will be reduced by a given crusher type. The paper examines the critical design parameters of jaw crushers. Crushers encounter considerable difficulties concerning external loads acting on their mechanical joints which make it almost impracticable to use theoretical calculations for design and performance evaluation. It is therefore necessary to use experimental studies to verify any theoretical methods used for these purposes. It should be noted however that considering the variety of applications as well as rock materials, minerals and ores, a truly optimal performance of a crushing application must be based on an optimized crusher design as well as a continuously optimized crusher operation.

1.0 Introduction

Jaw crushers are one of the most commonly used crushers in the world. They can easily be

distinguished by the presence of two plates. One plate is fixed where the other opens and closes. This process ensures that the materials are trapped and crushed. Three types of jaw crushers are presently widely used. They are the Blake, Dodge, and Universal jaw crushers. The classification is based on the location of the pivot point of the swinging jaw. The Blake crusher is most commonly used of the three and it was designed and patented by Eli Whitney Blake in 1858 (Weiss, 1985). Jaw crushers have found wide use in quarries, mining, ore crushing and metallurgical plants, where the material physical condition varies from dry to slightly wet, not sticky. The single toggle jaw crusher has found wide used because of its higher capacity and much lower cost when compare to other types of jaw crushers (Donovan, 2003). Jaw crushers are very suitable for rocks that has the hardness index of medium-hard to very hard and so are very common in quarries that requires the primary crushing of blasted rockpile. They can be applied to rocks or ore with edge lengths of more than 2,000 mm (Donovan, 2003).

2.0 Description of the Double Toggle and the Single Toggle Jaw Crusher

A noted characteristic of single toggle jaw crushers is that the swing jaw is suspended on the eccentric drive shaft (Figure 1) and the toggle plate that is placed against the crusher frame supports the swing jaw. The whole arrangement results in a motion that results in a higher capacity than that achieved by the double-toggle jaw crushers (Figure 2). The characteristics of different feeds have influenced the variation in design of the single-toggle jaw crushers by rock hardness.

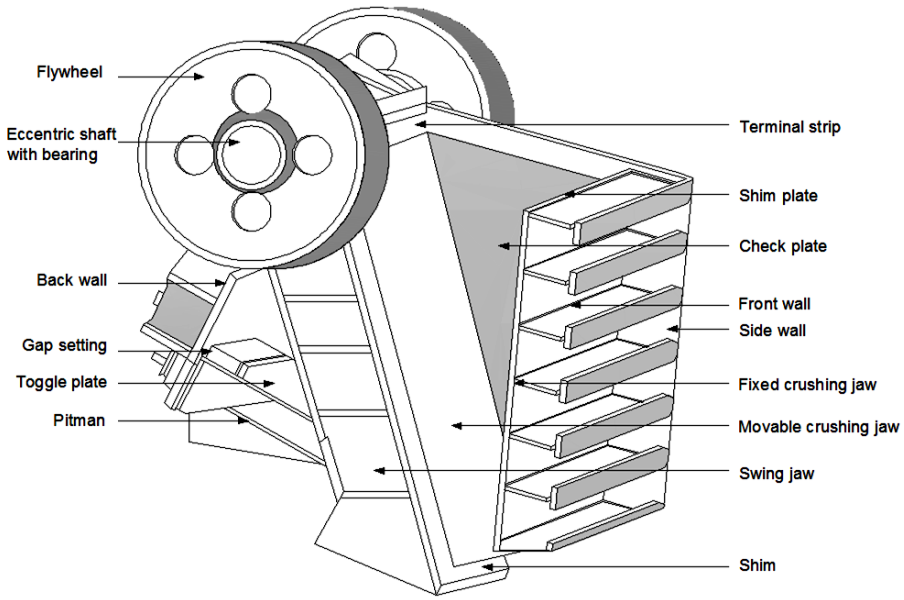

Figure 1: The various parts of a single-toggle jaw crusher ***(adapted from www.thyssenkrupp-industrial-solutions.com/backenbrecher_en.pdf)***

Double-toggle jaw crushers are fitted with a system of toggle levers which upward and downward movement is effected by a pitman by means of an eccentric shaft (Figure 3). The resultant effect of the upward and downward movement is the oscillating motion of the swing jaw. The ores or rocks to be crushed are fed to the crusher by allowing them fall by gravity and the necessary pressure to crush the material is achieved when the crushing chamber is narrowed by the movement of the swing jaw. To increase the crushing effect, the crushing jaw lining is toothed. The retraction of the swing jaw allows the crushed materials to leave the crusher. The crusher is designed in such a way that as crushed materials exits the crusher, new uncrushed materials enter concurrently (Figure 4). The transmission of the required power to the relevant parts of the crusher is effected

by the toggle lever system which makes this type of crusher the equipment of choice for the crushing of very hard, toughest and abrasive materials.

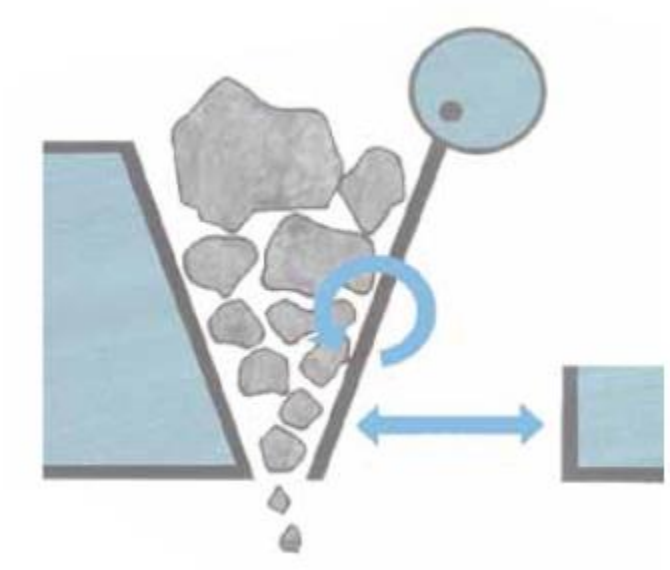

Figure 2: How a single-toggle jaw crusher with the toggle system operates *(www.thyssenkrupp-industrial-solutions.com/backenbrecher_en.pdf)*

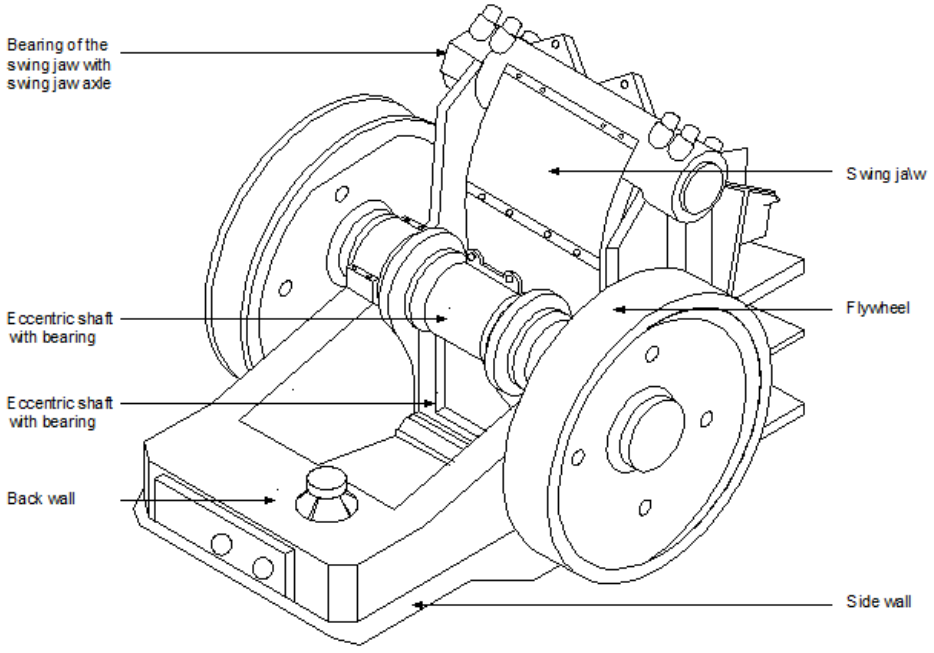

Figure 3: Double-toggle jaw crusher with its main components *(Adapted from www.thyssenkrupp-industrial-solutions.com/backenbrecher_en.pdf)*

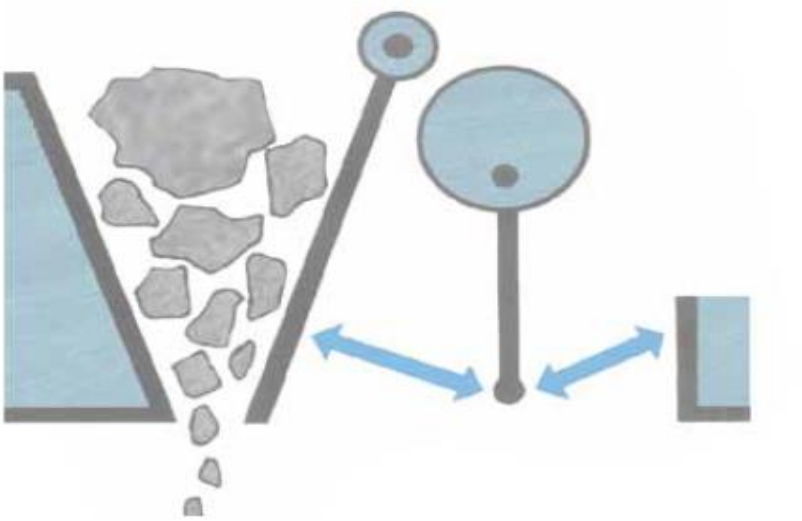

Figure 4: The Operating mechanism of a double-toggle jaw crusher with the toggle-lever system *(www.thyssenkrupp-industrial-solutions.com/backenbrecher_en.pdf)*

Table 1 shows the materials that the various parts of a jaw crusher are made. The selection of the materials is to ensure the jaw crusher last for long time even subject to very hard ore.

Table 1: Material for components of jaw crusher (Garnaik, 2010)

S/No	Component	Material / Function
1.	Body	Made from high quality steel plates and ribbed heavily in welded steel construction
2.	Swing jaw Plate	Manganese steel
3.	Fixed jaw plate	Manganese steel
4.	Pitman	Crushers have a light weight pitman having white-metal lining for bearing surface
5.	Toggle	Double toggles, for even the smallest size crushers give even distribution of load
6.	Flywheel	high grade cast iron
7.	Tension Rod	Pullback rods helps easy movement, reduces pressure on toggles and machine vibration
8.	Hinge plate	Strong hinge pin made from steel are used for crushing without rubbing
9.	Shaft and bearings	Massive rigid eccentric shafts made from steel along with roller bearing ensures smooth running.
10.	Diaphragm	Flexible diaphragm seals opening in oil chamber and protects components from dust

One of the trends in design solutions of crushers ensuring the crushing ratio of about 30 involves the application of the vibratory-impulse action to the material to be crushed. Crushers utilizing these effects are referred to as vibratory crushers. During the vibratory crushing the material to be disintegrated is subjected to the action of fast changing shearing forces, which leads to the material being crushed either by applied impulses or by fatigue action, unlike conventional crushers where the structure of the material is damaged by the applied pressure (Wolny, 2013).

3.0 Dimensions and Operating Parameters

Feed characteristics are important parameters when designing or selecting a jaw crusher for a specific job (Napier-Munn et al, 1999). The feed particle sizes of interest are those of the ore or rock that enters the crusher, the particle that can be nipped, particle that can fall through the chamber, and the particle that can fall through the chamber when the jaws are wide open (Donovan, 2003). The dimensions defined by these particle sizes include the gape which is the distance between the jaws at the feed opening, the Closed Side Set (CSS) which is the minimum opening between the jaws during the crushing cycle (minimum discharge aperture),the Open Side Set (OSS) which is the maximum discharge aperture, and the throw – the stroke of the swing jaw and the difference between OSS and CSS. Figure 5 shows a schematic of crusher dimensions (Donovan, 2003)

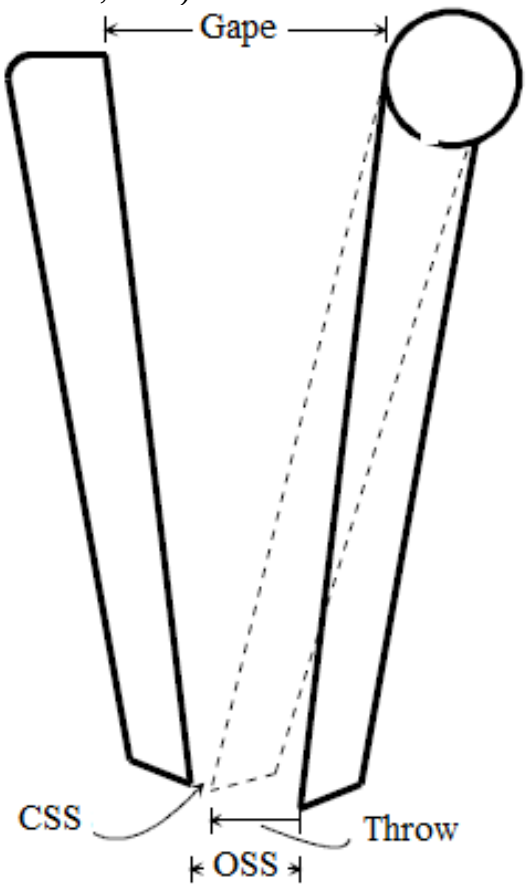

Figure 5: Schematic of crusher dimensions (Donovan, 2003)

The rating of jaw crushers are determined by the maximum dimensions of their feed opening, defined by the gape and the width of the plates. The fed openings of jaw crushers are known to vary from 250 mm by 500 mm to 1524 mm by 2032 mm. The largest particle size of the rock to be crushed should not be more than 80% of the rated gape (Weiss, 1985).The size of rectangular or square opening at the top of the jaws crusher defines the size the crusher. Therefore a 30 x 40 jaw crusher has an opening of 30" by 40". Primary jaw crushers generally come with square opening design while secondary jaw crushers have the rectangular opening design (Garnaik, 2010).

4.0 Selection of Crushers

The main factor that ensures effective control of the crushing process is proper selection of the crushing equipment. The principal factors that should be considered while selecting jaw crushers include (Donovan, 2003);

a. The petrographic nature of the rock
b. The abrasion index of the aggregate
c. The mechanical strength of the rock
d. The work index, or impact crushability, of the rock
e. The brittleness of the rock
f. The flakiness of the rock
g. The feed size
h. The desired product size (or reduction ratio)
i. The throughput to be crushed (tons per hour)
j. The capital cost
k. The long-term operating costs.
l. Project location, Operational considerations (e.g capacity per hour or day)
m. Climatic conditions,
n. Safety and environment,
o. Life of mine/expansion plans and Maintenance requirements.

The petrographic nature of the rock and its resistance to crushing forces (characterized by strength, work index, etc.) are used first to determine what type of crusher is needed and then in part to determine the power requirement of the crusher. When a jaw crusher is selected outright, the physical properties of the rock can be used to determine the mechanical features of the jaw crusher, but for the most part they are used along with the feed size and desired throughput to determine the size of the jaw crusher and its power requirement.

Usually, the feed size range or the desired throughput dictates the selection of specific jaw crusher. The current trend is to go to the largest feed opening that is economically feasible in order to avoid as much secondary breakage as possible (Donovan, 2003). Once a crusher is selected it can be determined whether or not the crusher will provide the desired reduction ratio or product size distribution. As was noted previously the size of a jaw crusher's discharge opening controls the product size distribution. Thus, determining whether a specific jaw can produce the desired product is dependent upon whether or not that crusher can have its discharge opening set to the required dimension. Table 2 shows the capacities for various Nordberg series jaw crushers.

Screen analysis graphs (Figure 6) and capacity charts (Table 2) have greatly simplified the task of selecting a crusher for a specific task. This been applied extensively in the selection of Nordberg C Series jaw crushers (Donovan, 2003; Metso Minerals, 2003) where computer program has been developed to speed up the process. The program known as the *Bruno* program requires inputs such as rock type, feed gradation, and the desired crusher to simulate expected capacities and product size distribution curves (Metso Minerals, 2003). The use of crusher efficiency index number based on crusher manufacturer's published data and the crushability factor of the rock has been proposed by Wagner (1990) to assist in crusher selection. However, the use of information based on standard rock size such as those presented in graphs, charts, etc, may be inaccurate because of the inhomogeneous nature of many rock types (Bearman, Barley and Hitchcock (1990). To carry out

a selection that may be consider accurate will therefore necessitate the need to fully characterize the rock which may require a lot of laboratory tests and experiments.

Table 2: Capacities for various Nordberg C Series jaw crushers (After Metso Minerals, 2003, Donovan, 2003)

CSS* mm	*C63* 440 × 630	*C100* 760 × 1000	*C110* 850 × 1100	*C140* 1070 ×1400	*C160* 1200 ×1600	*C200* 1500 ×2000
40	40					
50	55					
60	65					
70	80	150	190			
80	95	170	210			
90	110	190	235			
100	120	215	255			
125		265	310	385		
150		315	370	455	455	520
175		370	425	520	595	760
200		420	480	590	675	855
225				655	750	945
250				725	825	1040
275					900	1130
300					980	1225

Capacities in metric tons per hour

**CSS stands for closed side set (CSS) - the minimum opening between the jaws during the crushing cycle (minimum discharge aperture)*

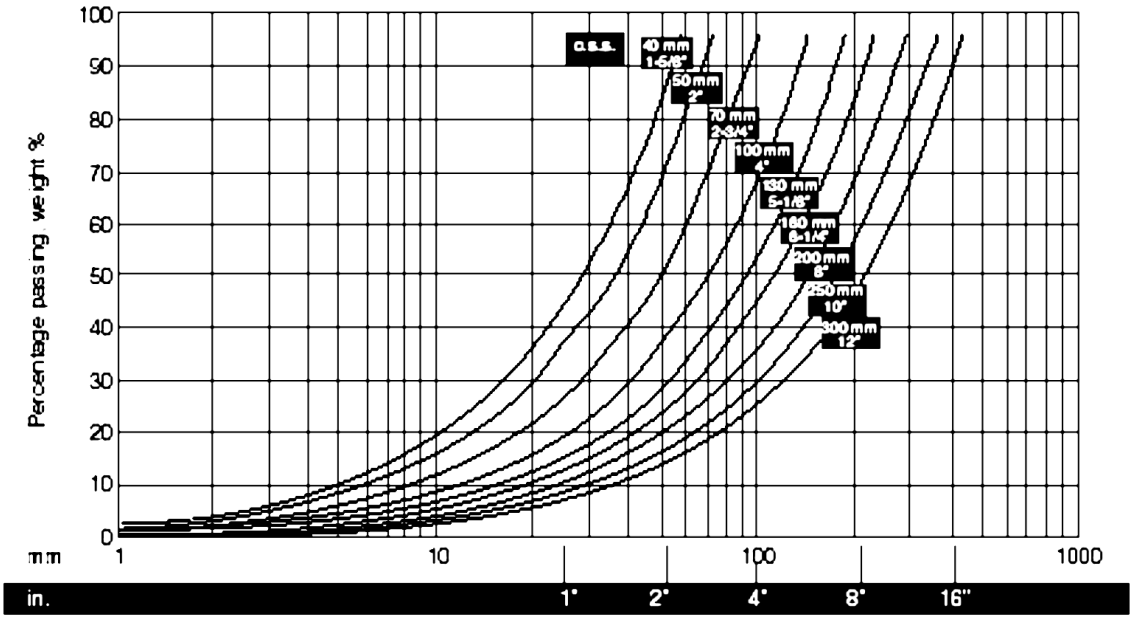

Figure 6: Product size distributions based on CSS (From Metso Minerals, 2003; Donovan, 2003)

For jaw crushers, a lot of considerations should be analysed such as (*Peter mayo; http:/www.quarry.com.au*):

a. The particle size of the should not be greater than 80% of the 'gape';
b. The crusher's operating setting (close side setting);
c. Maximum product particle diameter which normally is 1½ times the close side setting of the machine. This those not follow for slappy materials;
d. It is normally considered that 50% - 60% of the crushed product will pass the close side setting;
e. Jaw crushers reduction ratio are normally 6:1
f. When selecting a jaw crusher as a primary crusher, it should be noted that its output should exceed the average capacity of the plant, as primary feed to the plant is generally of a cyclical nature, relying on trucks or loaders in most cases.
g. For jaw crushers to operate optimally, all feed with particle size smaller than the closed side setting is removed to bypass the jaw crusher;
h. Generally, maximum feed size is critical in the selection of jaw crushers and not required capacity. This is because putting too fine a feed into a jaw crusher normally leads to equipment failure because of overload.

A lot of dynamic forces are present during a crushing process. These forces and the load also affect the supporting structures and foundations. It is therefore very important to consider how these forces and load affect the crusher structures and the outcome incorporated in the design (Rusiński, 2013).

5.0 Energy and Size Reduction

Crushing theory is concerned with the relationship between the amount of energy put into a rock or particle of a known size and the reduced particle size after the comminution process has taken place. The amount of energy required to do this work is referred to as the 'Work Index' and it is an expression of the resistance that a material has to crushing (or grinding). It is a measurement of how hard the ore is. Therefore 'Work Index' can be defined as *(http://gravel.gravelwasher.com/metalliferous-mining-processing-resource-book-crushing.html)*:

The amount of energy (work) required to break a rock from one size to another.

Each rock has a characteristic Work Index. For example, more energy is required to break quartz than sandstone so quartz will have a higher work index. Numerically the work index is known as the kilowatt-hours per tonne or kWh/t. A kilowatthour is the number of kilowatts consumed in an hour. For example, if you ran a 20kW motor for an hour, you would expend 20kWh. If you used that motor to do work to 2 tonnes of rock you would have used 20kWh/2 tonne, which is 10kWt/h. The higher the Work Index, the more work required to break the rock, hence the harder the rock. Whereas Work Index refers to the size fraction when rocks are reduced in size, **Specific energy input** refers to the amount of energy required to treat a certain tonnage. In simple terms if you crush 100t of rock from your feed size to your product size and it takes 180kWh, your specific energy input is 180kWh/100t = 1.8kWh/t.

The concepts of Work Index and Specific Energy make it clear that a certain (calculable) amount of energy is required to break a rock from one size to another. Experience has shown that to break a rock from coarse and medium size should require less energy per unit mass than to break a rock from coarse to fine, i.e. the smaller you want to break a rock, from a given starting size, the more energy you require. Because we are talking about specific energy, i.e. energy per tonne of ore, it

also follows that a given amount of energy spread out over a larger number of rocks will produce less breakage*(http://gravel.gravelwasher.com/metalliferous-mining-processing-resource-book-crushing.html)*. This can be demonstrated by looking at the numbers:

For example: Say it takes 100kWh to break 50t of rock from 50mm to 10mm. Then the Specific Energy Input from 50mm to 10mm is 100kWh/50t = 2kWh/t. If we then tried to use that same 100kWh to break 100t of rock, we would only be putting in 100kWh/100t or 1kWh/t.

Now, we know that to break a rock finer we need to increase the energy input, so a Specific Energy Input of 1kWh/t will produce a much coarser product than a Specific Energy Input of 2kWh/t.

6.0 Mechanisms of Particle Fracture

A size reduction process is analyzed by looking at the entire size distribution of its feed and product material. However as each particle breaks as a result of the stresses applied to it and it alone, it is of value to look at single particle fracture. For a particle to fracture, a stress high enough to exceed the fracture strength of the particle is required. The manner in which the particle fractures depends on the nature of the particle, and on the manner in which the forcer is applied. There are three main generalized mechanisms of single particle fracture and they are*(http://gravel.gravelwasher.com/metalliferous-mining-processing-resource-book-crushing.html)*.

6.1 Abrasion

Abrasion fracture occurs when insufficient energy is applied to cause significant fracture of the particle. Rather, localised stressing occurs and a small area is fractured to give a distribution of very fine particles. This type of breakage occurs predominantly in ball mills.

6.2 Cleavage

Fracture by cleavage occurs when the energy applied is just sufficient to fracture the particle. Only a few particles result and their size is comparatively close to the original particle. Typically this situation occurs under conditions of slow compression where the fracture immediately relieves the loading on the particle. This is the main type of fracture found in jaw crushers.

6.3 Shatter

Fracture by shatter occurs when the applied energy is well in excess of that required for fracture; under these conditions many areas in the particle are overloaded and the result is a comparatively large number of particles with a wide size distribution. In practice these events do not occur in isolation, rather breakages involve a combination of fracture mechanisms.

7.0 Predicting Jaw Crusher Performance

Comminution concerns the breakage of brittle particles under conditions of applied compressive stress. The nature of the failure mechanisms is governed by material properties of the particulate material and by the nature of the stress field around and within individual particles. The response of the particulate material to the stress field is largely elastic but significant non-elastic behavior occurs, particularly at the tips of growing cracks where large quantities of energy are dissipated when the criteria for fracture are met. The dissipation at the crack tip of the stored elastic energy in the particle turns out to be of critical interest in industrial comminution machines where energy efficiency is of major consequence because of its economic importance. Industrial comminution processes are typically inefficient in their use of energy in the sense that considerably more energy

is consumed by the operating equipment than is actually required to break the particles. In spite of the importance of this observation, it has not been possible to calculate precisely how much energy is actually required (Umucu et al; 2013).

Specific fracture energy of the particles is not the only fundamental property that is important. The particle strength also plays a significant role in determining the overall comminution properties of the material. A particle will be broken only if it is stressed beyond its strength which is determined by the intrinsic properties of the material, the presence of micro flaws which act as stress raisers when the particle is under load and the state of stress that is experienced by the particle (Umucu et al, 2013).

The performance of jaw crusher is mainly determined by the kinetic characteristic of the liner during the crushing process. The practical kinetic characteristic of the liners which are located in certain domain of the coupler plane are computed and discussed by Jinxi et al(2007) and Shrivastava (2012).

The performance of a jaw crusher is most aptly defined using the product size, the capacity or throughput, and the power consumption. The main object of size reduction in the aggregate industry is to generate a well-shaped product within a specified size range with a minimum of fines. It is also desirable to maintain target production rates and to crush the rock material as efficiently as possible.

There are various methods for the prediction of crusher performance. As noted previously in the discussion of crusher selection, technical literature provided by crusher manufacturers can be used to determine capacities and product size. Adjustments can be made to account for physical variations in feed materials using the aforementioned laboratory tests. When the actual performance of a jaw crusher is difficult to determine or unclear to the manufacturer, laboratory tests using small-scale jaw crushers are sometimes conducted in order to predict the performance of full capacity machines. The normal procedure is to test crush a representative sample of the feed material and determine the product size distribution. Comparison of the product distribution and associated properties of the feed material to other materials is used to estimate overall crushing performance, power requirements, and to detect characteristics that may require special design considerations. These tests provide an opportunity to evaluate the effects of various crusher settings, speeds, feeding methods, and the physical characteristics of the material (Pennsylvania Crusher Corporation, 2003).

In addition to charts, graphs, and lab-scale crushing tests, jaw crushers can also be evaluated using mathematical modeling techniques. Mathematical techniques are usually derived from laboratory data and can be used to predict crusher performance and possibly improve selection and design procedures (Rimmer et al, 1986). Models/equations are typically used to determine the product size, power draw, and capacity of crushers. The advantage of models is that they reduce complex operations to a few numbers or parameters and can provide guidance to improved performance and decision making (Napier-Munn et al, 1999).

7.1 Estimating capacity

The capacity of a jaw crusher is dependent upon the machine characteristics, the feed, and the nature of the rock material. The volumetric capacity of a jaw crusher can be estimated from the following equations (Sastri, 1994):

$$V = 60Nw\ (CSS + 0.5T)\ \left(\frac{DT}{G-(CSS+T)}\right) \text{ at low speeds}$$
$$V = 60Nw\ (CSS + 0.5T)\ \left(\frac{450g}{N^2}\right) \text{ at high speeds} \quad (1)$$

where N is the speed of the crusher in rpm
w is the width of the jaws in m
CSS is the closed side set in m
T is the throw in m
D is the vertical depth between the jaws in m
G is the crusher gape in m, and
g is gravitational acceleration in m/s^2.

Equation 1 gives volumetric capacity under ideal conditions. At low crusher speeds the material falls down the chamber due to gravity flow, and the distance of the fall is dependent on the geometry of the machine. At higher speeds there is less time between strokes/revolutions and movement of material down the chamber is constricted and controlled by the speed of the machine (Hersam, 1923).

In order to determine the actual capacity of a jaw crusher, Equation (1) needs to be corrected by accounting for the feed size, the degree of compaction resulting from vibration, and the nature of the material. Equation (2) gives the estimated capacity using these parameters (Sastri, 1994):

$$V = 60Nw\ (CSS + 0.5T)\ \left(\frac{DT}{G-(CSS+T)}\right)\ K_1\ K_2\ K_3 \text{ at low speeds}$$
$$V = 60Nw\ (CSS + 0.5T)\ \left(\frac{450g}{N^2}\right)\ K_1\ K_2\ K_3 \text{ at high speeds} \quad (2)$$

with

$$K_1 = 0.85 - \left(\frac{F_{avg}}{G}\right)^{2.5}$$
$$K_2 = 1.92 \times 10^{\frac{-6.5T}{G}} \quad (3)$$

where, F_{avg} is the average feed size in m, and K_3 is a parameter related to the nature of the material. The parameter K_3 does not have a suggested value but is considered to increase with increasing hardness or toughness.

7.2 Product Size Distribution for Crushers

Specific fracture energy of the particles is not the only fundamental property that is important. The particle strength also plays a significant role in determining the overall comminution properties of the material. A particle will be broken only if it is stressed beyond its strength which is determined by the intrinsic properties of the material, the presence of micro flaws which act as stress raisers when the particle is under load and the state of stress that is experienced by the particle.

For impact breakage mechanism, many stakeholders are using the model of the percentage of broken product passing 1/10 the original particle size, t_{10}. The parameter t_a is defined as one tenth of t_{10} as follows (Napier-Munn et al 1996):

$$t_a = \frac{t_{10}}{10} \quad (4)$$

The abrasion breakage parameter, t_a, is determined by performing a tumbling test. A lower value of t_{10} (hence a lower t_a value) indicates that there is a lower percentage of material passing 1/10th the original particle size, or greater resistance to abrasion breakage.

Equation (5) relates t_{10} to E_{CS} which is specific energy of comminution (Napier-Munn et al 1996):

$$t_{10} = A\,(1 - e^{-bE_{cs}}) \quad (5)$$

where: t_{10} = percentage passing 1/10th of the initial mean size,
E_{cs} = specific comminution energy (kWh/kg)
A, b = ore impact breakage parameters.

The impact breakage parameters, namely A and b, are determined using a high energy impact breakage device called JK Drop Weight Tester. Specific energy of comminution, E_{cs}, in Equation (5) can be calculated according to experimental setup data, as follows (Napier-Munn et al 1996):

$$E_{cs} = \frac{0.0272 M_d (h_i - h_f)}{\bar{m}} \quad (5a)$$

Where, M_d is drop weight mass (kg), m is the medium mass of per particle size class; (g), h_i is initial height of drop weight above the anvil (cm) and h_f is final height of drop weight above the anvil (cm).

It is noted that A is the maximum t_{10} value achieved. This is significant for higher energy breakage. The parameter b is related to the overall slope of t_{10} versus E_{cs} curve at the lower energies. A and b are interdependent, since the value of one will directly affect the other. Parameters A and b are related and usually are reported by $A.b$ as a single value to indicate the ore hardness in terms of impact breakage. The $A.b$ parameter is the slope of the t_{10} vs. E_{cs} curve at its origin and it is a measure of breakage of the ore at lower energy levels.

Napier-Munn et al indicate a possible correlation between the impact ($A.b$) and abrasion (t_a) parameters and the Bond ball mill work index given by the equations (Hasani et al; 2009):

$$A \times b = -3.5 W_i + 117 \quad (6)$$
$$t_a = 19.7 W_i^{-1.34} \quad (7)$$

Narayanan (1983), Pauw and Mare (1988), Bourgeois (1993) and King (2002), King (2002) proposed breakage distribution model as (Soni et al, 2013):

$$t_n = 1 - (1 - t_{10})^{\left[\left\{\frac{9}{n-1}\right\}^{\propto}\right]} \quad (8)$$

Where, t_n= cumulative fraction passing from 1/nth of the feed size
t_{10}= cumulative fraction passing from 1/10th of the feed size
α = a material characteristic

The t_n versus t_{10} relationships can then be used to predict the product size distributions at different grind times (Sand and Subasinghe, 2004).

King (2002) proposed the relationship of t_{10} to the specific comminution energy by the equation:

$$t_{10} = t_{10(max)} \left[1 - e^{\frac{\beta E_{CS}}{E_{50}}}\right] \quad (9)$$

where, E_{CS} = specific comminution energy (Kwh/ton).

The coefficient β and E_{50} (median impact energy at fracture) were considered as material characteristics by (Narayanan, 1987), (Napier-Munn, 1996) and (Weedon, 2001).

Umucu et al (2013) proposed a different size distribution relations for t_n values of crushing products obtained from different laboratory scale crushers (jaw, roller and hammer). The following equation was used to predict the cumulative percentage passing (t_n), depending on the Crushing Engine Power *(CEP)* and feed particle size (X) before crushing:

$$t_n = \left(\frac{56.12}{n^{1.168\,CEP^{-1.274}}}\right) X^{0.30} \quad (10)$$

The relationship has however not been tested on industrial crushers.

Narayanan (1986) used a novel procedure for estimation of breakage distribution functions of ores from the t-family of curves. In this method, the product size distribution can be represented by a family of curves using marker points on the size distribution defined as the percentage passing (t) at a fraction of the parent particle size. Thus, t_2 is the percentage passing an aperture of half the size of the parent particle size, t_4 is one quarter and t_{10} is one-tenth of parent particle size. Narayanan and Whiten (1988) have proposed empirical equations for relating the reference curve data t_{10} with the impact energy.

7.3 Product Size Models

Csoke et al (1996) developed an empirical method for determining the product size of "preliminary" crushers, i.e. jaw crushers and gyratory crushers. The product size resulting from breakage of the material larger than the CSS of the crusher can be modeled using the following function:

$$P(d) = \left(\frac{r}{r_{max}}\right)^m \quad (11)$$

With $r = \frac{d_p}{Gap}$ (12)

$$r_{max} = \frac{d_{PMAX}}{Gap} \quad (13)$$

where,
m is exponent describing the product size distribution
d_p is the particle size
d_{pMAX} is the largest size in the product (OSS), and

G_{ap} is the CSS (CSS is closed side set (CSS) - the minimum opening between the jaws during the crushing cycle (minimum discharge aperture)) of the crusher.

Based on operating data found in the literature, Equation (11) fits the product size of a jaw crusher with r_{max} equal to 1.223 and m of 0.842.

King (2001) outlined a model for the prediction of product size based on data from a crusher manufacturer. The main concept is that the size distribution of the product is characterized by the particle size relative to the OSS and by the product type, P_t, which is the fraction of the product smaller than the OSS. P_t is related to the nature of the material and is distinguished by the work index and a qualitative description of the material. The size distribution given by this model is determined from the following equations:

$$P(d) = 1 - e^{\left(-\left[\frac{r}{K_u}\right]^{1.5}\right)} \quad \text{for r > 0.5}$$
$$P(d) = 1 - e^{\left(-\left[\frac{r}{K_l}\right]^{0.85}\right)} \quad \text{for r < 0.5} \quad (14)$$

With

$$r_i = \frac{D_i}{OSS} \quad (15)$$

$$K_u = \left[In\left(\frac{1}{1-P_1}\right)\right]^{-0.67} \quad (16)$$

$$K_1 = 0.5\left[In\left(\frac{1}{1-P_b}\right)\right]^{-1.18} \quad (17)$$

$$P_b = 1 - e^{\left(-\left(\frac{0.5}{K_u}\right)^{1.5}\right)} \quad (18)$$

Equation (14) should only be used when the size at which half of the feed material passes is greater than the OSS.

Other product size models of note is the one developed by Whiten in 1972 (Donovan, 2003).

First the classification and breakage could be illustrated by Figure 7.

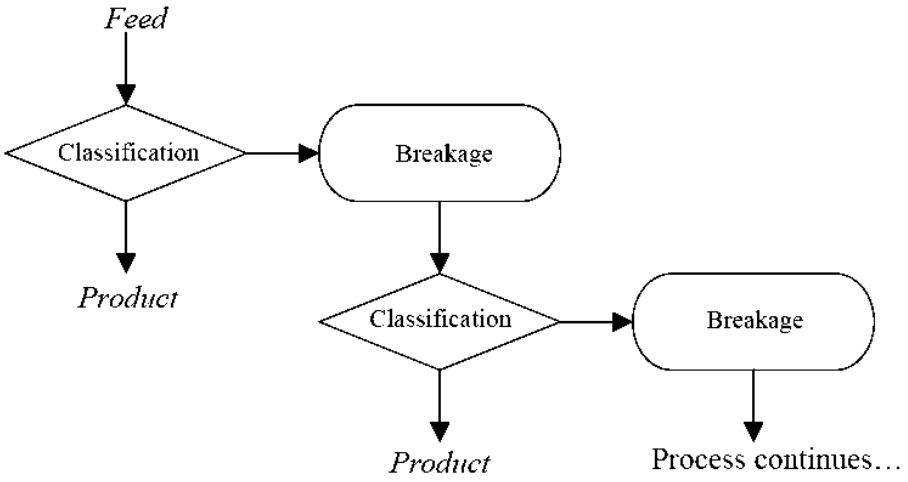

Figure 7: Flowchart of classification and breakage process (Donovan, 2003)

If the classification and breakage of particles in a jaw crusher is considered as a closed circuit process, Figure 7 can be represented by Figure 8, a representation of the Whiten crusher model (Donovan, 2003).

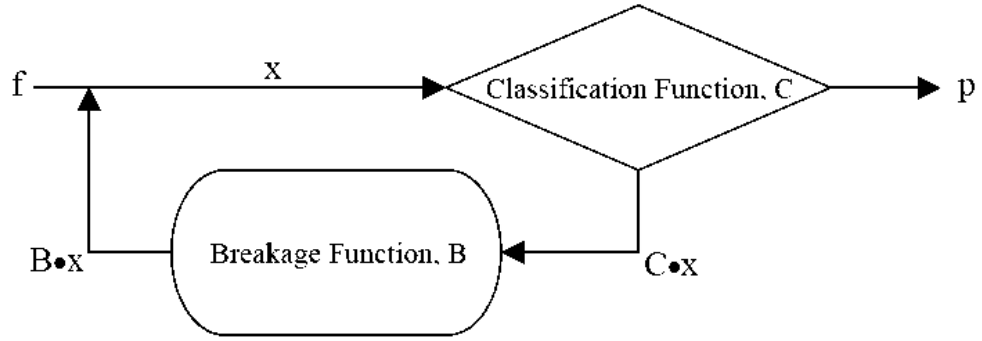

Figure 8: Whiten crusher model (Donovan, 2003)

The Mass balance equations written about each node of Figure 8 describe the repetitive process of classification and breakage and are expressed as (Kojovic et al, 1997, Donovan, 2003):

$$X = f + Bx \qquad (19)$$
$$X = p + Cx \qquad (20)$$

where, x is a vector representing the amount in each size fraction entering the crusher
f is the feed size distribution vector
p is the product size distribution vector
C is the classification (diagonal) matrix
B is the breakage distribution (lower triangular) matrix.

The classification matrix describes the proportion of particles in each size interval entering the crushing zone. The breakage distribution matrix gives the relative distribution of each size fraction

after a breakage event. Equations (19) and (20) can be combined resulting in the Whiten crusher model equation (Whiten, 1972):

$$P = (I - C).(I - BC)^{-1} \cdot f \quad (21)$$

where, *I* is the unit matrix. Equation (21) can be used to determine the product size of a jaw crusher given the feed size, classification function, and the breakage function (Donovan, 2003).

7.4 Power Models for Jaw Crushers

The classical comminution theories, which were derived by Rittinger, Kick and Bond (Lee, 2012) respectively, aim to describe the relation between energy and size reduction for a given feed size. The three theories, which are usually referred to as the first, second and third theory of comminution, are formulated in Equations (22) to (24) (Asbjörnsson, 2013; Lee, 2012).

$$E_{Rittninger} = C_{Ritt} \left(\frac{1}{p_{80}} - \frac{1}{f_{80}}\right) \quad (22)$$

Where $E_{Rittinger}$ is the energy input, C_{Ritt} is a material constant, p_{80} is the size which 80 % of the product passes, and f_{80} is the size which 80 % of the feed passes (Asbjörnsson, 2013; Lee, 2012).

$$E_{Kick} = -C_{Kick}\, In \left(\frac{p_{80}}{f_{80}}\right) \quad (23)$$

where E_{Kick} is the energy input and C_{Kick} is a material constant.

Rittinger's and Kick's laws lack precision in describing the shape of a size distribution curve as only a single point is used (Lee, 2012).

The third and final classical relationship was proposed by Bond in 1952. According to his theory, the energy input is proportional to the length of the produced crack tip and is equal to the difference in energy represented by the product and the feed, and is expressed as (Lee, 2012):

$$E_{Bond} = C_{Bond} \left(\frac{1}{\sqrt{p_{80}}} - \frac{1}{\sqrt{f_{80}}}\right) = W_1 \left(\frac{10}{\sqrt{p_{80}}} - \frac{10}{\sqrt{f_{80}}}\right) \quad (24)$$

where *p* and *f* are in microns. W_I is the Bond´s *work index* which expresses the resistance of a material to crushing or grinding. This constant is a function of material properties and the efficiency of the crusher. A lower efficiency in a crusher will give a higher work index (Asbjörnsson, 2013; Lee, 2012).

The above classical laws of comminution have not been found to accurate in many cases and others have worked to improve them with varying degree of success. Hukki in 1975 (Lee, 2012) suggested that all three relationships were in fact applicable but in different and relatively narrow size ranges (Will and Napier-Munn,2005; Morrel (2004). Based on Hukki's work, Morrell (2004) later successfully proposed a modification of Bond's equation. Unfortunately, as pointed out by Lindqvist (2008), Morrell's modified energy model still lacks precision due to the sole use of f_{80} and P_{80}. Egbe et al (2013) presented procedures for determining the Bond's work index of some Nigerian ores.

An alternative approach to calculate the energy cost to produce a given product size distribution from a given feed size distribution was suggested by Lindqvist (2008) and Lee (2012).

However, there is generally little confidence in the model results and it is also suspected that all these underlying ideas are incorrect and that the energy–size reduction relationship does not suitably define the process of size reduction (Napier-Munn, 1996, Lynch, 1977). Bond's "law" is an empirical law that only fits experimental data over a limited range of variables and only in certain cases (Choi, 1982). It can be corrected for other operating conditions but even with this correction it has been shown that the power consumption of a jaw crusher can be as much as 240% greater than the expected consumption based on Bond's equation (Eloranta, 1997). Rose and English have suggested a relationship for power consumption based on Bond's work index but take into account the material density and machine characteristics, i.e., gape, throw, CSS, etc. (Lowrison, 1974).

A more recent approach for predicting power consumption in crushers was presented Andersen and Napier-Munn (1988) and Morrell et al, 1992. In this case, they used using a single regression equation relating the power actually drawn by the industrial machine in producing a particular product size distribution, to the calculated power required to achieve the same size reduction in a laboratory test (Sabic and Forlin, 2002, Donovan, 2003).

$$P_c = AP_p + P_n \tag{25}$$

where P_c is the power drawn by the crusher under load in kW and P_p is the pendulum power in kW expressed as

$$P_p = \sum_{i-1}^{j} E_{cs} t_{10i} C_i \; x_i \tag{26}$$

P_n is the power drawn by the crusher under no load in kW.

This power model provides a means of comparing the power efficiency of different patterns and types of crushers, in terms of efficiency constant A, and has been found to provide satisfactory predictions for several crusher types. However, as the regression coefficients are not valid for all crushers, the tests must be repeated for some crusher types (Sabic and Forlin, 2002).

Today the energy-size relation in the comminution process is usually presented in the form of the differential equation proposed by Walker et al (1937) and revised by Hukki (1962). This is represented by Equation (27) (Asbjörnsson, 2013):

$$dE = -C \frac{dx}{x f^{(x)}} \tag{27}$$

The most common mathematical model used today for expressing the crusher performance is the empirical Selection-Breakage model proposed by Whiten (1972). This model is however empirically fitted to data from drop weight tests, which is more suitable for mills than compressive crushers and does not predict capacity.

More detailed analytical models based on the mechanical properties of the crusher have been proposed by Evertsson (2000) and Briggs (1997). These models can provide more accurate information from the process but require detailed information about crusher geometry, breakage behaviour and require considerable simulation time (Asbjörnsson, 2013).

7.5 Size Reduction Relationships

The general size reduction equation is as follows (Morrell, 2004):

$$W_i = M_i\, 4\left(x_2^{f(x_2)} - x_1^{f(x_1)}\right) \quad (28)$$

Where:
W_i = Specific comminution (kWh/tonne);
M_i = Work index related to the breakage property of an ore (kWh/tonne);
x_2 = 80% passing size for the product (microns)
x_1 = 80% passing size for the feed (microns)
$f(x_j)$ is calculated from the relationship: ((Morrell, 2006):

$$f(xj) = -(0.295 + xj \times 10^{-6}) \quad (29)$$

For grinding from the product of the final stage of crushing to a P_{80} of 750 microns (coarse particles) the index is labeled M_{ia} and for size reduction from 750 microns to the final product P_{80} normally reached by conventional ball mills (fine particles) it is labeled M_{ib}. For conventional crushing, M_{ic} is used and for High Pressure Grinding Rolls, (HPGRs), M_{ih} is used.

For coarse particle grinding in tumbling mills Equation (28) is written as:

$$W_a = K_1 M_{ia}\, 4\left(x_2^{f(x_2)} - x_1^{f(x_1)}\right) \quad (30)$$

where K_1 = 1.0 for all circuits that do not contain a recycle pebble crusher and 0.95 where circuits do have a pebble crusher; $x_1 = P_{80}$ in microns of the product of the last stage of crushing before grinding; x_2 = 750 microns and M_{ia}= Coarse ore work index and is provided directly by Semi-autogenous Mill Comminution(SMC) Test.

For fine particle grinding Equation (28) is written as:

$$W_b = M_{ib}\, 4\left(x_3^{f(x_3)} - x_2^{f(x_2)}\right) \quad (31)$$

where x_2 = 750 microns; $x_3 = P_{80}$ of final grind in microns; M_{ib} is provided by data from the standard Bond ball work index test using the following equation (Morrell, 2006):

$$M_{ib} = \frac{18.18}{P_1^{0.295}(Gbp)\left(p_{80}^{f(p_{80})} - f_{80}^{f(f_{80})}\right)} \quad (32)$$

where M_{ib} = fine ore work index (kWh/tonne); P_1 = closing screen size in microns; Gbp = net grams of screen undersize per mill; P_{80} = 80% passing size of the product in microns and f_{80} = 80% passing size of the feed in microns. Note that the Bond ball work index test should be carried out

with a closing screen size which gives a final product P_{80} similar to that intended for the full scale circuit.

Equation (28) for conventional crushers is written as:

$$W_c = S_c K_2 M_{ic}\, 4\left({x_2}^{f(x_2)} - {x_1}^{f(x_1)}\right) \quad (33)$$

Where S_c = coarse ore hardness parameter which is used in primary and secondary crushing situations. It is defined by Equation (34) with K_s set to 55; K_2 = 1.0 for all crushers operating in closed circuit with a classifying screen; $x_1 = P_{80}$ in microns of the circuit feed; $x_2 = P_{80}$ in microns of the circuit product and M_{ic} = Crushing ore work index and is provided directly by SMC Test. If the crusher is in open circuit, eg pebble crusher in an Autogenous/Semi Autogenous, AG/SAG circuit, K_2 takes the value of 1.19.

The coarse ore hardness parameter (S) makes allowance for the decrease in ore hardness that becomes significant in relatively coarse crushing applications such as primary and secondary cone/gyratory circuits. In tertiary and pebble crushing circuits it is normally not necessary and takes the value of unity. In full scale HPGR circuits where feed sizes tend to be higher than used in laboratory and pilot scale machines the parameter has also been found to improve predictive accuracy. The parameter is defined by Equation (34);

$$S = K_s(x_1 x_2)^{-0.2} \quad (34)$$

Where K_s = machine-specific constant that takes the value of 55 for conventional crushers and 35 in the case of HPGRs; $x_1 = P_{80}$ in microns of the circuit feed and $x_2 = P_{80}$ in microns of the circuit product.

High Pressure Grinding Rolls (HPGR)

Equation (28) for HPGR's crushers is written as:

$$W_h = S_h K_3 M_{ih}\, 4\left(x_2^{f(x_2)} - x_1^{f(x_1)}\right) \quad (35)$$

Where S_h = coarse ore harness parameter as defined by Equation 2.34 and with K_s set to 35 K_3 = 1.0 for all HPGRs operating in closed circuit with a classifying screen. If the HPGR is in open circuit, K_3 takes the value of 1.19. Also $x_1 = P_{80}$ in microns of the circuit feed; $x_2 = P_{80}$ in microns of the circuit product; M_{ih} = HPGR ore work index and is provided directly by SMC Test.

Specific Energy Correction for Size Distribution (Ws)

It should be noted that the feed and product size distributions are usually different (an assumption that was made in arriving in the above specific energy requirement) and so allowances for additional specific energy. However, for the purposes of this approach it has been assumed that the additional specific energy for ball milling is the same as the difference in specific energy between open and closed crushing to reach the nominated ball mill feed size. This assumes that a crusher would provide this energy. However, in this situation the ball mill has to supply this energy and it has a different (higher) work index than the crusher (that is, the ball mill is less energy efficient than a crusher and has to input more energy to do the same amount of size reduction). Hence from Equation (33), to crush to the ball mill circuit feed size (x_2) in open circuit requires specific energy equivalent to:

$$W_c = 1.19^* M_{ic}\, 4\left(x_2^{f(x_2)} - x_1^{f(x_1)}\right) \quad (36)$$

closed circuit crushing the specific energy is:

$$W_c = 1^* M_{ic}\, 4\left(x_2^{f(x_2)} - x_1^{f(x_1)}\right) \quad (37)$$

The difference between the two (Equation (36) and Equation (37)) has to be provided by the milling circuit with an allowance for the fact that the ball mill, with its lower energy efficiency, has to provide it and not the crusher. Thus Ws (specific energy correction for size distribution) is represented by:

$$W_s = 0.19^* M_{ia}\, 4\left(x_2^{f(x_2)} - x_1^{f(x_1)}\right) \quad (38)$$

It should be noted that in Equation (38), M_{ic} has been replaced with M_{ia}, the coarse particle tumbling mill grinding work index.

7.6 Sizes of aggregate produced by jaw crushers

Even though the setting of the discharge opening of a crusher will determine the maximum size of aggregate produced, the aggregate sizes will range from slightly greater than the crusher setting to fine dust. For any given setting for jaw or roll crushers, approximately 15% of the total amount passing through the crusher will be larger than the setting. If the opening of the screen which receives the output from such crusher are the same size as the crusher setting, 15% of the output will not pass through the screen.

Figure 9 (Assakkaf, 2003) provides the percentage of material passing or retained on screens having the size opening indicated for jaw and roll crushers. To read the chart:

a. Select the vertical line corresponding to the crusher setting
b. Then go down this line to the number which indicate the size of screen opening
c. From the size of the screen opening, proceed horizontally to the left to determine the percent of material passing through the screen or the right to determine the percentage of material retained on the screen.

Example 1 (Assakkaf, 2003)

A jaw crusher with a closed setting of 3½ in produces 60 tons per hour of crushed stone. Determine the amount of stone produced in tons per hour within the following size range: in excess of 1 in; between 1 and ½ in; between ½ and ¼ in.

It can be seen from Figure 9 that the amount retained on a 1-in screen is 71% of 60, which is 42.6 tons per hr. Also, details for each of the size range have been determined and calculations made as shown on Table 3:

Table 3: Sizes of aggregate produced by jaw crushers

Size Range (in)	% Passing Screen	%in Size Range	Crusher's Total Output (ton/hr)	Amount Produced in Size Range (ton/hr)
Over 1	100 – 29	71	60	42.6
1 – ½	29 – 17	12	60	7.2
½ – ¼	17 – 11	6	60	3.6
¼ - 0	11 – 0	11	60	6.6
Total		100%		60.0 tph

Examples 2 (Adapted from; Using The Smc Test® to Predict Comminution Circuit Performance (http://www.smctesting.com/documents/ Using_the_SMC_Test.pdf))

Calculate the overall specific energy to mill a rock in a primary crusher from a P_{80} of 110 mm to a product with a P_{80} of 116 microns for the following three circuit SAB mill crusher, SABC, HPGR/ball mill *and Conventional crushing/ball mill. SMC Test and Bond ball work index test on a similar sample has generated the following details: SMC Test:* M_{ia} *= 20.2 kWh/t,* M_{ic} *= 8.2 kWh/t,* M_{ih} *= 14.8 kWh/t Bond test carried out with a 160-micron closing screen:* M_{ib} *= 19.7 kWh/t.*

Solution

SABC Circuit

Coarse particle tumbling mill specific energy

Since it has a pebble crusher in the circuit, $k_1 = 0.95$. Also, 110mm = 110,000 microns. Combining Equations (29) and (30):

$$W_a = 0.95 * 20.2 * 4 * \left(750^{-(0.295+750 \times 10^{-6})} - 110{,}000^{-(0.295+110{,}000 \times 10^{-6})}\right)$$

= 10.14 kWh/t

Fine particle tumbling mill

specific energy

Combining Equations (29) and (31):

$$W_b = 19.7 * 4 * \left(116^{-(0.295+116 \times 10^{-6})} - 750^{-(0.295+750 \times 10^{-6})}\right)$$

= 8.27kWh/t

Pebble crusher specific energy

The assumption for this circuit is that the feed to the pebble crusher has a P_{80} of 60mm. Normally, this value is calculated by assuming that it is 0.75 of the nominal pebble port apertures which is 80mm in this case. The setting of the pebble crusher produces a product with P_{80} of

14mm. The feed rate of the pebble crusher feed rate is estimated to be 30% of new feed tph. Combining Equations (29) and (33):

Figure 9: Analysis of the size of aggregate by jaw crushers

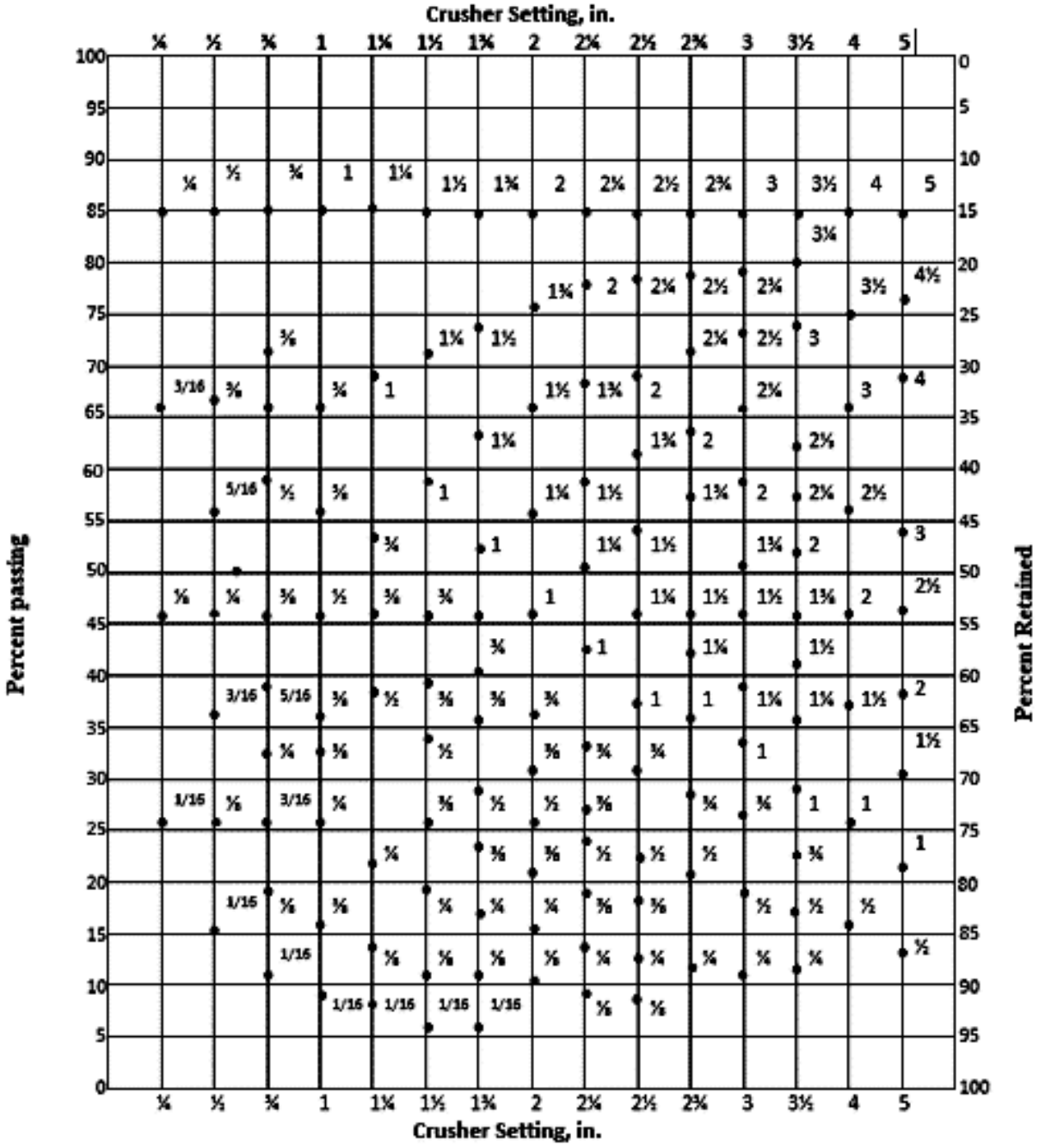

$$W_c = 1.19 * 8.2 * 4 * \left(14000^{-(0.295+14000\times10^{-6})} - 60000^{-(0.295+60000\times10^{-6})}\right)$$

= 1.26 kWh/t when expressed in terms of the crusher feed rate

= 1.26* 0.30 kWh/t when expressed in terms of the SABC circuit new feed rate

= 0.38kWh/t of SAG mill circuit new feed

Total net comminution specific energy:

W_T = 10.14+ 8.27+ 0.38 kWh/t

= 18.79kWh/t

HPGR/Ball Milling Circuit

The assumption in the circuit is that the primary crusher product is reduced to a HPGR circuit feed P_{80} of 38 mm by a closed circuit secondary crushing. The HPGR is also considered to be in the closed circuit and reduces the 38 mm feed to a circuit product P_{80} of 6 mm. after this, the product is feed to a closed circuit ball mill which takes the crushing down to a P_{80} of 116 microns.

Secondary crushing specific energy

Combining Equations (29), (33) and (34):

$$W_c = 1 * 55 * (38000 * 110000)^{-0.2} * 8.2 * 4 * \left(38000^{-(0.295+38000\times10^{-6})} - 110{,}000^{-(0.295+110{,}000\times10^{-6})}\right)$$

= 0.446kWh/t

HPGR specific energy

Combining Equations (29) and (34):

$$W_c = 1 * 35 * (6000 * 38000)^{-0.2} 14.8 * 4 * \left(6000^{-(0.295+6000\times10^{-6})} - 38000^{-(0.295+38000\times10^{-6})}\right)$$

= 1.90kWh/t

Coarse particle tumbling mill specific energy

Combining Equations (29) and (30):

$$W_a = 1 * 20.2 * 4 * \left(750^{-(0.295+750\times10^{-6})} - 6000^{-(0.295+6000\times10^{-6})}\right)$$

= 5.50kWh/t

Fine particle tumbling mill specific energy

Combining Equations (29) and (31):

$$W_b = 19.7 * 4 * \left(116^{-(0.295+116\times10^{-6})} - 750^{-(0.295+750\times10^{-6})}\right)$$

= 8.25kWh/t

Total net comminution specific energy:

W_T = 0.45+ 1.90+ 5.50+8.25 kWh/t
= 16.1 kWh/t

Conventional Crushing/Ball Milling Circuit

The assumption in this circuit is that the primary crusher product is reduced in size to P_{80} of 6.8 mm via a secondary/tertiary crushing circuit (closed) which is then fed to a closed-circuit ball mill which reduces the product to a P_{80} of 116 microns.

Secondary/tertiary crushing specific energy
Combining Equations (29) and (33):

$$W_c = 1 * 8.2 * 4 * \left(6800^{-(0.295+6800\times10^{-6})} - 110{,}000^{-(0.295+110{,}000\times10^{-6})}\right)$$
= 1.99kWh/t

Coarse particle tumbling mill specific energy

Combining Equations (29) and (30):

$$W_a = 1 * 20.2 * 4 * \left(750^{-(0.295+750\times10^{-6})} - 6800^{-(0.295+6800\times10^{-6})}\right)$$
= 5.76 kWh/t

Fine particle tumbling mill specific energy
Combining Equations (29) and (31):

$$W_b = 19.7 * 4 * \left(116^{-(0.295+116\times10^{-6})} - 750^{-(0.295+750\times10^{-6})}\right)$$
= 8.27 kWh/t

Size distribution correction

$$W_s = 0.19 * 20.2 * 4 * \left(6800^{-(0.295+6800\times10^{-6})} - 110{,}000^{-(0.295+110{,}000\times10^{-6})}\right)$$
= 0.93kWh/t

Total net comminution specific energy:

W_T = 1.99+ 5.76+ 8.27+ 0.93 kWh/t = 16.95 kWh/t

Worked Example 3: Feed Size

For a roll crusher, the diameter of the roll is directly proportional to the maximum particle diameter of the rock or ore that can be fed into it. This therefore means that very large diameter particles cannot be gripped by the rollers, and if they are too small, they simply fall through with size reduction.

For roll crusher that has an angle of nip, B, of 18.86^0, the maximum particle size that can be crushed by the roll crusher is calculated as follows:

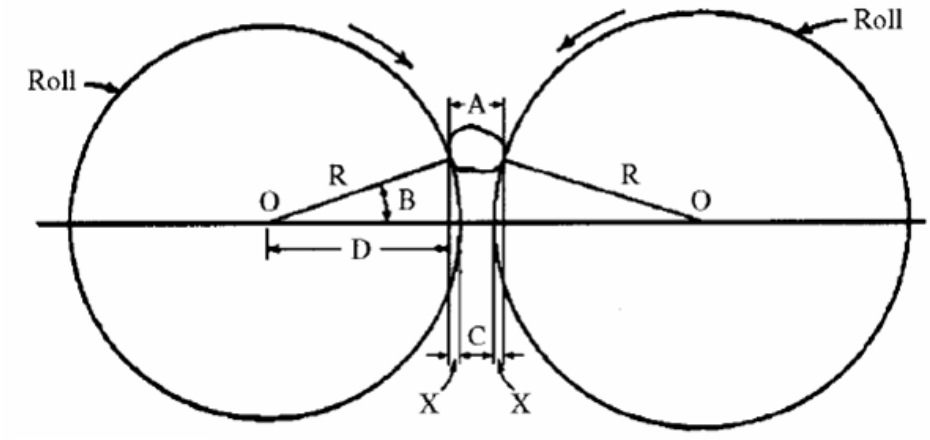

Figure 9: Crushing Rocks between two rolls

Let
R = radius of rolls
B = angle of nip
$D = R \cos B = R \cos (18.86) = 0.9463$ R
A = maximum particle size of the feed
C = roll setting which also equals the size of finished product
$X = R - D = R - 0.9463R = 0.0537R$
$A = 2X + C = 2\ (0.0537R) + C = 0.1074R + C$

∴ Maximum size Feed (A) = 0.1074R + C

Therefore, if we are to estimate the maximum particle size of rock or ore that can be crushed by a roll crusher with a roll of diameter, 80 cm, and a roll setting of 2.0 cm, then:

Maximum particle size of the feed (A) = 0.1074R + C
A = 0.1074(80) +2 = 10.59cm

8.0 Conclusion

This paper reviews the selection process as well as the theoretical performance evaluation procedures for jaw crushers. It is however important to note that Crushers encounter considerable difficulties concerning external loads acting on their mechanical joints which make it almost impracticable to use theoretical calculations for design and performance evaluation. It is therefore necessary to use experimental studies to verify any theoretical methods used for these purposes.

References

Assakkaf, I. (2003); Construction planning equipment and methods; Chapter 14, sixth edition, McGraw Hill.

Asbjörnsson, G. (2013); Modelling and Simulation of Dynamic Behaviour in Crushing Plants; Thesis for Licentiate of Engineering; Chalmers University of Technology

Andersen, J.S. and Napier-Munn, T.J. (1988); Power Prediction for Cone Crushers, 3rd Mill Operators Conference, AusIMM, Cobar, Australia

Aleksandar Sabic & Forlin Zhang (2002); Predicting Gyracone crusher performance using dynamic model (www.agg.net.com/resources/articles/).

Bearman, R.A., Barley, R.W., and Hitchcock, A. (1990); The Development of a Comminution Index for Rock and The Use of an Expert System to Assist the Engineer in Predicting Crushing Requirements, Minerals Engineering, Vol. 3, No. 1-2, pp. 117-127).

Bourgeois, F.(1993); Micro-scale Modelling of Comminution Processes. Thesis, University of Utah.

Briggs, C.A., A Fundamental Model of a Cone Crusher (1997); PhD thesis from University of Queensland: Brisbane, Australia.

Bond, F.C. (1952); The Third Theory of Comminution, Transactions of AIME/SME, Vol. 193, pp. 4884-494).

Bond, F.C. (1961); Crushing and grinding calculations, Part I-II. Br. Chem. Eng., vol. 6, 1961. pp. 378–385, pp. 543–548).

Choi, Woo-Zin (1982); Comminution and Liberation Studies of Complex Sulfide Ores, MS Thesis – Virginia Tech, Blacksburg, VA.

Csöke B., S. Petho J. Foldesi and L Meszaros (1996); Optimization Of Stone-quarry Technologies; International Journal of Mineral Processing - Vol. 44-45 - 1996 - pp. 447-459.

Donovan, James G. (2003); Fracture toughness-based models for the prediction of power consumption, product size and capacity of jaw crusher, Ph.D. thesis, U.S.A, Virginia Polytechnic Institute and state University.

Eloranta, J. (2006); Crushing and Screening Handbook, Sept 2006] [Http://www.infominerals.com/impact-crusher.html].

Egbe, E.A.P., E. Mudiare, O.K. Abubakre (2013); Determination Of The Bond's Work Index Of Baban Tsauni (Nigeria) Lead-Gold Ore; European Scientific Journal April 2013 edition Vol.9, No.12.

Evertsson, C.M. (1972); Cone Crusher Performance, in Department of Machine and Vehicle Systems. 2000, PhD thesis from Chalmers University of Technology: Gothenburg.

Garnaik, Sobhan Kumar (2009); Computer Aided Design of Jaw crusher, B.Tech Thesis, National Institute of technology, Rourkela, 2010.

Hasani, S., Dehghani, A., Khosravi, M. (2009); Determination of Work Index by abrasion mill and drop weight apparatus, 3rd Conference of Iran Mining Engineering, pp. 1786(http://www.maden.org.tr/resimler/ekler/ 3a8b724132b8e3d_ek.pdf).

Hasani, S., Dehghani, A., Khosravi, M. (2009); Breakage experiments for modeling of the AG and SAG mills; 3rd Conference of Iran Mining Engineering, pp. 1778 (http://www.maden.org.tr/resimler/ekler/ 3a8b724132b8e3d_ek.pdf).

Hersam, E.A. (1923); Factors Controlling the Capacity of Rock Crushers, Transactions AIME, Vol. 68, pp. 463-476

Hukki, R.T. (1962); Proposal for a Solomonic Settlement between the Theories of von Rittinger, Kick and Bond; AIME Transaction, 223: pp. 403-408

Jinxi Cao, Qin Zhiyu, Wang Guopeng, Rong Xingfu, Yang Shichun (2007); Investigation on Kinetic Features of Multi-Liners in Coupler Plane of Single Toggle Jaw Crusher" by, IEEE, College of Mechanical Engineering, Taiyuan University of Technology, Taiyuan.

King, R.P.(2002); Modeling and Simulation of Mineral Processing Systems, first ed. Butterworth-Heinemann Publishers, NY.

King, R.P., ed. (2001); Modelling and simulations of mineral processing systems, Butterworth-Heinemann.

Kojovic, T., Napier-Munn, T.J., and Andersen, J.S. (1997); Modeling Cone and Impact Crushers Using Laboratory Determined Energy-Breakage Functions, Comminution Practices, ch. 25, (edited by S. Komar Kawatra), SME, Littleton, CO.

Lee E. (2012); Optimization of Compressive Crushing; PhD Thesis; Department of Product and Production Development, Chalmers University of Technology, Göteborg, Sweden.

Lindqvist, M. (2008); Energy considerations in compressive and impact crushing of rock. Minerals Engineering, 21: p. 631-641.

Lowrison, G.C. (1974); Crushing and Grinding, CRC Press, Cleveland, Ohio.

Lynch, A.J., ed. (1977); Mineral Crushing and Grinding Circuits - Their Simulation, Optimisation, Design and Control. Developments in Mineral Processing. Vol. 1, Elsevier Scientific Publishing Company.

Morrell, S. (2004); An alternative energy–size relationship to that proposed by Bond for the design and optimisation of grinding circuits. International Journal of Mineral Processing, 74(1–4): p. 133-141.

Morrel, S., Napier-Munn, T.J., and Andersen, J.S. (1992); The Prediction of Power Drawfor Comminution Machines, Communition – Theory and Practice, (edited by S. Komar Kawatra), AIME, pp. 405-426.

Metso Minerals (2003); Nordberg C Series Jaw Crushers, Technical publication).

Morrell, S. (2004); An Alternative Energy-Size Relationship to that Proposed by Bond for the Design and Optimisation of Grinding Circuits; International Journal of Mineral Processing, 74, 133-141), (http://www.smctesting.com/documents/Using_the_SMC_Test.pdf)

Morrell, S. (2006); Rock Characterisation for High Pressure Grinding Rolls Circuit Design, Proc International Autogenous and Semi Autogenous Grinding Technology, Vancouver, vol IV pp 267-278.

Narayanan, S.S., Whiten W.J. (1983); Breakage characteristics of ores for ball mill modeling. Proceedings of AusIMM, 286, June, pp.31-39.

Napier-Munn, N., Morrell, S., Morrison, R.D., Kojovic, T. (1996); Mineral Comminution Circuits: Their Operation and Optimization, JKMRC, Brisbane, pp.413.

Napier-Munn, T.J., Morrell, S., Morrison, R.D., Kojovic, T. (1999); Mineral Comminution Circuits – Their Operation and Optimization, Julius Kruttschnitt Mineral Research Center, Queensland.

Pauw, O.G., Mare, M.S. (1988); The determination of optimum impact-breakage routes for an ore. Powder Technology, Vol 54, pp.3-13.

Pennsylvania Crusher Corporation (2003); Crusher Selection, Handbook of Crushing - http://penncrusher.com/1sol1_3.html.

Rimmer, H.W., Swaroop, S., Flavel, M.D., Leverance, N.C. (1986); Equipment Sizing and Process Design Procedures for Crushing and Screening Circuits, Advances in Mineral Processing, (edited by P. Somasundaran), SME/AIME, pp. 575-593.

Rusiński, E. Przemysław Moczko, Damian Pietrusiak, Grzegorz Przybyłek (2013); Experimental and Numerical Studies of Jaw Crusher Supporting Structure Fatigue Failure, Journal of Mechanical Engineering, 59(2013)9, 556-563.

Sand, G. W. and Subasinghe, G. K. N. (2004); A novel approach to evaluating breakage parameters and modeling batch grinding. Miner. Eng., 17 (11-12), 1111-16.

Sastri, S.R (1994); Capacities and Performance Characteristics of Jaw Crushers, Minerals and Metallurgical Processing, Vol. 11, No. 2, pp. 80-86.

Shrivastava Ashish Kumar, Avadesh k. Sharma; A Review on Study of Jaw Crusher (2012); International Journal of Modern Engineering Research (IJMER) www.ijmer.com Vol.2, Issue.3, May-June; pp-885-888

Soni, R.K, C. Eswaraiah and B.K. Mishra; (2013); Analysis of model parameters dependency on breakage characteristics (www.researchgate.net/.../235997803

Umucu, Y, Vedat Deniz, Nazmi Unal (2013); An Evaluation of a Modified Product Size Distribution Model Based On T-Family Curves for Three Different Crushers; Physicochem. Probl. Miner. Process. 49(2), 2013, 473−480.

Wagner, W.J. (1990); Rating Crushers by Formula, Rock Products, February, pp. 48-51.)

Walker, William H.; Lewis, Warren K.; McAdams, William H.; Gilliland, Edwin R. (1937); Principles of chemical engineering. 1937: McGraw-Hill Book Company, inc.

Weedon, D.M. (2001); A perfect mixing matrix model for ball mills. Minerals Engineering, Vol 14, No.10, pp.1225-1236.

Weiss, N.L. (1985); Jaw Crushers, SME Mineral Processing Handbook, ch. 3B-1, (edited by N.L. Weiss), SME/AIME, New York.

Whiten, W.J. (1972); The simulation of crushing plants with models developed using multiple spline regression; Journal of the South African Institute of Mining and Metallurgy, May 1972.

Wills, B.A. and Napier-Munn, T. (2005); Comminution, in Wills' Mineral Processing.

Technology (Seventh Edition), Butterworth-Heinemann: Oxford. p. 108-117.

Wolny, S. (2013); Dynamic Behaviour of a Vibrating Jaw Crusher for Disintegration of Hard Materials; Archives of metallurgy and Materials; Volume 58, Issue 3.

Nigerian Journal of Renewable Energy Research
Volume 1, Number 1, pp 39-49, 2023

Application of the Novel Proportional Nodes Curve Fitting Method to develop Correlations for the Dynamic Viscosity of Ammonia-Water Solution

S. N. Mumah[1*], H.F. Akande[1] and S. Alexander[2]
[1]Department of Chemical Engineering, Kaduna Polytechnic, Kaduna, Nigeria
[2]Department of Marketing, Kaduna Polytechnic, Kaduna, Nigeria

[*]Corresponding author: *mumahsndoyi@kadunapolytechnic.edu.ng*; Tel: *+234- 8037619719*

https://www.tetfundkadpolycoex.org.ng

ARTICLE INFORMATION

Article history:
Received 28 Jun, 2023
Revised 26 Sep, 2023
Accepted 03 Oct, 2023
Available online 30 Dec, 2023

Keywords:
Correlations
Proportional nodes
Curve fitting
dynamic viscosity
ammonia-water solution

Abstract

This study used the 'Proportional Nodes Method,' a novel curve fitting approach to correlate data for dynamic viscosity of ammonia-water solution. The approach integrates polynomial equations, generated at various temperatures, with those calculated at selected mole fraction nodes. These nodes are scaling factors that account for variations in dynamic viscosity at different temperatures at selected mole fractions. The polynomial equations provided a high degree of fitting accuracy, with R^2 values ranging from 0.999663 to 0.99985. The proportional nodes, computed systematically, were integrated into a robust and highly accurate polynomial model. This model exhibited minimal average percentage differences between predicted and actual viscosity values, indicating a high level of predictive accuracy. The Proportional Nodes Method offers a significant contribution to both academic research and industry. It provides a more precise and adaptive model for predicting the dynamic viscosity of ammonia-water solution, which is critical for optimizing and designing various industrial applications, including refrigeration systems.

1.0 Introduction

Data fitting gives the user a mathematical function that best fits to a series of data points while considering the constraints of the data. Curve fitting is a technique that is used to determine a mathematical equation that fits a given set of data points in such a way that the deviation of the points from the equation is minimized. In order to fit two or three-dimensional data, polynomial regression is used. Establishing precise data correlations is a fundamental necessity for effective design, simulation, and optimization of chemical processes. While several correlation-generating methods for data fitting exist, each brings a unique degree of complexity and accuracy.

This study introduces and evaluates the effectiveness of the 'Proportional Nodes Method,' a novel approach for curve fitting. The proportional nodes method was introduced by Mumah (2021). The method is applied to calculate dynamic viscosity of ammonia-water solution. The dynamic viscosity of ammonia-water solution is a key property necessary for design and optimization

purposes of refrigeration systems. Previous studies have employed polynomial equations to describe the viscosity of such solution based on temperature and composition (Kumar and Gardas, 2010). However, these models tend to lack adaptability to temperature changes, potentially leading to inaccuracies in predictive scenarios.

2.0 Methods

In this paper, we used data for dynamic viscosity of ammonia-water solution at various temperatures and mole fractions presented by Conde-Petit (2006) to demonstrate the effectiveness of the Proportional Nodes Method. The approach integrates polynomial equations, generated at all temperatures, with those calculated at selected mole fraction nodes. These nodes are scaling factors that account for variations in dynamic viscosity at different temperatures at selected mole fractions. These proportional nodes act as scaling factors that account for variations in dynamic viscosity at different temperatures for a selected mole fraction. This research addresses a significant gap in the literature by introducing a method that offers more precise and temperature-adaptive predictions for the dynamic viscosity of ammonia-water solution. By achieving R^2 values very close to 1 and minimal differences between predicted and actual values, this study validates the robustness and high reliability of the proposed model, presenting a significant contribution to both the academic community and relevant industries.

3.0 Results

In this study, the dynamic viscosity values of an ammonia-water solution presented by Conde-Petit (2006) were used. They are tabulated in Table 1, which clearly depict a decrease in dynamic viscosity as the temperature increases for various mole fractions. This is a common behaviour observed in fluids where an increase in temperature tends to reduce the internal resistance to flow, thereby reducing the viscosity (Lide, 2005).

Table 1. Dynamic Viscosity of Ammonia-Water Solution for various temperatures and mole fraction

T (K)	Mole fraction (-)										
	0	**0.1**	**0.2**	**0.3**	**0.4**	**0.5**	**0.6**	**0.7**	**0.8**	**0.9**	**1**
273.15	1.749E-03	2.122E-03	2.363E-03	2.301E-03	1.970E-03	1.500E-03	1.027E-03	6.492E-04	3.971E-04	2.478E-04	1.631E-04
283.15	1.328E-03	1.596E-03	1.771E-03	1.728E-03	1.490E-03	1.147E-03	7.982E-04	5.152E-04	3.233E-04	2.073E-04	1.367E-04
293.15	1.012E-03	1.201E-03	1.326E-03	1.297E-03	1.128E-03	8.811E-04	6.258E-04	4.144E-04	2.678E-04	1.769E-04	1.168E-04
303.15	7.819E-04	9.134E-04	1.002E-03	9.834E-04	8.651E-04	6.878E-04	5.004E-04	3.411E-04	2.274E-04	1.547E-04	1.023E-04

Generally, data are not depicted into 2 forms in published papers, but we have chosen to do so for a particular reason. The variation of dynamic viscosity of ammonia-water solution for various mole fractions and temperatures is shown in Figure 1.

The next step is to generate polynomial equations for each curve. There are shown in Figures 2 to 5. The polynomial equations and coefficient of determination, R^2, generated by Microsoft Excel as shown in Table 2, provided a high degree of fitting accuracy, as indicated by R^2 values very close to 1. These R^2 values range from 0.999663 to 0.99985, indicating that over 99.96% of the variation in dynamic viscosity can be explained by the variation in the mole fraction of ammonia

in the solution for a given temperature. This high degree of fit is consistent with the previous studies on the viscosity of ammonia-water mixtures (Kumar and Gardas, 2010).

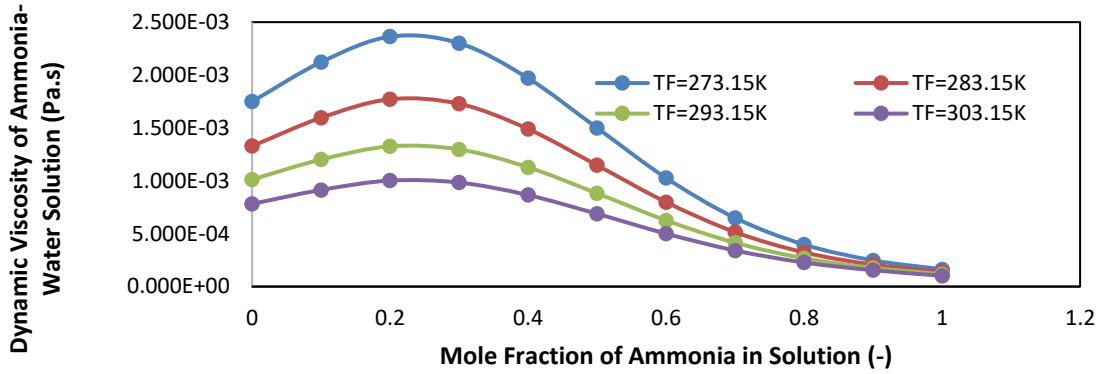

Figure 1. Variation of dynamic viscosity of ammonia-water solution for various mole fraction and temperatures

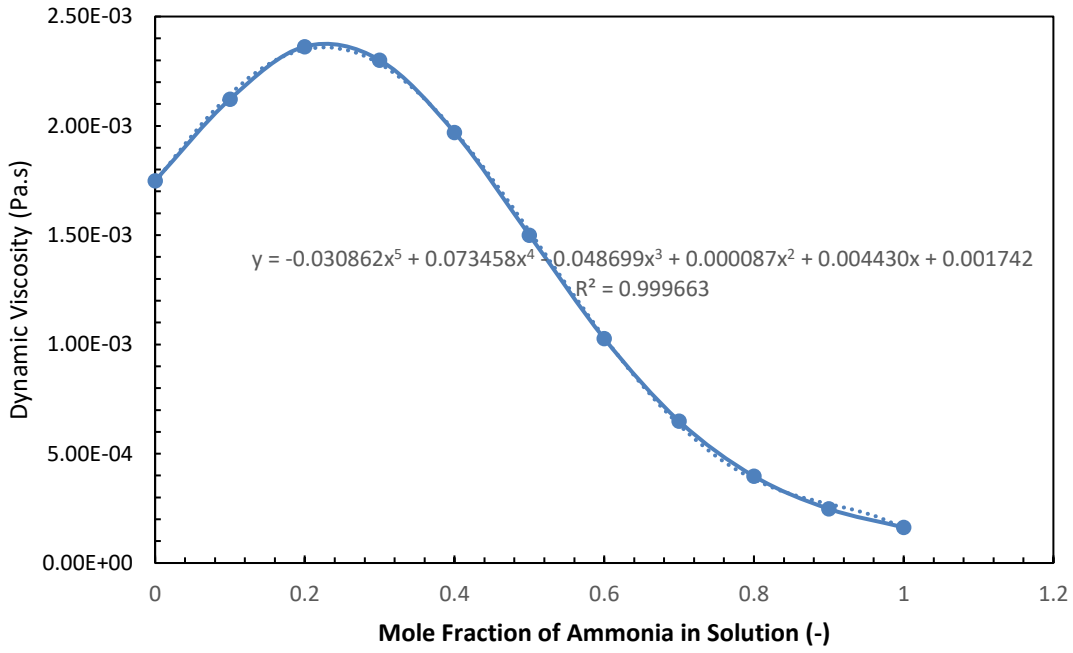

Figure 2.. Equation at T = 273.15K

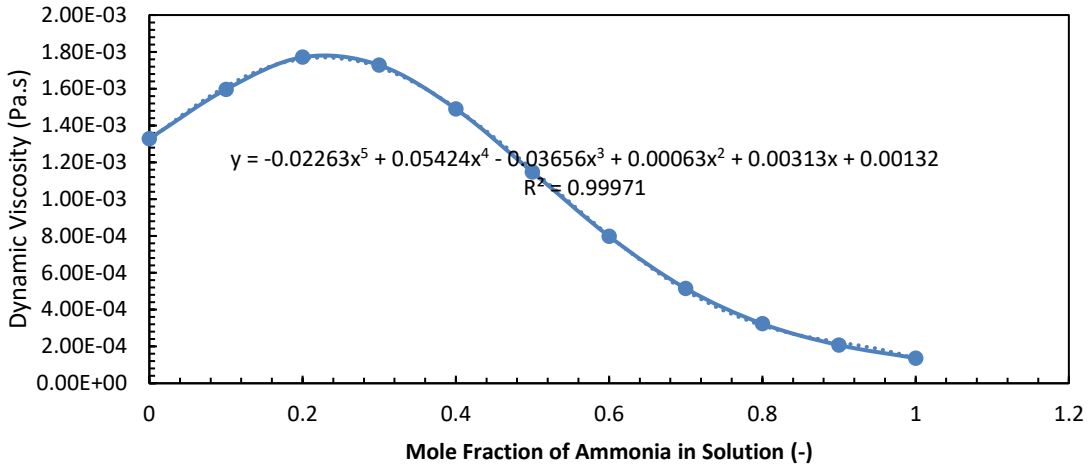

Figure 3. Equation at T = 283.15K

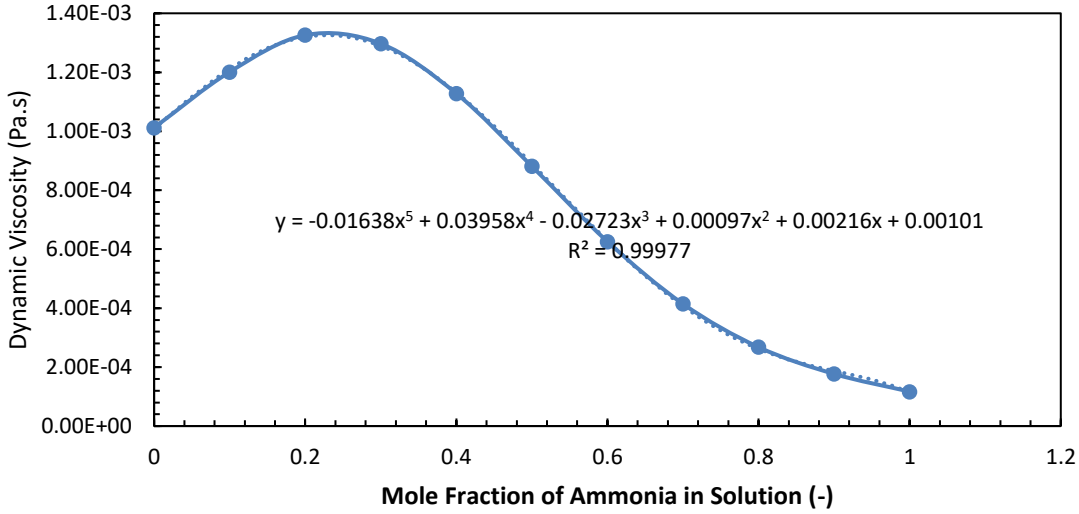

Figure 4. Equation at T = 293.15K

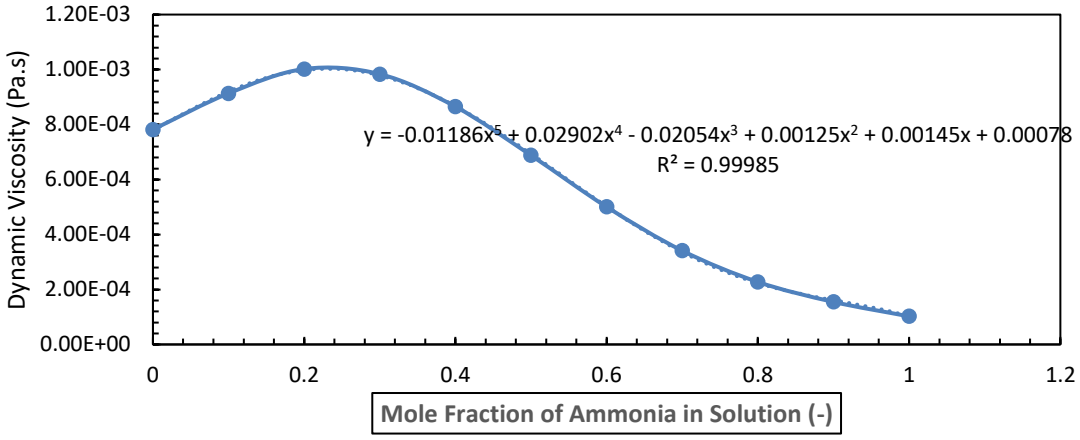

Figure 5. Equation at T = 303.15K

The equations generated for each temperature show that a fifth-order polynomial was used to fit the data. The choice of a fifth-order polynomial, as maintained across different temperatures, is guided by the R^2 values as per the analysis. It is observed that the coefficients of the polynomials change with temperature, which is a logical outcome, considering that temperature is a fundamental factor affecting viscosity.

In this study, the novel concept of 'proportional nodes' was introduced to account for variations in the dynamic viscosity of the ammonia-water solution at different temperatures. To illustrate this method, the mole fraction with the greatest difference in dynamic viscosity was considered, which, for demonstration purposes, was assumed to be at 0.2 moles. That is the reason a graphical illustration is necessary. Generally, a computer program can be generated to determine the exact mole fraction. Table 3 highlights that as temperature increases, the dynamic viscosity decreases consistently, affirming the inverse relationship between temperature and viscosity, commonly observed in fluid dynamics (Holman and Gajda, 2001).

Table 2. Equations and coefficient of determination for dynamic viscosity at each temperature

Mole Fraction of Ammonia in Solution	0	0.1	0.2	0.3	0.4	0.5	0.6	0.7	0.8	0.9	1
273.15K	1.749E-03	2.122E-03	2.363E-03	2.301 E-03	1.970 E-03	1.500 E-03	1.027 E-03	6.492 E-04	3.971 E-04	2.478 E-04	1.631 E-04
Generated Equation 1 and R^2 from Microsoft Excel	$\eta = -0.030862x^5 + 0.073458x^4 - 0.048699x^3 + 0.000087x^2 + 0.004430x + 0.001742$ $R^2 = 0.999663$										
283.15K	1.328E-03	1.596E-03	1.771E-03	1.728 E-03	1.490 E-03	1.147 E-03	7.982 E-04	5.152 E-04	3.233 E-04	2.073 E-04	1.367 E-04
Generated Equation 2 and R^2 from Microsoft Excel	$\eta = -0.02263x^5 + 0.05424x^4 - 0.03656x^3 + 0.00063x^2 + 0.00313x + 0.00132$ $R^2 = 0.99971$										
293.15K	1.012E-03	1.201E-03	1.326E-03	1.297 E-03	1.128 E-03	8.811 E-04	6.258 E-04	4.144 E-04	2.678 E-04	1.769 E-04	1.168 E-04

Generated Equation 3 and R^2 from Microsoft Excel	$\eta = -0.01638x^5 + 0.03958x^4 - 0.02723x^3 + 0.00097x^2 + 0.00216x + 0.00101$ $R^2 = 0.99977$										
303.15K	7.819E-04	9.134E-04	1.002E-03	9.834 E-04	8.651 E-04	6.878 E-04	5.004 E-04	3.411 E-04	2.274 E-04	1.547 E-04	1.023 E-04
Generated Equation 4 and R^2 from Microsoft Excel	$\eta = -0.01186x^5 + 0.02902x^4 - 0.02054x^3 + 0.00125x^2 + 0.00145x + 0.00078$ $R^2 = 0.99985$										

Table 3. Dynamic Viscosity Values of Ammonia-water Solution at 0.2 wt fraction for Various Temperatures

Temperature (K) (y Value)	Dynamic Viscosity (Pa.s) (x value)
273.15	2.363E-03
283.15	1.771E-03
293.15	1.326E-03
303.15	1.002E-03

The procedure for calculating the proportional nodes for each temperature is shown in Table 4.

The equation of the proportional nodes is gotten by applying Microsoft Excel. The details are extracted from Table 4 and is shown in Table 5.

Table 4. Procedure for calculating the proportional nodes

Temperature (K) (y value)	Dynamic viscosity (Pa.s) (X value)	Values of proportional nodes (x values)	
273.15=E	2.363E-03 =A	(A-A)/(A-D)	0.0000
283.15=F	1.771E-03 = B	(A-B)/(A-D)	4.35E-01
293.15=G	1.326E-03 = C	(A-C)/(A-D)	7.62E-01
303.15=H	1.002E-03 = D	(A-D)/A-D)	1.0000

Table 5. Proportional nodes data

Temperature (K)	Nodes
273.1500	0.0000
283.1500	4.35E-01
293.1500	7.62E-01
303.1500	1.0000

The Microsoft Excel plot of Table 5.is shown in Figure 6.

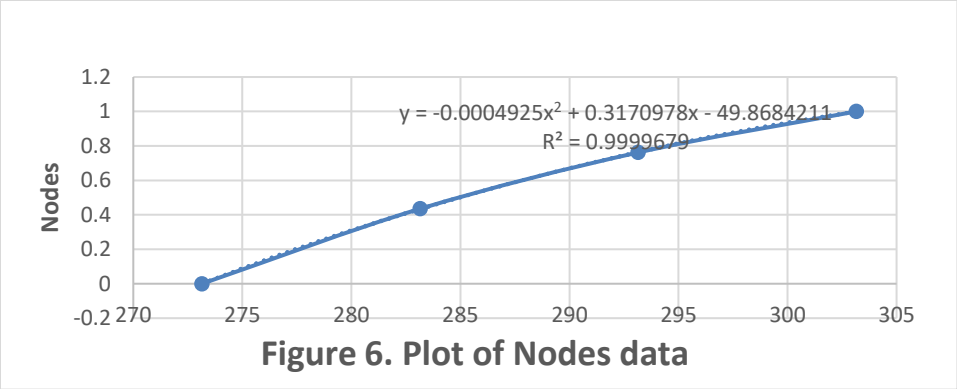

Figure 6. Plot of Nodes data

$$Nodes = -0.0004925\,T^2 + 0.3170978\,T - 49.8684211 \quad (1)$$
$$R^2 = 0.9999679$$

The proportional nodes were computed using a methodical procedure, as outlined in Table 4. These nodes were then utilized to generate a second-degree polynomial as seen in Equation (1), with an impressive R^2 value of 0.9999679. This polynomial represents how the viscosity changes as the temperature changes for a specific mole fraction, essentially acting as a scaling factor.

We have the equations of each line as shown in Table 2 and the proportional nodes equation. It must be stressed that for this method, the power of the polynomial should be maintained for each temperature. In addition, the Trendline Option (Microsoft Excel) should also be maintained for each process.

Therefore, the dynamic viscosity at any point within the temperature range is given by Equation (2).

η (Pa.s)= (Equation of enthalpy at point where nodes =0) - [(Equation of enthalpy at point where nodes =1) – (Equation of enthalpy at point where nodes =0)] x Nodes Equation* (2)

* Please note that the sign is minus and not plus because dynamic viscosity decreases as temperature increases.

The dynamic viscosity of ammonia water solution can be represented by;

$$\eta\,(Pa.s) = y = (-0.030862X^5 + 0.073458X^4 - 0.048699X^3 + 0.000087X^2 + 0.00443X + 0.001742)-((-0.030862X^5 + 0.073458X^4 - 0.048699X^3 + 0.000087X^2 + 0.00443X + 0.001742)-(-0.01186X^5 + 0.02902X^4 - 0.02054X^3 + 0.00125X^2 + 0.00145X + 0.00078))x\ Nodes \quad (3)$$

or

$$\eta\,(Pa.s)=(-0.030862X^5 + 0.073458X^4 - 0.048699X^3 + 0.000087X^2 + 0.00443X + 0.001742)-((-0.030862X^5 + 0.073458X^4 - 0.048699X^3 + 0.000087X^2 + 0.00443X + 0.001742)-(-0.01186X^5 + 0.02902X^4 - 0.02054X^3 + 0.00125X^2 + 0.00145X + 0.00078))\,(-0.0004925T^2 + 0.31709775T - 49.868421081) \quad (4)$$

Simplifying;

$-0.030862x^5 + 0.073458x^4 - 0.048699x^3 + 0.000087x^2 + 0.004430x + 0.001742$
-
There is a bracket here

$-0.030862x^5 + 0.073458x^4 - 0.048699x^3 + 0.000087x^2 + 0.004430x + 0.001742$ - $(-0.01186x^5 + 0.02902x^4 - 0.02054x^3 + 0.00125x^2 + 0.00145x + 0.00078)$	* $(-0.0004925T^2 + 0.31709775T - 49.868421081$

Subtracting first the coefficients in the bracket;

-0.030862	0.073458	-0.048699	0.000087	0.004430	0.001742
-					
-0.01186	0.02902	-0.02054	0.00125	0.00145	0.00078
=					
-0.01900	0.04444	-0.02816	-0.00116	0.00298	0.00096

Thus

$-0.030862x^5 + 0.073458x^4 - 0.048699x^3 + 0.000087x^2 + 0.004430x + 0.001742$
-
There is a bracket here

$-0.01900x^5 + 0.04444x^4 - 0.02816x^3 - 0.00116x^2 + 0.00298x + 0.00096$	* $(-0.0004925T^2 + 0.31709775T - 49.868421081)$

Or;

$$\eta\ (Pa.s) = (-0.030862x^5 + 0.073458x^4 - 0.048699x^3 + 0.000087x^2 + 0.004430x + 0.001742) - (-0.01900x^5 + 0.04444x^4 - 0.02816x^3 - 0.00116x^2 + 0.00298x + 0.00096) * (-0.0004925T^2 + 0.31709775T - 49.868421081) \quad (5)$$

To prove that this equation satisfactory represent the data, the Percentage Difference for values from correlation and actual values, $[(\eta_{actual} - \eta_{calculated})/\eta_{actual}] * 100.0)$, is calculated and from these values, the average percentage difference (Sum of Percentage Difference/Number of Points) calculated. The values are presented in Table 6.

Table 6. Percentage difference for dynamic viscosity values from correlations and actual values

Mole Fraction of ammonia in Ammonia in Solution	0	0.1	0.2	0.3	0.4	0.5	0.6	0.7	0.8	0.9	1
273.15K	1.749E-03	2.122E-03	2.363E-03	2.301E-03	1.970E-03	1.500E-03	1.027E-03	6.492E-04	3.971E-04	2.478E-04	1.631E-04
Calculated value from Proportional Nodes Method 273.15	0.001741086	0.002143045	0.002348	0.002283	0.001975	0.001517	0.001032	0.000632	0.000383	0.00027	0.000156
Percentage Difference $[(\eta_{actual} - \eta_{calculated})/\eta_{actual}]*100.0$	0.452487	-0.99175	0.634786	0.782269	-0.25381	-1.13333	-0.48685	2.649415	3.550743	-8.95884	4.353158
Generated Equation 1 and R^2 from Excel	$\eta = -0.030862x^5 + 0.073458x^4 - 0.048699x^3 + 0.000087x^2 + 0.004430x + 0.001742$ $R^2 = 0.999663$										
Mole Fraction of Ammonia in Solution	0	0.1	0.2	0.3	0.4	0.5	0.6	0.7	0.8	0.9	1
283.15K	1.328E-03	1.596E-03	1.771E-03	1.728E-03	1.490E-03	1.147E-03	7.982E-04	5.152E-04	3.233E-04	2.073E-04	1.367E-04
Calculated value from Proportional Nodes Method 283.15K	0.001326272	0.001615056	0.001766	0.00172	0.001497	0.001162	0.000803	0.000504	0.000314	0.000223	0.000132
Percentage Difference $[(\eta_{actual} - \eta_{calculated})/\eta_{actual}]*100.0$	0.13012	-1.19398	0.282326	0.462963	-0.4698	-1.30776	-0.60135	2.173913	2.876585	-7.57356	3.438186
Generated Equation 2 and R^2 from Excel	$\eta = -0.02263x^5 + 0.05424x^4 - 0.03656x^3 + 0.00063x^2 + 0.00313x + 0.00132$ $R^2 = 0.99971$										
Mole Fraction of Ammonia in Solution	0	0.1	0.2	0.3	0.4	0.5	0.6	0.7	0.8	0.9	1
293.15K	1.012E-03	1.201E-03	1.326E-03	1.297E-03	1.128E-03	8.811E-04	6.258E-04	4.144E-04	2.678E-04	1.769E-04	1.168E-04
Calculated value from Proportional Nodes Method 293.15K	0.001006214	0.001207676	0.001316	0.001286	0.001128	0.000887	0.000627	0.000406	0.000261	0.000186	0.000113
Percentage Difference $[(\eta_{actual} - \eta_{calculated})/\eta_{actual}]*100.0$	0.571739	-0.55587	0.754148	0.848111	0	-0.66962	-0.19175	2.027027	2.539208	-3135.16	3.253425
Generated Equation 3 and R^2 from Excel	$\eta = -0.01638x^5 + 0.03958x^4 - 0.02723x^3 + 0.00097x^2 + 0.00216x + 0.00101$ $R^2 = 0.99977$										
Mole Fraction of Ammonia in Solution	0	0.1	0.2	0.3	0.4	0.5	0.6	0.7	0.8	0.9	1
303.15K	7.819E-04	9.134E-04	1.002E-03	9.834E-04	8.651E-04	6.878E-04	5.004E-04	3.411E-04	2.274E-04	1.547E-04	1.023E-04
Calculated value from Proportional Nodes Method 303.15K	0.000780914	0.000920907	0.001	0.00098	0.000868	0.000694	0.000503	0.000337	0.000224	0.000161	0.0001
Percentage Difference $[(\eta_{actual} - \eta_{calculated})/\eta_{actual}]*100.0$	0.126103	-0.82187	0.199601	0.345739	-0.33522	-0.90142	-0.51958	1.201994	1.495163	-4.0724	2.248289
Generated Equation 4 and R^2 from Excel	$\eta = -0.01186x^5 + 0.02902x^4 - 0.02054x^3 + 0.00125x^2 + 0.00145x + 0.00078$ $R^2 = 0.99985$										

The average percentage difference for the surface (Sum of percentage deviation/Number of points) is calculated from values in Table 6 and presented in Table 7.

Table 7. Values of percentage deviation for various temperatures and mole fractions

	Mole Fraction										
Temp (K)	**0**	**0.1**	**0.2**	**0.3**	**0.4**	**0.5**	**0.6**	**0.7**	**0.8**	**0.9**	**1.0**
273.15	0.452487	-0.99175	0.634786	0.782269	-0.25381	-1.13333	-0.48685	2.649415	3.550743	-8.95884	4.353158
283.15	0.13012	-1.19398	0.282326	0.462963	-0.4698	-1.30776	-0.60135	2.173913	2.876585	-7.57356	3.438186
293.15	0.571739	-0.55587	0.754148	0.848111	0	-0.66962	-0.19175	2.027027	2.539208	-5.14415	3.253425
303.15	0.126103	-0.82187	0.199601	0.345739	-0.33522	-0.90142	-0.51958	1.201994	1.495163	-4.0724	2.248289
	Average percentage difference for the surface ±0.2614293										

The very low average percentage difference for the surface proves that the Equation (5) satisfactorily represents the final expression for calculating the dynamic viscosity of the ammonia-water solution at any given temperature and mole fraction for the selected temperature range

4.0 Discussion

Equation (5) satisfactorily represents the correlation for calculating the dynamic viscosity of the ammonia-water solution at any given temperature and mole fraction for the selected temperature range. It incorporates the polynomial equations at the extreme temperatures (273.15K and 303.15K), as well as the proportional nodes equation. The resulting equation is less complex and offers a robust and highly accurate model for predicting the dynamic viscosity of an ammonia-water solution under varying conditions.

The R^2 values associated with each generated equation (as shown in Table 6) are consistently very close to 1, ranging from 0.999663 to 0.99985. This is an indication of the model's exceptional ability to accurately predict the dynamic viscosity of ammonia-water solution under different conditions. These R^2 values further substantiate the validity and reliability of the derived model, reflecting its strong alignment with actual observations (Motulsky and Ransnas, 1987). The inverse relationship between temperature and viscosity, as indicated in our results, is consistent with existing literature on fluid dynamics (Bergman et al., 2011). For example, it has been previously established that an increase in temperature generally corresponds to a decrease in viscosity due to the increased kinetic energy of the molecules, resulting in a reduced internal resistance to flow (Incropera and DeWitt, 2002).

The average percentage differences between the actual and calculated dynamic viscosity values for various mole fractions and temperatures are tabulated in Table 7. These percentage differences are generally very low, affirming the strong correspondence between the model's predictions and the actual measured data. Notably, the deviations are not systematic and fluctuate around zero, indicating no apparent bias in the model's predictions.

5.0 Conclusion

This study provides a comprehensive and highly accurate model for predicting the dynamic viscosity of an ammonia-water solution under varying temperatures and mole fractions. The

innovative concept of 'proportional nodes,' introduced in this study, allows for temperature-adaptive predictions, a significant advantage over standard polynomial fitting techniques. The R^2 values, close to 1, and the minimal percentage differences between actual and calculated values at various conditions, demonstrate the model's exceptional predictive capability and reliability. Overall, this study makes a noteworthy contribution to the understanding and calculation of the correlation for dynamic viscosity of ammonia-water mixtures, promising implications for various applications where such data arrangement for mixtures exist.

Acknowledgement

The author wishes to acknowledge the funds provided for this research by the Tertiary Education Trust Fund (TETFund), Nigeria, under the Institution-Based Fund (IBR) Grants. *REF: TETF/DR&D/POLY/KAD/IBR/VOLII(2022).*

References

Bergman, T. L., Lavine, A. S., Incropera, F. P., & DeWitt, D. P. (2011). Fundamentals of Heat and Mass Transfer (7th ed.). John Wiley & Sons.

Cheng, N. S. (2008). Formula for the viscosity of a glycerol-water mixture. *Industrial & Engineering Chemistry Research*, 47(9), 3285-3288. https://doi.org/xxxxxxx

Conde-Petit, M. (2006). Thermophysical Properties of NH3/H2O Mixtures for the Industrial Design of Absorption Refrigeration Equipment. A formulation for Industrial Use. M. Conde Engineering, Zurich, Switzerland

Holman, J. P., & Gajda, W. J. (2001). Experimental Methods for Engineers (7th ed.). McGraw-Hill.

Incropera, F. P., & DeWitt, D. P. (2002). *Introduction to Heat Transfer* (4th ed.). John Wiley & Sons.

Kumar, A., & Gardas, R. L. (2010). Viscosity of aqueous ammonia solution at high pressures. *Journal of Chemical Engineering Data*, 55, 3983-3986. https://doi.org/xxxxxxx

Lide, D. R. (2005). CRC Handbook of Chemistry and Physics (86th ed.). CRC Press.

Motulsky, H., & Ransnas, L. (1987). Fitting curves to data using nonlinear regression: A practical and nonmathematical review. *FASEB Journal*, 1(5), 365-374. https://doi.org/xxxxxxx

Mumah, S.N. (2022). Introduction of a novel curve fitting approach: The use of Proportional Nodes [Unpublished Research and Innovation Report].Kaduna Polytechnic, Kaduna, Nigeria

Nigerian Journal of Renewable Energy Research
Volume 1, Number 1, pp 50-61, 2023

Safety Requirements in Blasting at Edile Rock Nigeria Ltd. Quarry, Talata Mafara, Zamfara State, Nigeria

Salawu, O.M*, Bida, A.D and Godiya, Z.M

Department of Mineral Resources Engineering, Kaduna Polytechnic, Kaduna, Nigeria
*Corresponding author: adbida@gmail.com

https://www.tetfundkadpolycoex.org.ng

ARTICLE INFORMATION

Article history:
Received 28 Jun., 2023
Revised 26 Sep., 2023
Accepted 03 Oct., 2023
Available online 20 Oct., 2023

Keywords:
Explosives Act
Explosives Regulations
Optimum Safety
Compliance and Blasting

Abstract

This study considered essentially an observation of safety considerations in blasting at Edile Rock Nigeria Limited Quarry. Field visitation was undertaken along with digital camera and questionnaires. Explosives Acts 1964 and Explosives Regulations 1967 were used in the analysis of this study to compare the level of compliance to safety rules in terms of storage, transportation, handling and use of explosives. The explosives used in the quarry for blasting includes Ammonium Nitrate and Fuel Oil (ANFO), Gelatine 90% strength, detonating cord, detonating fuse, Ohmmeter and exploder. The results from the analysis of questionnaires show that the level of compliance to the Explosives Acts and Regulations is not up to the required standard required for optimum safety in the aspect of blasting operation. Thus, it was recommended that the company should improve on standards of Explosives Acts of 1964 and Explosives Regulations of 1967 in the aspect of storage, transportation, handling and general applications of explosives at quarry sites.

1.0 Introduction

In Mining business, an improved safety record means a lot to the employees and the entire company which becomes a daily routine. Safety considerations in blasting entail all safety measures that must be observed so as to be able to have successful operations with little or no casualty. In the aspect of blasting, some safety apparel such as safety boots, helmet, hand glove, nose mask as well as explosive needed for the operation must be properly taken into consideration. Blasting is also a process of fracturing rock materials by use of calculated amount of explosives, which on initiation, either by light or shock, will break the pre-determined volume of rock at high temperature and pressure. Accidents do occur due to unsafe blasting practice and unsafe use of explosives and the siting of mines close to settlements constitutes risk to residents in terms of ground vibrations and fly rocks. Therefore, the need for safety considerations in blasting becomes necessary.

This study focused on safety consideration in blasting operations at Edile Rock Quarry. It specifically investigated safety practices in blasting at the quarry; process involved in safe blasting operations considering depth and diameter of holes, type of explosives and proximity of settlement

and recommended effective safety measures to attain level of compliance to Nigeria Mining Safety Regulations.

2.0 Location and Accessibility of the Study Areas

Zamfara State is a state in North – Western Nigeria region; study area lies between longitudes 12º22/ N and12^{0}55.5/N and latitudes 6º13/E and 6^{0}40.9/E. The area of study is found in western part of Zamfara state, it's located at Fangaltama, Talat Mafara Local Government Area of Zamfara state which is about 64km from the state capital. The project area covers Fangaltama, Mayanchi, kukan Mairai which are few kilometers away from area of study as shown in Figure1.

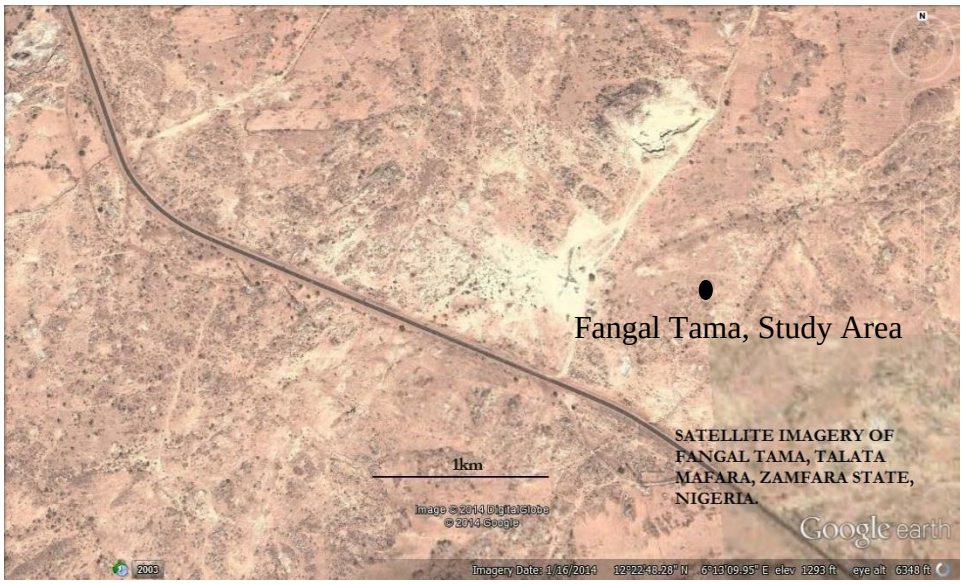

Figure 1: Satellite Imagery of the Study Area (*Source*: Google Earth, 2014)

3.0 Theory of Drilling and Blasting

Simon (1950) has presented a theory of drilling to include effect of drilling by percussion and vibration with rotary bits, cable tool and pneumatic hammer. The formula developed is for rate of penetration of chisel shaped bit into brittle rock. The rate of drilling may be defined by the following equation:

$$R = \frac{NAF}{D} \qquad (1)$$

where,
R = rate of bit penetration
N = number of wings of bits;
F = number of impact per units time
A = area of the bit, and;
D = diameter of the bit.

Drilling is the boring of cylindrical holes into a rock mass either inclined, vertical or horizontally and of a suitable diameter for insertion of explosive to fragment rock. This is always done when the overburden proves to be very hard for bulldozers to rip off (Eugene, 1968). On the other hand, blasting entails the constructive use of calculated amount of explosives for the breakage splitting

or loosing of massive overburden ore bodies to fragments of sizes. Here, the operation consists of charging and loading, stemming and initiation. Holes drilled at certain depths as determined by length of drill rode (9 or 11 metres).

Drilling patterns is manifested when the drill holes is being arranged within the limits of the blasted block in a single or a multi row pattern which could be in square, rectangular or staggered pattern. Both the staggered and square patterns are shown in Figure 2. The square pattern has equal burden and spacing behind the other row of holes. The staggered pattern has equal burden and spacing of 1.5m though this depends on the climate and season of blasting the holes less spacing and burden leads to high fragmentation of rocks because of high effectiveness of the explosive. The application of any of the pattern depends on the mineral to be mined, physical characteristics of the rock, type of product required, the geological characteristics of the deposits and also management policy from the economic point of view.

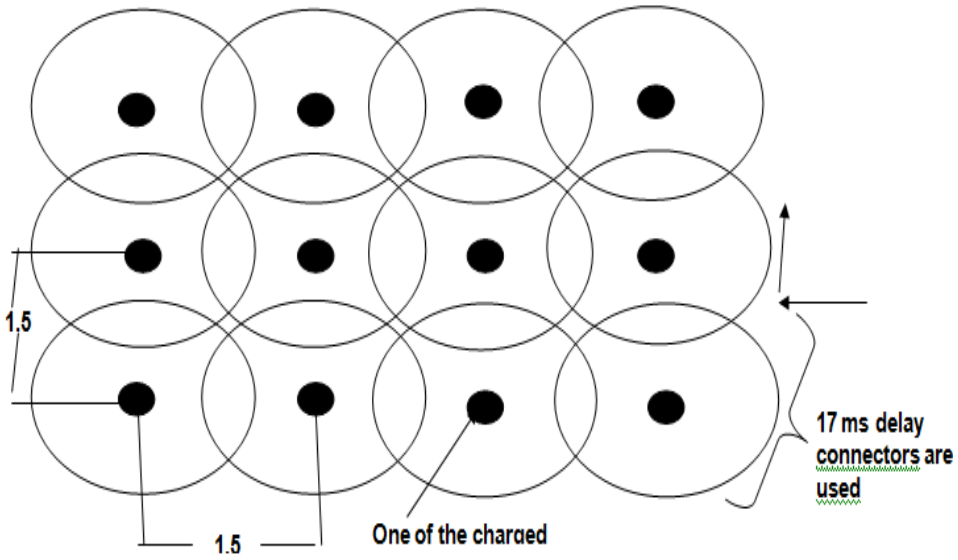

Figure 2: Showing Square Pattern of Drilling

3.1 Drilling Methods

Several methods of drilling are applicable and these include percussion, rotary, percussion-rotary and rotary-percussion drilling.

3.2 Blasting Methods

3.2.1 Pre-Splitting Blasting

Involves blasting certain area before drilling the rest of the boreholes for blasting pattern workers drill a row of holes at three sides of the main blasting block and charged them with fewer explosive then the main, production blast. This creates a fracture line on the desired break line thereby exposes the half barrel of the blast hole after excavation. Presplitting is rare in underground works than surface.

3.2.2 Cushion Blasting

This method of blasting is when workers must train excess materials from the final high walls. The holes are drilled in a single row along the excavation line. Holes are usually between two to four centimetres (12 – 4 cm) in diameter. Blast holes have small well–distributed charges and completely stemmed. Workers perform cushion blasting after the main blast has been excavated. By firing cushion holes with minimum or no delay between the blasts, the detonation shears the work web between holes and produces smooth wall with minimal over break.

3.2.3 Smooth Blasting

Blasters mainly used smooth (perimeter or contours) blasting underground. An ideal blast causes minimum damage to the host rock. They drill hole in a roof of tunnels and headings, parallel to the direction of the excavation and space them closely, loading them with decoupled charges which are fired simultaneously.

4.0 Blasting Equipment and Accessories

Explosives are substances (compound or mixture of compounds) which undergo a rapid chemical change when shocked or heated. They produce gases in large quantity and set up light pressure in the modern commercial explosive (Anon, 2014).

4.1 High Explosives

High explosives have high density and usually consist of oxidizing salts, fats and sensitizers dissolved or dispersed in a continuous liquid phase the active system is thickened and could be made H_2O resistant by the addition of gallant and cross lolling agents. Sensitization may be provided by chemical sensitization such as the nitrate salt of organic amines, nitrate esters of alcohol, percolate silt or small particles of aluminium. High explosives have velocity of detonation (V.O.D) from 1500 – 7500m/s depending on how they are initiated and their compound. The gases produced are large in quantities and causes high pressure to be set in the rock e.g., Trinitrotoluene (TNT), Nitroglycerine Dynamite etc. This category usually contains chemical component with a more or less unstable molecular structure capable of detonation of molecular arrangement into more stable forms; the reaction is supersonic and generates high pressure shock wave accompanied by rapid expansion of the reactive production. High explosives reaction is needed for better blasting of rocks (Obafemi, 2006).

4.2 Low Explosives Ammonium Nitrate and Fuel Oil (ANFO)

These are, however, low intensity compared to high explosives. The explosive case usually pentaerythritol tetra nitrate (PETN) is covered with water proofing materials and plastic so as to protect frond damage cause by physical abuse or exposure to external temperature, water, oil and other foreign elements. The cord is relatively insensitive and requires proper detonation for initiation. Despite the low sensitivity, PETN detonate at velocity of about 6700m/s over about 5km/second. It has a food tensile strength and easy to handle and connect, low explosive do not burn with intense shock, it can be lighted by a fuse head used when rocks are not hard. Examples of low explosive are ANFO (ammonium Nitrate and Fuel Oil is ratio 94) and 6% respectively, gum powder, black powder (pulverized potassium or sodium nitrate, sulphur and charcoal mixture) etc.

5.0 Explosives Acts

5.1 Explosives Act 1964 and Explosives Regulation 1967

Section 34 subsection (1)a of the Explosive Act 1964 and Regulations 1967 recommends that:

> *"Explosives are expected to be stored in a magazine which should be surrounded by an adequate fence of pattern approved by the licensing officer through which access shall be obtained by means of a gate which when not in use, be kept securely locked".*

Section 22 subsection (2), requests the outer gates of every magazine as well as the door to be marked in the manner prescribed by the regulations and license number are likewise painted.

Every magazine licensed for the storage of two thousand pounds (907.18kg) of explosive and over shall comprise at least two compartments, namely, a lobby communicating directly for receipt and issuance of explosives and a storage room through which access could be gain from the lobby and must be 100 meters apart from each other. The door of the lobby should be wooden protected by light fire-proof sheet on the other side to overlap the sill, a reliable maximum and minimum thermometer should be kept in storage room of every magazine, pairs of shoes for entering into the magazine kept in the lobby, screws, locks, nails, keys and other metals fastening used are expected to brass or copper. Subjected to the regulations, the materials in use for construction of magazine should be non-inflammable nature as the case may be.

The Explosive Regulation Act Section 35 Subsection (1) states that

> *"Every magazine has to be protected by all sides by a sand or earth bank as high as the roof eaves and at least three feet in thickness at the top and at the bottom of the inner slope should be less than three feet or more than six feet from the walls except at the entrance which should be either in broken line or be protected by a an outer earth wall. Fence as required by the Regulations Act, Section 34 Subsection (1) shall not be more than three feet and magazines fitted with reliable lightning conductor (thunder arrestor) supported on a vertical post four feet from the nearest part of the magazine building, foundation should be such as to render the magazine proof against termites, the walls consisting of concrete blocks, burnt bricks, stone or sand Crete blocks. Ventilation channels should be constructed in the gables side and walls and when required in the roof."*

5.2 Use of Explosives

The Explosive Acts and Regulations in Section 44 - (1) states that

> *"it will be an offence under these regulations for any person other than the holder of a blasting certificate issued under these regulations or under the Safe Mining Regulations 2011, to prepare or fire any charges, charge any hole with explosive or conduct any blasting operations."*

Under section 46 - (1), it states,

> *"All drilled holes should be thoroughly cleaned before being charged, explosives of all kinds shall be used only in the form of cartridges or as supplied by the manufacturer or as may be approved by an inspector save that ammonium nitrate blasting powder, ammonia and explosives similar thereto may be used loose in surface works."*

In Section 46 – (3), when blasting with explosives requiring use of detonators, the fuse with the attached detonator may only be inserted in the primer cartridge immediately before use. In making up a charge, a hole shall be made in the primer cartridge with a picker made of non-ferrous material and the fuse with detonator attached shall after being inserted in the primer cartridge, be securely fastened thereto by means of a string or other suitable material so that the fuse with detonator cannot be inadvertently withdrawn, the detonator shall be fastened on the fuse by properly designed crimping pliers.

6.0 Data Description

A well-structured questionnaire was adopted in gathering of data at the study area. It was designed to test effectiveness on how blasting operations was handled, the performance and statistics of handling this performance. Group interview was also conducted to aid in acquiring more information.

7.0 Data Presentation and Analysis

Based on the aspect of storage of explosives, transportation and handling, and the use of explosives, the information and data obtained during the course of assessing the Safety Considerations in Blasting at Edile Rock Nigeria Limited Quarry, Zamfara State. Fifteen sets of questionnaires were designed and administered to the study area for data and information gathering. Same numbers of copies were retrieved back after obtaining the results. The percentage gender distribution of quarry workers, the questionnaire distributed shows 93.3% are male while 6.7% are female, there was no percentage record of death at the company but there was prevalence of accident recorded up to 80% of respondents which was caused by uncaring attitude towards safety practice. Accident cases were reported to the mines officer which carries 80% of respondents and in terms of safety awareness, mode of safety in transportation and handling of explosives as well as the company Explosives magazines is really not up to the standard as required by the Explosives Act 1964 and 1967.Lastly during observing blasting at the site, the rate of safety in the use of explosives 80% of the respondents fair which indicates that proper safety practice is not observed and stand to have some lapses which needs to be corrected (Figure 3).

8.0 Storage of Explosives

Regarding the safety consciousness at the project site, we observed that their method of storage of explosives is not up to the standard recommended by the Explosive Act 1964 and Regulations 1967 as shown in Figure4. That is to say, there are two magazines, the low explosive magazines where they store the ANFO and Electric fuse which is contained in a box in the lobby and are demarcated in a trailer mounted magazine (container) and its wooden lined. Also, the high explosive magazine which contains the Gelatin super power 90 and other accessories as the cortex etc. are also kept in a reinforced concrete building which is just about 15 feet (9.32m) apart from each other which is not up to standard.

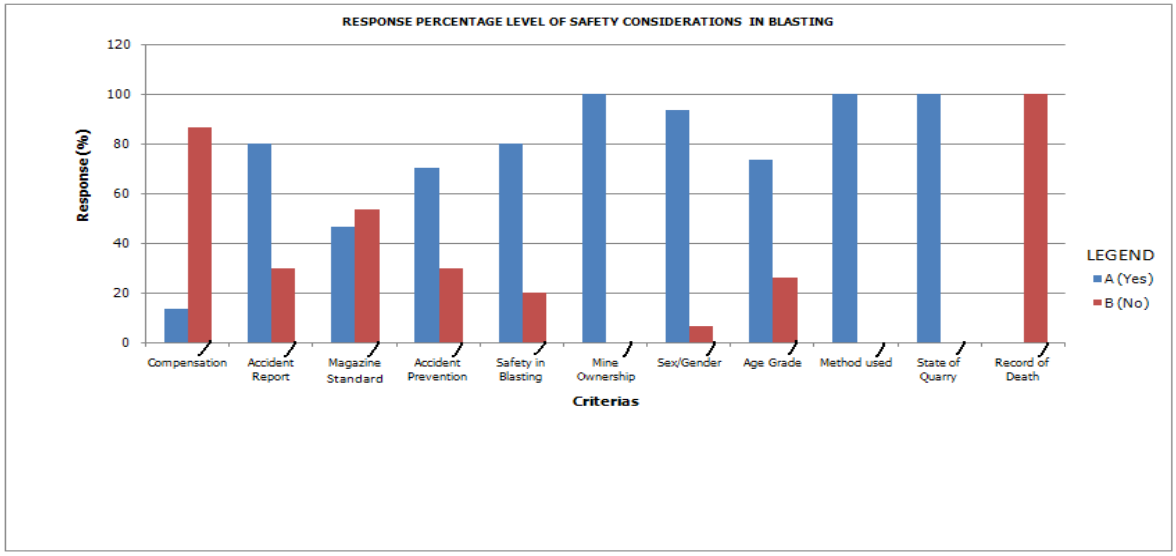

Figure 3: Bar Chart of Responses from Questionnaires

Other facilities that a standard magazine need to have as been approved by the Act are not in place like the drainage, embankment, danger sign, thermometer, thunder arrestor, etc.

Figure 4: Explosive Magazines

9.0 Handling and Transportation of Explosives

Explosives at sites are conveyed in a wooden lined truck for safety reasons which need to be observed and not any kind of vehicle as prescribed in explosives act and regulations of 1964 and 1967. But at the site, their mode of transporting explosives is by using a pay loader (FEL) to convey both the high and low explosives to quarry face during blasting as shown in Figure 5 which is about 1 kilometre away and could be dangerous due to ignition which is likely to occur in the process of transportation and therefore caution need to be taken for safety reasons.

Figure 5: A Pay Loader Conveying Explosives

10.0 Blasting

Two methods of blasting are practised in Edile Rock Nig.Ltd- primary and secondary. Primary blasting is carried out with the aim of loosening rocks in order that it may be excavated or removed from its host or existing position. Electric method of blasting is practised using the exploder to do the initiation. Holes to be blasted are drilled at certain depth of 9 metre and number of holes is between 60 and 70 for particular blasting. Explosive are properly primed, and lowered to the bottom ensuring it reached the bottom depth of the hole, another high explosive is dropped to touch the primer. Ammonium nitrate and fuel oil (ANFO) is then added to the high explosive (gelatine super power 90) to about half the depth of hole (4.5m) another high explosive is split into two and one half dropped into the hole and ANFO added to cover it at certain intervals the other half in then splitted into two and dropped at intervals at about one metre to the surface, stemming is done using the chippings from drilled holes. For a particular hole the blaster uses 3 gels of Galantine and almost a bag of Ammonium Nitrate and fuel oil (ANFO) to do the charging distance of one meter to the surface is used for stemming for an effective blasting and to avoid too much vibration and flying rock which could be disastrous, finally, ohms meter is used to test resistivity of holes to ensure proper connection is done to observe a safe blasting practice at the site. And balance of materials (explosive) used after blasting are taken back to the magazine for record purpose (Figures 6 and 7).

Figure 6: Charging of Holes for Primary Blasting

Figure 7: Priming of Holes for Primary Blasting

Secondary Blasting is method is used to reduce boulders that are too large for the primary crusher after primary blasting. At EDILE Rock , Secondary blasting is done to break the oversize boulders using the hand held drill (Jack hammer) to bore hole and charged with ANFO (Ammonium Nitrate and fuel oil), detonating cord and properly stemmed or use of the impact hammer(Rock breaker) to be able to break rock to required size suitable for the crushing plant (Figure 8).

Figure 8: Handheld Drill (Jackhammer) Machine for Secondary Blasting

Figure 9: Rock Breaker attached to Power Excavator

At site they, they either use a jackhammer or impact hammer (rock breaker) to break the holes into required fragments to fit in the crushing plants which is being shown Figure 9.

Safety Considerations: After initiation and charging is done confirming to be properly connected, labourers were assigned to go to the various corners with red flags alerting people by shouting to leave the vicinity of the blasting area because they are yet to have a siren for alarm. By so doing, they ensure nobody remains anywhere around the vicinity, the blaster then make enquiring by making phone call to be sure everywhere is clear and safe for blasting, he then do the initiation to ensure total and absolute safety of lives and properties.

11.0 Conclusions and Recommendations

The Safety Consideration in Blasting at Edile Rock Nig. Ltd was assessed and analysed. It was discovered that the company practiced safe blasting method as can be seen from the records and performance. However, some aspects of explosives handling and transportation and type of explosives required for required fragmentations produced need to be further appraised. This will even reduce some unnecessary expenses and eventually improve profit margin.

This study leads to the following recommendations:

i) There is need to improve method of transporting explosives which should be wooden lined truck and not the pay loader ass presently being used.
ii) A four-wheel drive vehicle to be used to monitor people in the vicinity before any blasting takes place.
iii) Use of Siren for alerting people around whenever blasting is to take place.
iv) Charging methods should be appraised to attain optimal fragmentation, which will reduce secondary blasting and downtime.

References

Anon (2014). "Definition of Explosives." (www.thefreedictionary.com/explosive, accessed 28/04/2014).

Nigerian Explosive Act (1964) and Explosive Regulations (1967), published by Ministry of Mines and Steel Development PP 44-45. Pp 4-6; 8-16.

Nigerian Minerals and Mining Act (2007), published by Ministry of Mines and Steel Development PP 44-45.

Nigerian Minerals and Mining Regulations, (2011), published pp 23-27.

Obafemi O. (2006), Mechanics of Rocks Fragmentations, Department of Mineral Resources Engineering, HND Project Page 13-17, pp 22-27. Unpublished

Simon, H.A (1950) the effect of atomic power on national or regional economics. In S.H Schurr And J.Marschak (Eds) Economics Aspect Of Atomic Power (Chapter 13) University Press.

Nigerian Journal of Renewable Energy Research
Volume 1, Number 1, pp 62-68, 2023

Characterisation of Mica from Bukkuyum Area of Zamfara State, Nigeria

Abubakar G. Salisu*[1], Hadiza A. Isa[1], Hamisu Adamu[1] and Zalihatu M. Idris[2]

[1]Department of Applied Science, Kaduna Polytechnic, Kaduna, Nigeria.
[2]Department of Science Laboratory Technology, Abdu Gusau Polytechnic, Zamfara State, Nigeria.
*Corresponding author: abasal012@gmail.com

https://www.tetfundkadpolycoex.org.ng

ARTICLE INFORMATION

Article history:
Received 28 Jun., 2023
Revised 26 Sep., 2023
Accepted 03 Oct., 2023
Available online 20 Oct., 2023

Keywords:
Evaluation
Mica
XRD
XRF
SEM

Abstract

The term mica is a generic term that applies to a group of aluminosilicate minerals that possess a sheet-like structure. The most common commercial micas are Muscovite is a potassium-based mica, usually colorless to pale green, others include Phlogopite, Lepidolite, Zinnwaldite, Biotite and Roscoelite. Muscovite mica enjoys the most diverse market applications. Muscovite and phlogopite possess unique characteristics and are highly valued because of their physical, chemical, electrical, thermal, and mechanical properties. These properties include high dielectric strength, low coefficients of expansion, cold and heat resistance, and high tensile strength, making these minerals excellent raw materials for electrical insulators, reinforcing materials, and high-temperature applications. As with all industrial minerals, several factors determine the test program implemented in any evaluation project. The material to be tested could be from new, unexploited deposit or from existing. This paper is aimed at evaluating Mica from Bukkuyum local government area of Zamfara state of Nigeria, using Empyrean diffractometer DY 674 (2010) for XRD phase analysis of the powdered sample. The peaks generated matched those of a muscovite in ICDD PDF 2 (2010) database. Minipal 4 energy dispersive X-ray Fluorescence (XRF) provided the elemental analysis in their oxides with 48.7% SiO_2, 33.3% Al_2O_3, 10.2% K_2O,1.04% Fe_2O_3 as major composition with loss on ignition (LOI) of 0.79% and SEM provided the photomicrograph picture with the fiber histogram giving the particle size statistics of 959.92nm, 4.22µm and 11.23µm, with the objective of giving adequate information for any of it numerous industrial applications.

1.0 Introduction

The term mica is derived from the Latin micare, meaning to shine or glitter. Today, it is a generic term that applies to a group of aluminosilicate minerals that possess a sheet-like structure. Mica is a mineral that has a rich history of industrial applications, over the centuries, mica uses have evolved from decorative ornaments, mirrors, stove windows, and shock-resistant materials in early

military applications to its more high-tech applications today in construction materials, paper, plastics, paints, electronics, and others (John and James, 2006; Bailey, 1984),.

The most common commercial micas are Muscovite: a potassium-based mica, usually colorless to pale green. Phlogopite: a magnesium-based mica that is yellow to dark brown. Lepidolite: a lithium-based mica with a purplish hue. Other micas with less commercial value include Zinnwaldite: a lithium/iron-based mica that is gray to brown; Biotite: a magnesium/iron-based black mica; and Roscoelite: vanadium/potassium/ magnesium mica that can be green or brown, Muscovite mica enjoys the most diverse market applications, followed by phlogopite and veimiculite (Harben, 2002). Muscovite and phlogopite possess unique characteristics and are highly valued because of their physical, chemical, electrical, thermal, and mechanical properties. These properties include high dielectric strength, low coefficients of expansion, cold and heat resistance, and high tensile strength, making these minerals excellent raw materials for electrical insulators, reinforcing materials, and high-temperature applications (Hendrick, 2002).

Elemental substitution takes place within the various micas quite readily. The mica group includes the more common and most widely used mica species such as muscovite, paragonitc. and phlo-sopite. Other micas in this group are biotite and lepidolite. Muscovite and paragonite (both are commonly referred to as muscovite) enjoy the most industrial uses and subsequent exploitation. Muscovite is the most common of all the micas, having a chemical formula $KAl_2(OH)_2(AISi_3O_{10})$ with a theoretical composition of 11.8% K_2O, 45.2% SiO_2. 38.5% Al_2O_3 and 4.5% H_2O. Paragonite is similar in composition, with the potassium replaced by sodium (Sinkankas, 1964; Skillen, 1992).

As with all industrial minerals, several factors determine the test program implemented in any evaluation project. The material to be tested could be from new, unexploited deposit or from existing. This paper is aimed at evaluating Mica from Bukkuyum local government area of Zamfara state of Nigeria, using Empyrean diffractometer DY 674 (2010) for XRD phase analysis of the powdered sample. The peaks generated match those of a muscovite in ICDD PDF 2 (2010) database. Minipal 4 energy dispersive X-ray Fluorescence (XRF) provided the elemental analysis in their oxides, and SEM provided the photomicrograph picture with the fiber histogram giving the statistics of particle size, with the objective of giving adequate information for any of it numerous industrial applications.

2.0 Experimental Procedure

2.1 Materials and Methods

The sample of Mica sheets was collected from Bukkuyum local government area, Zamfara state of Nigeria. Using, Empyrean diffractometer DY 674 (2010) for (XRD) phase composition analysis, Minipal 4 energy dispersive X-ray Fluorescence for (XRF) elemental analysis and PhenomProX Scanning Element Microscope (SEM) for micrograph morphological picture of the Mica sample.

2.2 XRD Analysis of the Sample

The sample was finely ground, homogenized, and sieved to pass through the 75 microns. A representative portion of the powdered sample was then prepared using the sample preparation block and compressed in the flat sample holder to create a flat, smooth surface that was later

mounted on the sample stage in the XRD cabinet.

The samples were analyzed using the reflection-transmission spinner stage using the Theta-Theta settings. Two-Theta starting position is 0.00483 and ends at 75,000 with a two-theta step of 0.026 at 3.57 seconds per step. Tube current was 40mA and the tension was 45VA. Fixed Divergent Slit size of 1° is used and the goniometer radius was 240mm. The intensity of diffracted X-rays is continuously recorded as the sample and detector rotate through their respective angles. A peak intensity occurs when the mineral contains lattice planes with d-spacings appropriate to diffract X-rays at that value of θ, although each peak consists of two separate reflections ($K_{\alpha 1}$and $K_{\alpha 2}$), at small values of 2θ the peak locations overlap with $K_{\alpha 2}$ appearing as a hump on the side of $K_{\alpha 1}$, Greater separation occurs at higher values of θ. Typically these combined peaks are treated as one. The 2λ position of the diffraction peak is typically measured as the center of the peak at 80% peak height.

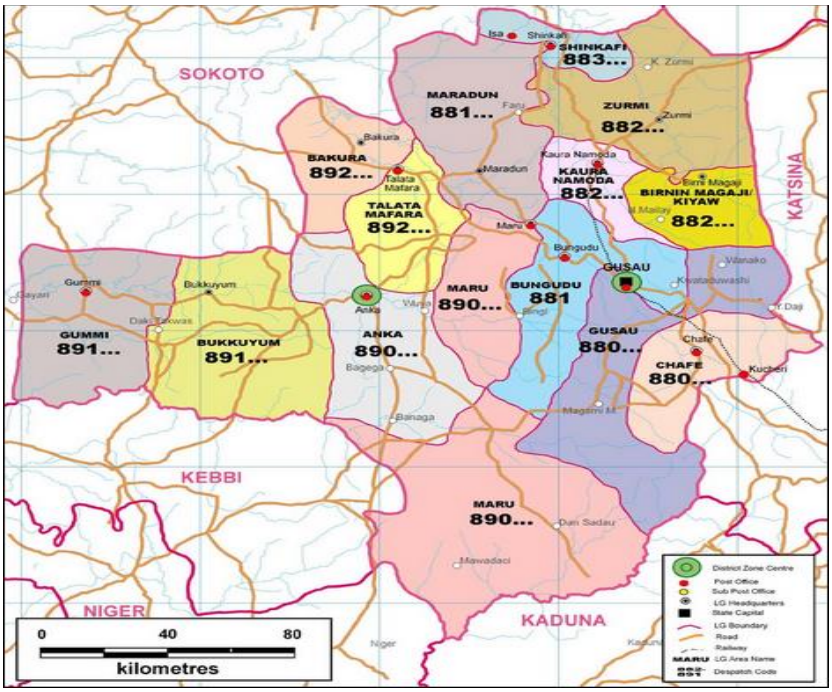

Figure 1: Map of Zamfara state showing fourteen local government areas, with Bukkkuyum local government area where the barite found second from left.

Results are presented as peak positions at 2θ and X-ray counts (intensity) in the form of a table, and x-y plot. Intensity (*I*) is reported as peak height intensity. That is intensity above background, or as integrated intensity, the area under the peak. The relative intensity is recorded as the ratio of the peak intensity to that of the most intense peak (*relative intensity = I/I_1 x 100*).

The d-spacing of each peak is then obtained by solution of the Bragg equation for the appropriate value of λ. Once all d-spacing have been determined, automated search/match routines compared the unknown to those of known materials. Because each mineral has a unique set of d-spacing, matching these d-spacings provides an identification of the unknown sample. A systematic procedure was used by ordering the d-spacings in terms of their intensity beginning with the most

intense peak. Files of d-spacings for hundreds of thousands of inorganic compounds are liable from the International Centre for Diffraction Data as the Powder Diffraction File (PDF). The peaks obtained from the analyses were matched with the minerals from ICDD database which was attached to the software of the machine.

2.3 XRF Analysis of the Sample

Solid sample pellet of l0g was placed in the special "dekat" plastic cup sample holders. The sample was then loaded on the sample changer and the position was noted. Beads used for the major oxide analysis which are SiO_2, AI_2O_3, Fe_2O_3, MgO, TiO, MgO, CaO, K_2O and P_2O_5 expressed in weight percent were precast. l.0g of pulverized sample was weighed and mixed exactly with 5times of X-Ray flux (66.0% lithium Tetraborate, 34.0% Lithium Metaborate). This weighed mixture was mixed properly in a Platinum crucible and ignited in a pre-set furnace at 1150°C for 10 minutes. Immediately the weighed mixture in the crucible was placed on the crucible holder, the preparation process commenced as the start button was pressed on. It was heated, mixed and automatically cast into a dish (mold). During this process a releasing agent was added (ammonium iodide tablet). Upon completion of cooling the cold glass bead was unloaded ready for analysis. The glass bead was labeled and slotted into the Minipal 4 energy dispersive XRF for major oxide analysis. For XRF Trace elemental analysis, the pellets were prepared by weighing l.0g of oven dried pulverized sample and 5.0g flux (cellulose powder) added as a binder. This is mixed thoroughly with glass rod in a bowl. The well mixed was then compressed by applying a pressure of 1500kgm using manual compressor. The steps carried out for measurements were; Loading the sample, and opening the measure window for the required application i.e.**:**

- Selected measure application from the menu bar
- clicked on the required application to select it
- Clicked on the "sample identity" file to insert the 'text cursor.
- Typed a name for the sample to be measured.
- clicked on the position of the sample in the "select changer position" to measure

2.4 SEM of the Sample

The Solid samples pellet was prepared for scanning electron microscopy by crushing and grinding, to acquire such images on the morphology and surface features of the samples at micrometer scales. The SEM has an electron optical column in which a finely focused high intensity electron beam was scanned over a specified area of the specimen small particles mounted on a stub, the impact of the electron beam on the surface of a solid sample causes various types of radiation signals that were recorded by detector above the specimen.

3.0 Results and Discussion

3.1 XRD Phase analysis

From Figure 2 show the XRD peaks of the crude Mica powder, which indicates peaks corresponding to muscovite pattern with reference code 01-070-1869 on ICSD card.

3.2 XRF Elemental analysis

From table 1 the elemental composition mica from bukkuyum local government area of Zamfara state, Nigeria are presented in their oxides.

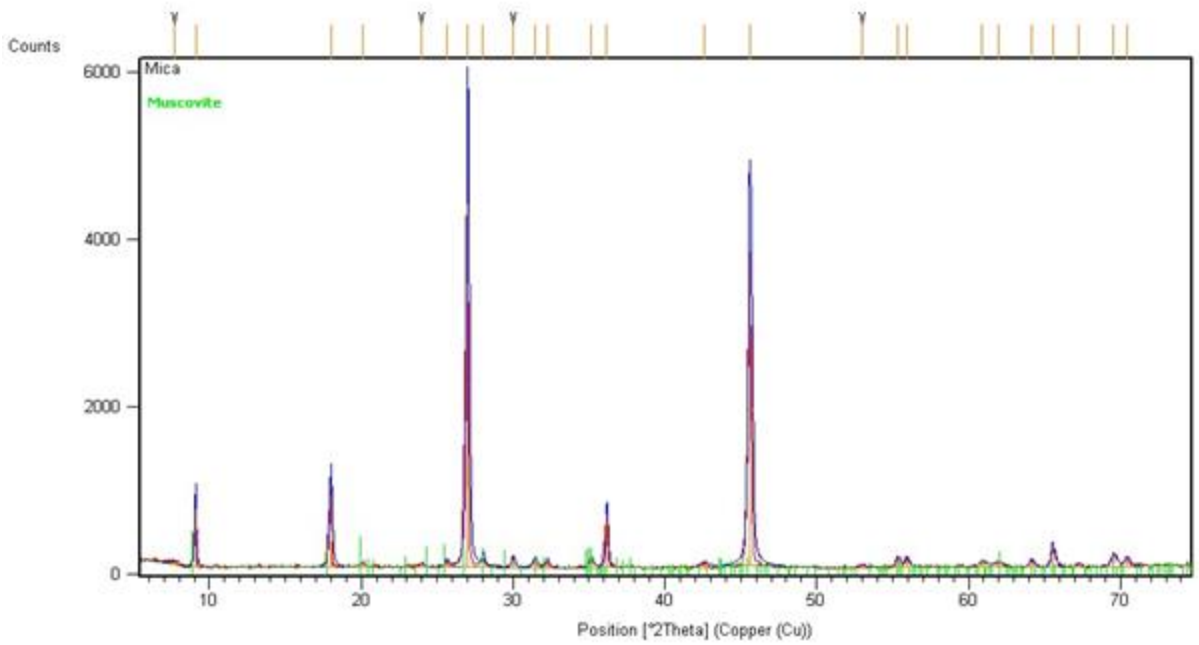

Figure 2: X-ray diffraction of crude Mica from Bukkuyum local government, Zamfara State, Nigeria.

Table 1: X-Ray Fluorescence(XRF)Elemental Analysis Result of crude Mica From Bukkuyum Local Government Area, of Zamfara State, Nigeria

OXIDES	PERCENTAGE PRESENCE
SIO_2	48.7
Al_2O_3	33.3
K_2O	15.2
Na_2O	0.67
CaO	0.01
MgO	0.04
TiO_2	0.17
Fe_2O_3	1.04
MnO	0.02
BaO	0.03
LOI	0.79

3.3 SEM Morphological Analysis

From the figure 3 and figure 4 it shows the surface, the fracture pattern of the sheet and range of fiber particle size respectively.

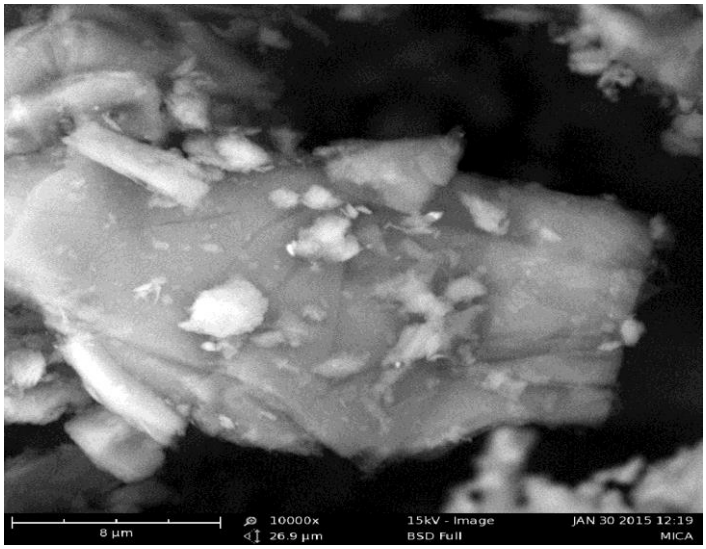

Figure 3: Scan Electron Photomicrograph showing the fracture surface of fine crude Mica that is representative of the Mica deposit in Bukkuyum local government area of Zamfara State, Nigeria.

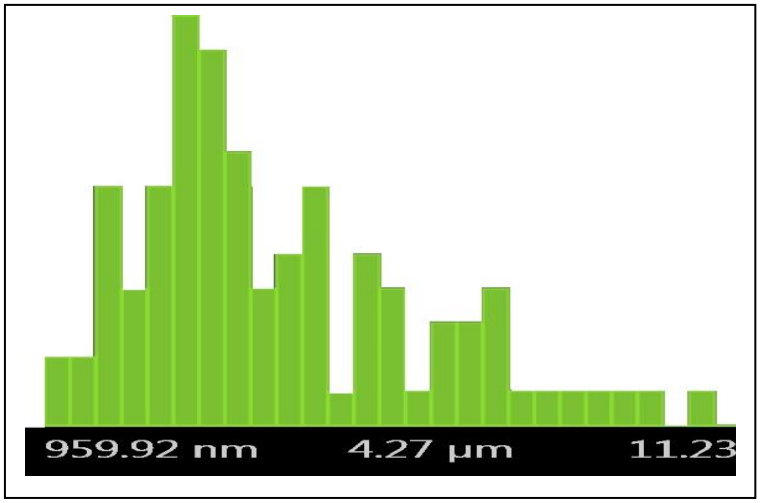

Figure 4: The fiber histogram showing the particle size distribution of the crude crushed Mica that is representative of the Mica deposit in Bukkuyum local government area of Zamfara State, Nigeria.

4.0 Conclusion

From the evaluation results and analysis, the following conclusions are deduced.

1. From XRD analysis confirms the muscovite phase
2. The XRF provided the elemental composition in their oxides SiO_2 of 48.7, Al_2O_3 of 33.3, k_2O of 15.2, Na_2O of 0.67, CaO of 0.01, MgO of 0.04, TiO_2 of 0.17, Fe_2O_3 of 1.04, MnO of 0.02, BaO of 0.03 and LOI of 0.79

3. The SEM shows the morphology along with statistics of fiber particle size of 959.92 nm, 4.27µm and 11.23µm
4. Finally, it can be concluded that the Mica from bukkuyum local government area of Zamfara state of Nigeria is a muscovite with chemical formula $K_{0.77}Al_{1.93}(Al_{0.5}\ Si_{3.5})\ O_{10}\ (OH)_2$ from the XRD result and contains impurities of Fe_2O_3 of 1.04%, and CaO of 0.01%, MgO of 0.16%, TiO_2 of 0.17% with LOI of 0.79% from the XRF result. The morphology results 959.92nm, 4.27µm and 11.23µm. This result can be improved on by numerous beneficiation processes depending on the area of industrial or engineering application.

Acknowledgements

Authors would like to thank (NGRL), Kaduna for their kind help of XRD and XRF analysis, and also Department of Chemical Engineering, ABU, Zaria for the SEM morphology analysis.

References

Bailey, S.W 1984. Classification and Structures of the Micas. Pages 1-12 in reviews in mineralogy. Volume 13. Washington, DC: mineralogical society of American.

Harben, P.W 2002, Mica, pages 220-227 in Industrial Minerals Handbook 4th edition, survey. UK; Industrial Mineral Information.

Hendrick, J.B 2002, Mica. Pages 51.1-51.5 in Mineral Yearbook Washington DC, US, Geological Survey

John W.S and James T. T Jr.2006 mica pages 637-652 in 7th Edition Industrial Minerals & Rocks. Commodities, Markets and Uses, edited by Jessica E.K, Nikhil C.T, James M.B and Stanley T.K Published by SMME Inc. USA.

Sinkankas, J 1964. Phyllosilicates, pages 480-486 in Mineralogy for Amateurs, New York; Van Nostrand Reinhold.

Skillen A. 1992, Mica, grounds for optimism. Industrial Minerals 302-25

Nigerian Journal of Renewable Energy Research
Volume 1, Number 1, pp 69-79, 2023

Performance Prediction of Xanthogenate Collectors Using Flotation Kinetic Equation

Damisa, E.O.A.

Department of Metallurgical and Materials Engineering, Ahmadu Bello University, Zaria, Nigeria
All correspondences to: eoadamisa@yahoo.com, +234-803 785 0992

https://www.tetfundkadpolycoex.org.ng

ARTICLE INFORMATION

Article history:
Received 18 Jun., 2023
Revised 06 Sep., 2023
Accepted 03 Oct., 2023
Available online 20 Oct., 2023

Keywords:
Kinetics
Flotation
xanthogen collectors
separation efficiency

Abstract

The kinetics of flotation using xanthogen collectors - $C_2H_5OCSSNa$, $C_3H_7OCSSNa$, $C_4H_9OCSSNa$ and $C_5H_{11}OCSSK$ were studied in the flotation of lead sulphide with sodium ethyl xanthate –SEX ($C_2H_5OCSSNa$) as control. Sodium ethyl xanthates (SEX) as control gave a recovery of the mineral of interest being lead sulphide of 94% and high-grade recovery of gangue as 24% which indicated that SEX has high selectivity but low recovery. The SIPX has a flotation kinetics of gangue that are greater than for SEX, which indicates its relative greater strength than SEX. At optimum time the concentrate grades are 12.1% Pb and the separation efficiency is greater, reaching 80.5% but with lower selectivity than SEX. SIBX is a collector with much more rapid flotation kinetics for the lead sulphide but with lower recovery, being less selective than SEX. The optimum separation time for SIBX is around 7 minutes, which demonstrates its high flotation rate for the lead sulphide giving recovery of 88.9% with separation efficiencies of 76.6%, better parameters than those of SEX. PAX is a collector of great strength with recovery characteristics similar to SEX, with rapid flotation kinetics for lead sulphides but less selective. In comparison with SEX, it has lower recovery of lead sulphide but the rapid recovery percent is 91.9%. Its separation efficiency is very similar to SEX at their respective optimum times, with concentrate level of 7.4% Pb and efficiency of 73.8%

1.0 Introduction

Reagents used in flotation are collectors, frothers and modifiers. Of these, collectors are the most important and continuous efforts are made to evaluate and improve their functionalities. These collectors are organic compounds which render selected minerals water-repellent by adsorption of molecules or ions on to the mineral surface, reducing the stability of the hydrated layer separating the mineral surface from the air bubble to such a level that attachment of the particle to the bubble can be on contact (Wills, 2006). The most common collectors in use today are the alkaline collectors, known as xanthates. For successful flotation operation, addition of optimum quantities of the collectors is very essential. Too little or excess quantity of collector have either beneficial

or adverse effects on the flotation process. Therefore, extant and new reagents are constantly being evaluated with regard to their effectiveness in any particular flotation process, taking into consideration the minerals and conditions of operation in each plant. Also, for ore bodies, as the mineralogical characteristics of different zones are change, periodic reviews of the reagents used in the flotation process are carried out. (Marin and Molina, 1985).

It is the convention to evaluate the performance of flotation reagents using laboratory batch flotation tests to determine the recovery and grade of concentrates on the basis of varied dosages of the reagent under study. Small scale batch test results should be evaluated with caution due to several limitations. The most important limitations are associated with recycle streams, site water and test size (Thompson, 2002). Another method is the use of statistical approach. The use of statistical analysis in the selection of a reagent scheme is usually limited to optimizing reagent dosages after a preliminary scheme has been selected. Statistical methods are also extensively used to evaluate the relative importance of various reagents in existing reagent scheme at operating plants. The two most common types of statistical methods that are used in reagent scheme evaluation are *screening tests* and *response surface design.* The most common type of screening statistic used is the Plackett Burman (1946) analysis. This is a special two-level factorial design that is used as a preliminary screening tool to determine which reagents have a significant effect on recovery, grade, or both. Thus, it is used to reduce the number of batch tests necessary to optimize the combination of reagents, permitting the development of a more effective formula during the process. More sophisticated statistics such as response surface design are used to optimize reagent additions. These methods are based upon factorial design of experiments and may be used to evaluate several variables at several levels. This type of analysis is quite complex and software packages are used to simplify the experimental design and interpret the results. In all these cases, it is necessary to carry out intensive experimental work.

To obviate the need to carry out intensive experimental work for the evaluation of reagents in flotation processes is to consider that flotation separation can be described very simply using a kinetic equation, which not only describes the effect of the reagents, but also helps in the design and optimization of the separation process.

2.0 Modeling Flotation Process

According to King (1982), many batch flotation tests conducted in the laboratory have indicated that the kinetic model for flotation does describe the essential nature of the flotation process at least in a well–stirred flotation environment where the solid particles are kept in suspension and are available for capture by the bubbles. Also, according to Gochin and Smith (1987), state that research has shown that flotation can generally be regarded as a first-order rate process with respect to the concentration of the floating species in the pulp. Therefore, flotation separation can be described in kinetic terms using a first order rate equation. The first order rate equation can be expressed (Lynch et al, 1981) as:

$$R = 1-\exp(-kt) \quad (1)$$

A modified first order rate equation is of this form (Wills, 2006) in equation (2) in which the parameter of maximum recovery is $R_{m.}$

$$R = R_m[1-\exp(-kt)] \quad (2)$$

Where:
R = cumulative recovery at time t,
R_m = maximum recovery that is approximately asymptotic as $t \rightarrow \infty$
K = flotation rate constant (min^{-1})
t = flotation time (min)

This equation can be applied to all the components of the flotation system, including water. Of course, some gangue will float and dilute the concentrate Gochin and Smith (1987). The longer flotation continues the more will be this dilution and cumulative concentrate grade will decrease Gochin and Smith (1987). Hence it is evident that there is an optimum flotation time beyond which the incremental increase in recovery in the unwanted minerals begins to exceed that of valuable mineral. Also, it has been shown that through the use of this equation, a continuous circuit can be simulated from batch data, and even more, the time used in the various stages can be optimized.

The premise on which this application is based is that a variation in the quantity of reagents or the introduction of reagents into the flotation system affects in some way K and R_m. This is valid for any agent in the process, whether they are collectors, frothers or modifiers.

To interpret the data kinetically, only one flotation test would be necessary. The froth bearing the concentrate is collected in concentrate launder over an increasing period of time. The unknown parameters of the rate equation can be calculated from the first order kinetic equation. A first estimate of the value of maximum recovery R_m is obtained by plotting the cumulative recovery as a function of time (Figure 1), when the curve becomes asymptotic after a long period of flotation. The initial estimate of R_m can be corrected by preparing a logarithmic plot of (R_m –R/R_m) as a function of the flotation time (Figure 2). If the estimate of the value of R_1 is too great, the line will curve downwards. The value of the constant K is obtained as a slope of that straight line.

With the parameters K and R_m determined, the first order equation can be used to calculate the optimum separation time. The optimum time is defined as the time at which the difference between the recovery of valuable mineral and the gangue ΔR is at a maximum.

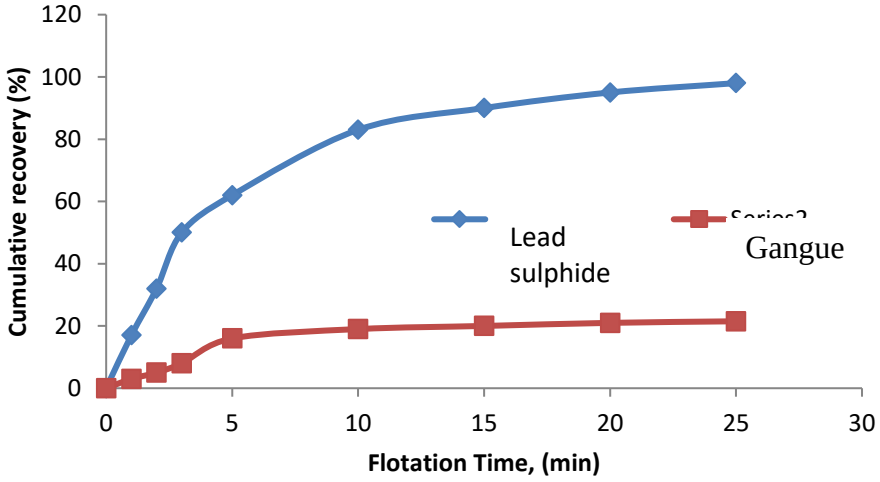

Figure 1: Kinetic flotation curve for estimating R_m (SEX)

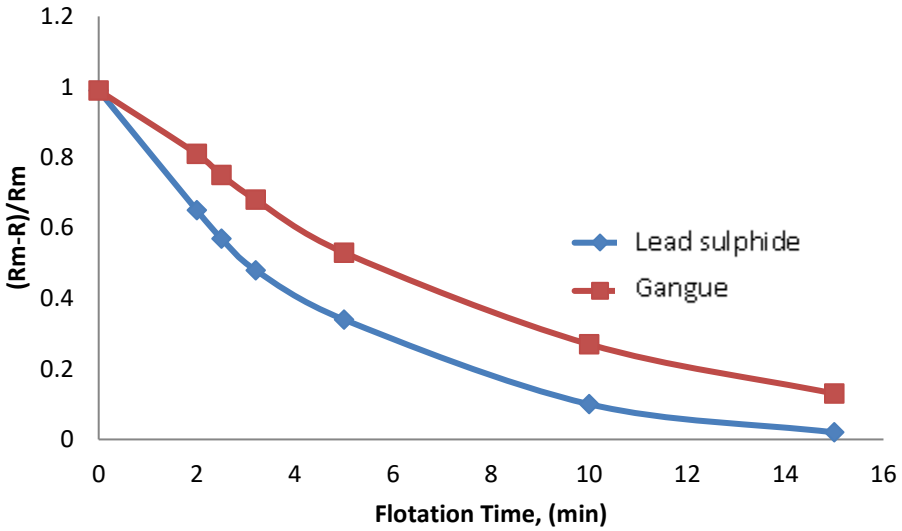

Figure 2: Adjustment of Rm in a first order equation (SEX)

$$\Delta R = Rv\text{-}Rg \quad (3)$$

Where:
R_v = recovery of valuable mineral
R_g = gangue recovery

$$\partial R/\partial t = \partial Rv/\partial t - \partial Rg/\partial t = 0 \quad (4)$$

$$\partial Rv/\partial t = \partial R_g/\partial t \quad (5)$$

$$\frac{\partial(R_{mV}[1\text{-}\exp(-K_V t)])}{\partial t} = \frac{\partial(R_{mg}[1\text{-}\exp(-Kgt)])}{\partial t} \quad (6)$$

$$t_{,optimum} = 1/K_A\text{-}K_B \ln (R_{mV} K_V/R_{mg} K_g) \quad (7)$$

The optimum time corresponds to the time when the rate of transfer of solids to the froth phase is equal for both components. When plotting the flotation rate as the slope of the kinetic curve as a function of time (Figure 3) both curves will cross at the optimum time.

Once the optimum time is determined using the rate equation, the recovery of both components is determined for that time and the difference is the optimum separation. The term ΔR is the separation efficiency and it is a measure of the fraction of the feed that can be perfectly separated. Higher flotation times than the optimum reduce the concentrate grade, due to the higher flotation of the gangue, considering that the maximum recovery of valuable mineral or mineral of interest (R_m) has already been reached.

The application of this technique, permits the evaluation of the behaviour of sulphydryl collector type of reagents.

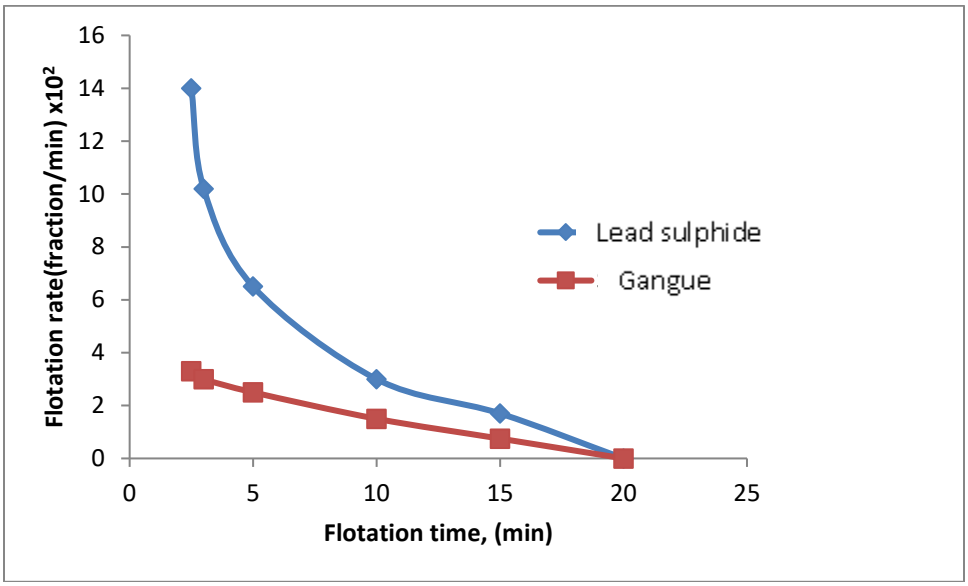

Figure 3: Flotation rate as a function of time for SEX

3.0 Experimental

Ore: the sample used in the experiment was a complex Nahuta lead sulphide ore, Bauchi State, Nigeria. Its mineralization consists principally of galena, PbS. Sample preparation was done by coning and quartering followed by rifling. Comminution of the material was by Denver laboratory jaw crusher, classifying the product through a 90µm.

Reagents: The collectors under study were synthesized through the reaction of an alkali hydroxide, an alcohol and carbon disulphide (Wills, 2006):

$ROH + CS_2 + KOH = RO.CS.SK + H_2O$

These products were purified by means of low-pressure distillation. The structure of the thiol collectors, otherwise known as xanthogenates (technically known as xanthates) was checked through the use of infrared spectrophotometry and magnetic nuclear resonance and compared with the xanthates obtained from *ALS Metallurgy* Western Australia. The results were consistent with the proposed structures. The xanthates studied were:

Sodium ethyl xanthates	SEX	$C_2H_5OCSSNa$
Sodium isopropyl xanthates	SIPX	$C_3H_7OCSSNa$
Sodium isobutyl xanthates	SIBX	$C_4H_9OCSSNa$
Potassium amyl xanthates	PAX	$C_5H_{11}OCSSK$

Other Reagents:
Frother: Pine oil; Type of water: Tap water

3.1 Techniques and Equipment

Grinding: The samples were ground in a Denver Ball Mill lined with rubber the grinding was done with 67% solids.

Flotation Tests: The flotation tests were carried out in a Denver flotation machine at 1800 rpm and with a pulp volume of 3 litres. The design of the experiments that would evaluate the xanthate collectors took into account the following variables: liberation degree, pulp pH, agitation seed, pulp density, frother type and dosage, type of water, collector dosage and its conditioning; all of which remained constant so as to study only one variable, a particular collector. The reagents dosage as follows:

a. Frother: Pine oil at 10 g/tonne of the ore
b. Collector: 50 g/tonne of ore in each case

With this collector dosage and frothers in the case of SEX, a recovery after 10 minutes of flotation of 86% was found under the prevailing conditions which left a sufficient margin of improvement. The flotation lasted 25 minutes and the launders for the concentrate were changed at the following times: 1, 2, 3, 4, 5, 10, 15 and 25 minutes. During this period, water was added to the flotation cell so as to maintain the pulp volume at 3 litres

.

At the end of the experiment, the concentrate samples that corresponded to each flotation time concentrate and final tailings were filtered and then afterwards dried and weighed. Finally, as a product of a rigorous sampling 30g were separated which were analyzed for Pb and total Pb content. The difference between them gives the percentage of insoluble Pb needed for calculations.

4.0 Results

The kinetics flotation curves for the lead sulphide and the gangue from the data in Table 2 for SEX, are shown in Figure 1. From both curves an estimation of R_m, are summarized in Fig. 2, giving for the lead sulphide minerals a value of 94.1% and for the gangue 24%. The slopes of the straight lines correspond to the first order rate constants, in the case of the sulphide minerals they are 0.233 (min^{-1}) and for the gangue 0.144 (min^{-1}).

Table 1: Kinetic parameters in the flotation of lead sulphide using different collectors.

Collector	Ore K (min-1)	Lead Sulphide R_m	K (min-1)	R_m	Optimum separation time	S.E. (%)	Conc. Grade (%) (optimum time)	Tail grade Pb % (optimum time)
SEX	0.23	0.94	0.14	0.24	20	72.6	6.4	0.15
SIPX	0.36	0.92	0.14	0.14	13	80.6	12.1	0.22
SIBX	0.56	0.89	0.13	0.21	7	76.7	11.8	0.30
PAX	0.44	0.92	0.24	0.24	10	73.8	7.4	0.19

Taking the slopes of the kinetic curves of Fig.1 at different times Fig.3 was constructed for the flotation rate, the intersection of both curves giving the optimum time of separation which gave 20 minutes. With the value for optimum time, using the kinetic curves ΔR was found to be 72.5%,

which is the value for the greatest separation efficiency. With the data in Table 2 the concentrate grades and tailings for the optimum were calculated to be 6.4% and 0.14% Pb, respectively.

5.0 Discussion

The primary role of a collector is to adsorb selectively and impart hydrophobicity to particles of the mineral to be floated (Fuerstenau and Somersudaran, 2003). SEX as a collector has moderate rate of recovery of the mineral of interest in the first four minutes and begins to slow down. From five minutes upward the rate of flotation is slow and it was observed that recovery of gangue minerals became constant following the trend of the mineral of interest. Its application would be principally in rougher and scavenger flotation circuits where these metallurgical objectives are required.

Table 2: Flotation kinetic data for SEX

Flotation time (min)	Conc. Weight (g)	Grade of Pb (%)	Cumulative Recovery Sulphide (%)	Cum. Recovery gangue (%)
0	38.7	10.3	3.4	0.5
1	51.4	9.6	14.5	2.4
2	70.0	8.4	31.8	5.6
3	74.1	8.0	49.2	9.1
5	77.0	7.0	64.9	12.7
10	114.3	5.6	83.9	18.2
15	60.9	4.0	91.0	21.2
20	71.3	3.3	92.7	23.4
25	82.0	2.1	96.1	25.3

Table 3: Flotation kinetic data for SIPX

Flotation time	Concentrate Weight (g)	Grade Pb (%)	Cum. Recovery of lead sulphide (%)	Cumulative recovery gangue (%)
0	36.21	19.14	14.69	0.78
1	39.82	18.90	22.09	1.59
2	50.21	17.40	47.78	3.81
3	30.69	14.47	60.89	5.11
5	43.78	10.88	74.91	7.09
10	50.81	6.49	84.68	9.48
15	60.51	3.48	91.40	12.78
20	62.81	3.51	93.59	13.47
25	65.28	3.41	97.88	15.68

In Figures 4, 5 and 6, the kinetic flotation curves can be seen, obtained from data in Tables 3, 4, and 5 for SIPX, SIBX and PAX respectively. Those which have been drawn are those obtained for SEX (dotted line) in order to demonstrate their differences. The data for the kinetic parameters of the first order expressions for these reagents are presented in Table 1. For the collector SIPX, a K of 0.360 (min^{-1}) and a R_m of 14.3%. The optimum time value was 13 minutes, which gives a

separation efficiency (S.E) with grades of 12.1% and 0.21% Pb in the concentrate and tailings respectively.

For the collector SEX, a K of 0.562 (min^{-1}) and a R_m of 88.9% was obtained and for the gangue there was a K of 0.127 (min^{-1}) and a R_m of 20.7%. The optimum time was 7 minutes which gives a separation efficiency (S.E) of 76.6% with grades of 11.8% and 0.29% Pb in concentrate and tailings respectively.

Table 4: Flotation kinetic data for SIBX

Flotation time (min)	Concentrate weight (g)	Pb grade (%)	Cumulative recovery sulphide mineral (%)	Cumulative recovery gangue (%)
0	38.59	17.22	18.58	1.81
1	54.69	16.51	26.62	2.32
2	60.51	15.31	53.79	4.89
3	40.51	14.87	71.58	6.67
5	60.68	6.01	82.30	9.61
10	80.88	2.52	83.21	13.62
15	75.68	1.13	90.61	17.40
20	78.31	0.85	91.51	19.50
25	79.01	0.71	92.31	21.39

Table 5: Table Flotation kinetic data for PAX

Flotation time (min)	Concentrate weight (g)	Pb grade (%)	Cumulative recovery sulphide mineral (%)	Cumulative recovery gangue (%)
0	131.4	12.41	36.71	3.79
1	128.01	11.31	42.58	5.88
2	66.71	8.30	60.0	8.92
3	52.96	7.68	70.21	11.47
5	81.31	5.39	83.81	15.38
10	88.59	2.58	90.58	19.77
15	60.70	1.10	92.47	23.00
20	56.21	0.85	91.87	23.81
25	45.97	0.61	93.29	25.21

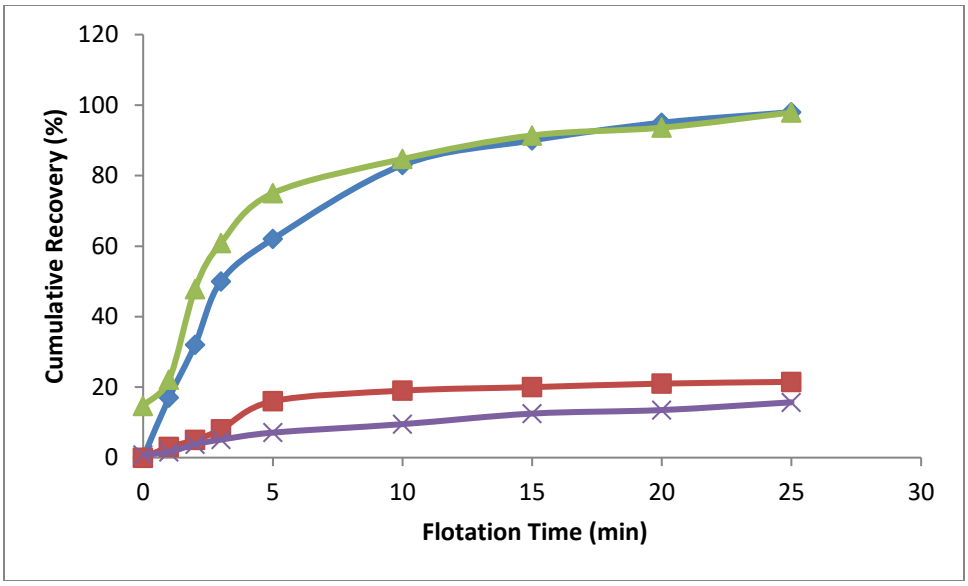

Figure 4: Flotation kinetics for SIPX

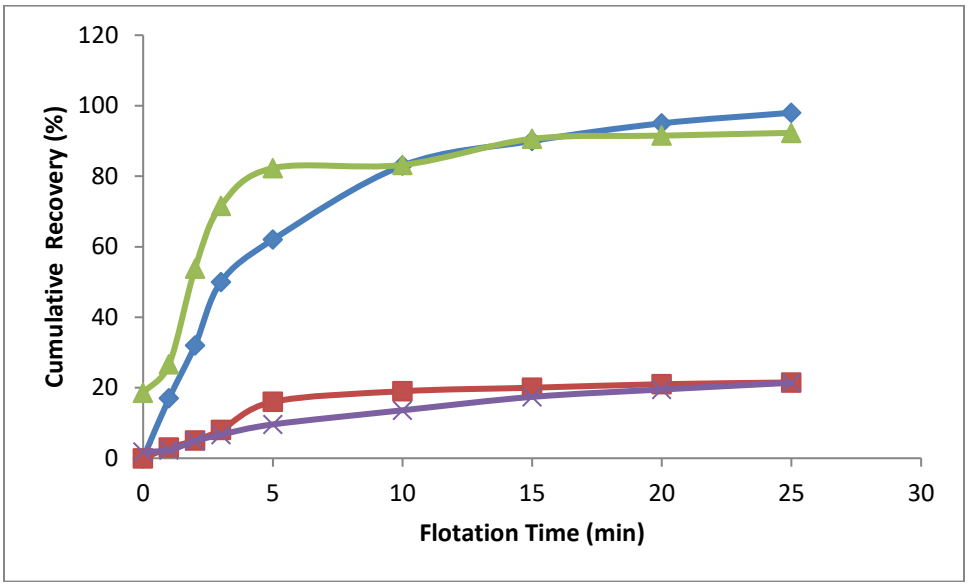

Figure 5: Flotation kinetics for SIBX

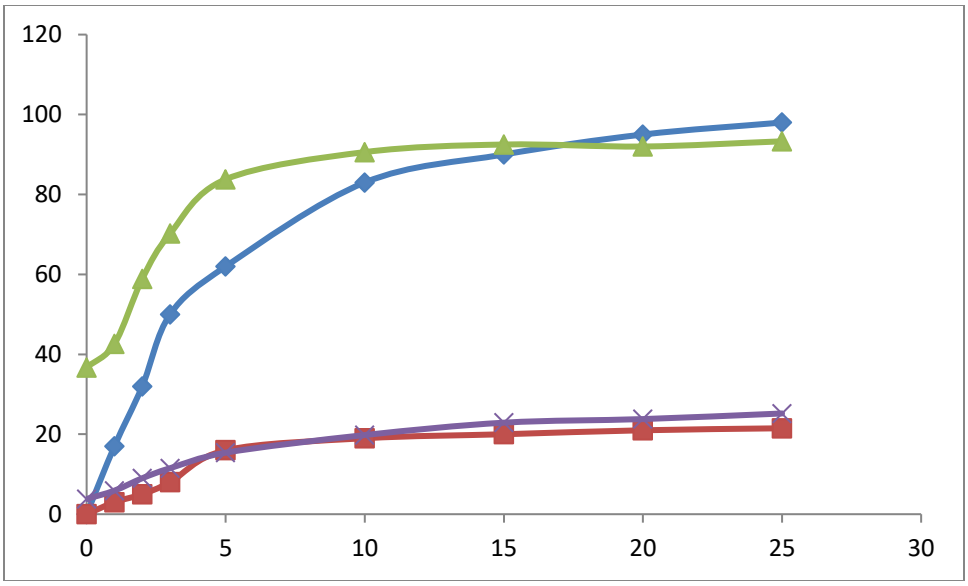

Figure 6: Flotation kinetics for PAX

The collection of lead sulphide which was the mineral of interest took place over a relatively long period of time of about 20 minutes, with a maximum efficiency of 72. 5%. The concentrate grades are low with fairly clean tailings, with recovery of 94%. As SEX is very selective, the recovery of the gangue is high, around 24%, which is reflected in a lowering of the grades.

The SIPX has very high flotation kinetics rate than SEX and with greater collecting power for lead sulphide. The rate constant K for sulphide mineral is greater for SEX, which gave, in only 13 minutes, a recovery of 92%. The SIPX has flotation kinetics of gangue that are greater than for SEX, which indicates its relative greater strength than SEX. At optimum time the concentrate grades are 12.1% and the separation efficiency is greater, reaching 80.5% but with lower selectivity.

SIBX is a collector with much more rapid flotation kinetics for the lead sulphide but with lower recovery, being less selective than SEX. The optimum separation time for SIBX is around 7 minutes, which demonstrates its high flotation rate for the lead sulphide giving recovery of 88.9% with separation efficiencies of 76.6%, better parameters than those of SEX.

PAX is a collector of great strength with recovery characteristics similar to SEX, with rapid flotation kinetics for lead sulphides but less selective. In comparison with SEX, it has lower recovery of lead sulphide but the rapid recovery percent is 91.9%. Its separation efficiency is very similar to SEX at their respective optimum times, with concentrate level of 7.4% Pb and efficiency of 73.8%. At high level of flotation time, PAX showed tendency to recover more of the gangue and in this case it is advisable to find the optimum time of flotation to avoid more gangue recovery when the time exceeds 15 minutes in the course of the flotation process. It is evident that this time recovery of the valuable mineral (lead sulphide) starts to decrease.

6.0 Conclusion

As a general approach, the above is a good approximation of what happens with a simple two component ore where one is the valuable mineral and the other species is the gangue. Of course

most ores have several waste minerals that have significant and different values rate constant. In this case, the k for the waste materials can be taken as a weighted average of the individual rate constants. With this it can be taken that the determination of kinetics flotation parameters, associated with a first order rate expression is valid for characterizing collectors in the flotation process.

The SIPX is a collector similar to SEX, but with a greater flotation rate and less selective for lead sulphides than SEX. SIBX is a collector of lower selectivity than SEX and fewer recovery properties than SEX. It has a greater flotation rate for the lead sulphide, reaching a very high separation efficiency in a very short flotation time.

The PAX has a lower selectivity than SEX with a greater flotation rate for sulphides and lower recovery at longer times, reaching very similar separation efficiency with SEX at about 16th minute of the flotation process and tendency to diminish in recovery properties than SEX afterwards.

Acknowledgement

Appreciation to Mr. Mike Holland of ALS Metallurgy, Western Australia for assistance in the provision of reagents.

References

Gochin, R.J. and Smith, M.R. (1987) The methodology of froth flotation testwork *in* Mineral Processing Design, Yarar, B and Dogan Z.M. (eds) Martinus Nijhoff Publishers

King, R.P. (ed) (1982) *The Principles of Flotation*, South African Institute of Mining and Metallurgy

Marin, G and Molina, E (1985) Characterization of collectors through flotation rate data, *in Developments in Mineral Processing, Proceedings of the 2nd Latin-American Congress on Froth Flotation*, Concepcion, Chile Edited by Castro Flores S.H. and Moisan, J.A.

Fuerstenau, M.C and Somersudaran, P (2003) *Flotation* in Principles of Mineral Processing, Fuerstenau, M.C and Han, K.N. (Eds) published by Society for Mining, Metallurgy, and Exploration, Inc Colorado

Thompson, P (2002) The selection of flotation reagents via batch flotation tests in *Mineral Processing Plant Design, Practice and Control Proceedings*, Vol 1. Mular, A.L, Halbe, D.N. and Barratt, D.J. (Eds)

Wills, B.A. (2006) *Wills Mineral Processing Technology*, An introduction to the practical aspects of ore treatment and mineral recovery, Napier-Munn T (Ed.) 7th Edition Elsevier

Nigerian Journal of Renewable Energy Research
Volume 1, Number 1, pp 80-83, 2023

Determination of Liberation Size of Agwada Chalcopyrite Ore, Nasarawa State, Nigeria

Ali M, Aye, A.E. and Akindele. U.M[*].

Department of Mineral Resources Engineering, Kaduna Polytechnic, Kaduna
[*]Corresponding author: usmanakindele44@gmail.com.

https://www.tetfundkadpolycoex.org.ng

ARTICLE INFORMATION

Article history:
Received 28 Jun., 2023
Revised 26 Sep., 2023
Accepted 03 Oct., 2023
Available online 20 Oct., 2023

Keywords:
Mineral processing
Comminution
Particle size
Liberation
Chalcopyrite

Abstract

This research work centered on the determination of Liberation Size of Agwada chalcopyrite Ore in Nasarawa State, Nigeria. This study reviewed the Comminution process for the release or liberation of the valuable minerals particles from the associated gangue. The ore was comminuted and sieved to liberation size. The mesh of grind was found to be 189µm and liberation size established to be 125µm, sieve size having the highest percentage of copper of 8.17% which was assessed by using x-ray fluorescence spectrometer (XRF).

1.0 Introduction

Most minerals are finely disseminated and intimately associated with gangue, as such, they must be intimately unlocked or liberated before separation can be undertaken. The liberation of the valuable minerals from the gangue is accomplished by comminution to release the valuable mineral from the associated gangue mineral at the coarsest possible particle size. If such an aim is achieved, this could not only save energy, but also reduce the amount of fines produced, hence subsequent separation stages becoming easier and cheaper to handle (Wills and Atkinson,1993).

Comminution in mineral processing plant or "mill" takes place as a sequence of crushing and grinding processes. Crushing precedes grinding, which can be carried out until the mineral and gangue are substantially produced as separate particles (Flavel, 1978). Crushing is the first mechanical stage in the process of comminution in which the main objective is the liberation of the valuable minerals from the gangue (Lewis et al, 1976). Crushing is accomplished by compression of the ore against rigidly constrained motion path as against abrasion and impact of the ore by the free motion of unconnected media such as rods, balls or pebbles in the case of grinding (Wills, 2006).

Grinding is the last stage in the process of comminution. In this stage, the particles are reduced in size by a combination of impact and abrasion, either dry or in suspension in water. It is performed

in rotating cylindrical steel vessel which contains a charge of loose crushing bodies, the grinding medium which is free to move inside the mill, thus comminuting the ore particles (Wills, 2006).

Particle size analysis is of great important in establishing the degree of liberation of the values from the gangue at various particle sizes. Therefore, size analysis must be accurate and reliable, as important changes in plant operation may be made on its outcome. Size analysis is accomplished by passing a known weight of sample materials through fine sieves usually by agitation and material retained are weighed. The effectiveness of a sieving test depends on the amount of materials put on the sieve (the "charge") and the type of movement imparted on to the sieve. A comprehensive account of sampling techniques for sieving is given in BS 1017 (Levin, 1989).

2.0 Methodology

The following techniques were adopted in order to determine the liberation size of Agwada chalcopyrite ore:

2.1 Sample Collection

The samples were obtained from the main bulk in Agwada, Nasarawa State from seven different locations spaced at 15m interval and depth of 3.5m.

2.2 Sample Preparation

The samples collected in lumps size were broken manually with sledge hammer to provide a required size acceptable to laboratory jaw crusher. The samples were crushed and pulverized, then coned and quartered to yield a representative sample

2.3 Sieve Analysis

100g of the prepared sample was subjected to sieve analysis. The selected and arranged of the sieves were with respect to root of two ($\sqrt{2}$). Five sieves were arranged in a stack with the coarsest one on the top and the finest at the bottom. A tight fitting pan was placed below the bottom sieve to receive the final undersize and a lid was placed on top of the coarsest sieve to prevent escape of the sample. The arranged sieves were placed in a sieve shaker which vibrates the materials vertically. The duration of the screening was set at 30minutes.

After a successful operation, each size fraction retained on each sieve was collected, weighed and recorded.

2.4 Chemical Analysis

XRF spectrometry was used to determine the elemental composition of inorganic based materials. It is typically used for bulk chemical analysis on solids and powders. The pellet loaded in the sample chamber of the spectrometer and voltage (30kV maximum) and a current (1mA maximum) applied to produce the x-rays to excite the sample for a present time (10 minutes in this case). The system controlled by a PC, running the dedicated mini analytical software (Anon, 2015).

3.0 Results and Discussions

Results of various laboratory experiments and analysis carried out are presented and discussed below.

3.1 Sieve size

It was observed from the sieve test results presented in table 1 that 13.63g of the total weight was retained on the 250μm sieve size, 10.09g on 180μm, 17.63g on 125μm, 15.84g on 90μm and 17.32g on 63μm. From the table, the mesh of grind was calculated by correlating the cumulative weight passing value of 76.28% of 180μm to establish equivalent value at 80% leading to189μm.

Table 1: Result of Sieve Analysis

Sieve size Range (µm)	Weight retained (g)	% weight retained	Nominal aperture	Cumulative % Weight retained	Cumulative % Weight passing
+250	13.63	13.63	250	13.63	86.37
-250+180	10.09	10.09	180	23.72	76.28
-180+125	17.63	17.63	125	41.35	58.65
-125+90	15.84	15.84	90	57.19	42.81
-90+63	17.32	17.32	63	74.51	25.49
-63	25.49	25.49	-	100	0.00
Total	100.0	100.0			

If 180 µm ⟶ 76.28
X µm ⟶ 80%

$X = \frac{180 \times 80}{76.28}$ = 188.8µm at 80%

3.2 Chemical analysis

The chemical analysis of the sample was conducted on all the five sieve sizes (Table 2). The result in its elemental form indicated that 250μm contain 4.16%Cu,180μm contains 1.02% Cu, 125μm contains 8.17%Cu, 90μm contains 6.48% Cu while 63μm contain 3.03% Cu. The result has confirmed 125μm having the highest deportment of copper in its elemental form.

4.0 Conclusion

Therefore, from the foregoing, the research work established the mesh of grind to be 189μm for Agwada chalcopyrite ore and liberation size to be 125μm sieve size having the highest recovery of mineral of interest copper (Table 2) of 8.17%. It is hoped that with the above figure, further research work can be done to estimates reserve and develop beneficiation routes.

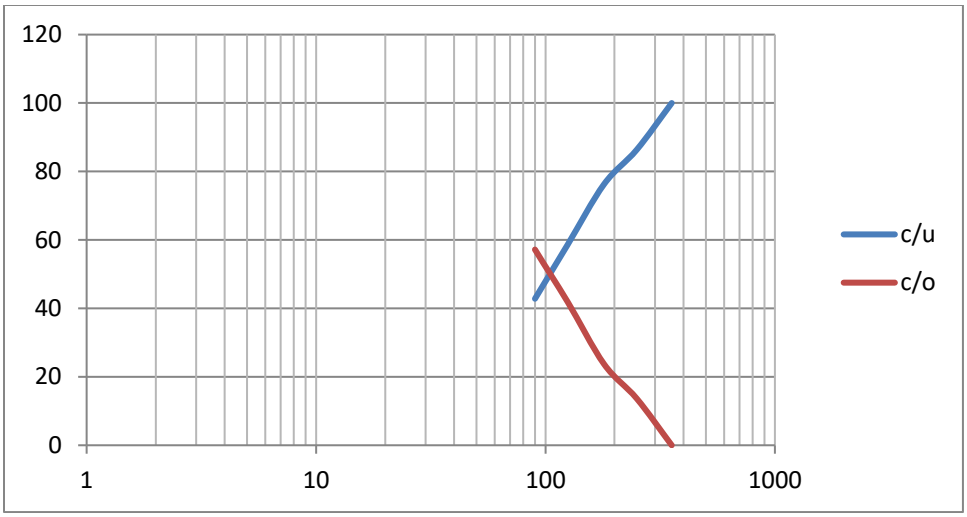

Figure 3: PSD Curve For Agwada Chalcophyrite Ore

Table 2: Result of the Chemical Analysis of Head Sample in Element form

Aperture size (μm)	K	Al	Si	Ca	Fe	Mn	Zn	S	Cu
250	4.48	2.91	9.02	9.17	29.69	1.95	6.56	5.56	4.16
180	2.27	0.59	3.36	1.26	21.29	0.19	1.13	0.22	1.02
125	4.49	4.96	10.83	14.51	26.89	0.21	0.97	2.56	8.17
90	6.03	3.97	7.90	6.22	19.04	0.51	0.23	1.26	6.48
63	4.50	2.17	15.54	8.29	23.46	0.15	1.13	1.95	3.03

Acknowledgement

The authors are grateful to Engr. Dr. E.O.A. Damisa, for his assistance and value added contributions to this research work.

References

Anon (2015). X-Rays Fluorescence Spectrometry, www.ceram.com/testing.analysis/techniques/x-rays-fluorescence-spectrometry-xrf. Accessed; May 1st, 2015.

Flavel, M.A (1978). Control of crushing circuits will reduce capital and operating costs mining magazine Vol. 207

Jatau B.S, Akindele U.M, Aye A.E (2014) Physico-Chemical Appraisal Agwada Chalcopyrite Ore, Nasarawa State. Nigerian Mining Journal Vol. 12, No I, 46-50pg.

Levin, J. (1989). Observations on the bond standard grindability test and a proposal for a standard grindability test for fine materials, J.S Afr. Inst Min. metallurgy.

Obaje N.G, Ukaonu C.E (2005). Geology and Mineral Resources of Nasarawa State, Nasarawa State University, Department of Geology & Mining, Nigeria.

Wills B.A and Atkinson, K. (1993). Some observation on the tract and liberation of mineral assemblies, minerals engineering Vol. 697.

Wills, B.A (2006). Will's Mineral Processing Technology: An Introduction to the Practical Aspect of Ore Treatment and Mineral Recovery, 7th Edition, Published by Elsevier Limited, U.S

Nigerian Journal of Renewable Energy Research
Volume 1, Number 1, pp 84-99, 2023

Performance Evaluation of an Active Solar Still under Forced Circulation Mode

S. N. Mumah[1*], Tanimu Garba Ibrahim[2], H.F. Akande[1] and Abdullahi Ismail Belli[3]
[1]Department of Chemical Engineering, Kaduna Polytechnic, Kaduna, Nigeria
[2]Department of Mechanical Engineering, Kaduna Polytechnic, Kaduna, Nigeria
[3]Department of Electrical & Electronics Engineering, Kaduna Polytechnic, Kaduna, Nigeria
[*]Corresponding author: *mumahsndoyi@kadunapolytechnic.edu.ng*; Tel: *+234- 8037619719*

https://www.tetfundkadpolycoex.org.ng

ARTICLE INFORMATION

Article history:
Received 21 Jun., 2023
Revised 24 Sep., 2023
Accepted 13 Oct., 2023
Available online 20 Oct., 2023

Keywords:
Solar Still
Forced Circulation
Design
Performance Evaluation

Abstract

Water is fundamental to human life on earth for survival and good health. Access to safe water is a major challenge to many communities both urban and rural in Nigeria. As Nigeria's population continues to grow with the social-economic problems already quite visible, communities will continue to be challenged to provide fresh water to meet those needs for all of their people. Growing demands of freshwater resources are creating an urgent need to develop self-sustained systems to meet the demand of fresh water. Among the conventional distillation process, solar distillation process seems to be a suitable solution for resolving this existing demand of fresh water. This is quite true especially in areas where the water table is already contaminated or polluted such as in the artisanal mining areas of Northern Nigeria. The purpose of this work was to design and fabricate a solar water distillation system that can purify the water from various sources. Such sources include water from contaminated wells and boreholes, streams and rivers and even runoff water from plants and domestic buildings. Solar water distillation removes impurities such as salts and heavy metals such as lead, arsenic and mercury as well as eliminates microbiological organisms. A Solar Still has been designed and fabricated because of the portable water and energy challenges of the rural areas in the country. The incoming solar radiation from the sun heats the water, which placed in the basin in impure form, and this water gets evaporated and condensed into pure drinkable water. In this work, a basin types double slope active solar still was designed and fabricated, and a performance evaluation was carried out. To determine the efficiency of the still.

1.0 Introduction

The need for good drinking water is on increase over the years due to importance of good health. Rapid economic growth and climate change have resulted in increasing pressure on quality and quantity of water resources-especially in tropical and developing countries. There is often enough water available, but it is salty, brackish and need technique to make it safe to drink. Most people

in Nigeria have no access to good drinking water. This is particularly so for areas where artisanal mining is rampant.

During many of the processes used by artisanal miners, toxic materials are released into the environment, posing large health risk to the miners, their families and surrounding communities. For instance, gold mining operations are particularly dangerous, as they often use mercury amalgamation process to extract gold from ores. Furthermore, these materials find their way into the water table poisoning wells and other water sources. Remediation is very expensive for most State governments because of the cost involved.

Heavy metals are dangerous because they tend to bioaccumulate. Bioaccumulation means an increase in the concentration of a chemical in a biological organism over time, compared to the chemical's concentration in the environment. Heavy metal toxicity can result in damaged or reduced mental and central nervous function, lower energy levels, and damage to blood composition, lungs, kidneys, liver, and other vital organs. Long-term exposure may result in slowly progressing physical, muscular, and neurological degenerative processes that mimic Alzheimer's disease, Parkinson's disease, muscular dystrophy, and multiple sclerosis. Allergies are not uncommon and repeated long-term contact with some metals or their compounds may even cause cancer (International Occupational Safety and Health Information Centre, 1999). Lead and mercury exact their most devastating toll on the developing brain (http://www.purewaterservices.co.nz/contaminants/other-contaminants-issues/heavy-metals):

a. Children exposed to lead at a young age are more likely to suffer from shorter attention spans and are less able to read and learn than their peers.
b. Children with above-average mercury exposures have learning difficulties.
c. Recent studies also suggest that arsenic can harm the developing brain.
d. Many other health effects of these metals are well-known.

Emerging distillation technology using renewable energy is viewed as a feasible alternative to supply water as it can be cost effective but also has potential to transform the lives of people living in small communities in remote and rural areas.

Various researchers have been carried out research works on design, fabrication methods, and performance analysis of solar distillation. Kabeel and El-Agouz (2011) investigated an active system of conventional solar still integrated with a flat plate collector under thermo siphon mode and found that up to 33% increase in the distillate yield when the water is preheated in the collector. An air-blown, multiple effect solar still with heat energy recycle to increase in yield has been proposed by Mink et al. (1998). Kwatra (1996) simulated the relationship between the evaporation area and distillate yield and shows that an enlarged evaporation area increases the yield. Khalifa *et al*. (1999) studied the effect of feed water preheating on single and double slope solar stills and concluded that yield output and efficiency of the solar still has been increased by preheating. Sethi and Dwivedi (2013) developed the convective mass transfer relation for double condensing chamber solar still. In relation Nu = C(GrPr)n, the values of C and n were determined using regression analysis for different temperature ranges and found that the values of C and n proposed by Dunkle (1961) are valid only for lower temperature ranges, however for higher temperature

ranges the values of C and n change. Rubio et al. evaluated the distillate yield for a double-slope solar still under controlled conditions for basin water and collector temperatures within typical operating ranges and propose a new empirical model for estimating mass flow rates in single slope solar stills. Nafey *et al.* (2001) has studied the various parameters affecting solar still performance and developed an equation relating the dependent and independent variables to predict the single-slope solar still productivity.

Thermal models to establish the energy balance equations of active and passive solar still have been developed by Tripathi and Tiwari (2005) and validated the theoretical results with the experimental results. Abu-Hijleh *et al.* (2003) studied the effects of sponge cube and showed that the daily production of solar still can be greatly improved. Radhwan (2005) studied the performance of a stepped solar still with built-in latent heat storage and conclude that efficiency and fresh water production rate increased. El-Sebaii *et al*. (2009) studied an analytical solution of the energy-balance equations for the thermal performance of a triple-basin solar still and found that productivity of the bottom basin is higher than the productivity of the upper basins during the daytime. Sow et al. have carried out the exergy analysis for distiller driven by solar energy and reported that the exergetic efficiencies less than 4% for single effect system, 17-20% for double effect system and 19-26% for triple effect solar distiller system. Stephen *et al.* (2012) fabricated plastic solar still and studied the effect of water depth on mass and heat transfer and found that distillate output of 2.1 L/m^2/day, at water depth of0.02m in still basin, could be achieved. Lindblom (2010) have shown that the efficiency of single slope solar still using the black granite gravel reaches up to 52%maximum which is 8% higher than the conventional single slope solar still. Ahsan and Fukuhara (2009, 2010) proposed a new mass and heat transfer model of a tubular solar still incorporating various mass and heat transfer coefficient taking account of the humid air properties inside the still.

Stephen *et al.* (2012) study the effects of orientation and depth of water in the basin of the still on the productivity of a double slope solar still and compared the same with that of a single slope solar still. The authors have done work on new design of solar collector by replacing the conventional collectors with the GI plate sandwiched collectors and compared the steady state outlet temperature and efficiencies.

2.0 Importance of Solar Stills

It has been established through experimental and mathematical model results that the best performance of solar powered systems is achieved if the high intensity of insulation, minimum wind velocity and full insulation exist. Nigeria climatic conditions meet these criteria.

Growing demands of freshwater resources are creating an urgent need to develop self-sustained system to meet the demand of fresh water. Among the conventional distillation process, solar distillation process seems to be a suitable solution for resolving this existing demand of fresh water. Solar water distillation removes impurities such as salts and heavy metals as well as eliminates microbiological organisms. The water produced by the process can be considered pharmaceutical grade.

In order to tap this seemingly boundless resource (solar energy), the purification of water from polluted wells, crude oil polluted water sources, salty sea water, using solar still should be the most

promising process, as this process basically removed impurities such as dirt, microorganisms, crude oil and its related constituents, salt, etc., from these polluted sources to produce purified water. It is one of the most important methods of getting potable water. Besides of being inexhaustible, clean and universally available, the use of solar energy in renewable energy based-solar still, is moreover significantly more economical than the use of fossil fuels (Stephen *et al*., 2012). To rationalize the use of this energy source in water purification, an improved solar still that can produce purified water from various sources has been designed and evaluated. A double solar heat collection system is being proposed. We expect that our configuration will improve the overall efficiency of the still. In addition, all equipment on the fabricated rig will be solar powered making it possible to be installed in rural communities where electric power is unavailable.

In this work, a double slope active solar still under forced circulation mode was designed and fabricated, and distillate output and instantaneous thermal efficiency calculated at different water depths.

3.0 Design View/ (Isometric Sketch)

The isometric, Orthographic Projections and exploded view are shown in Figures 1a to 1f.

4.0 Design Assembly

The Complete Design Assembly is presented in Figure 2.

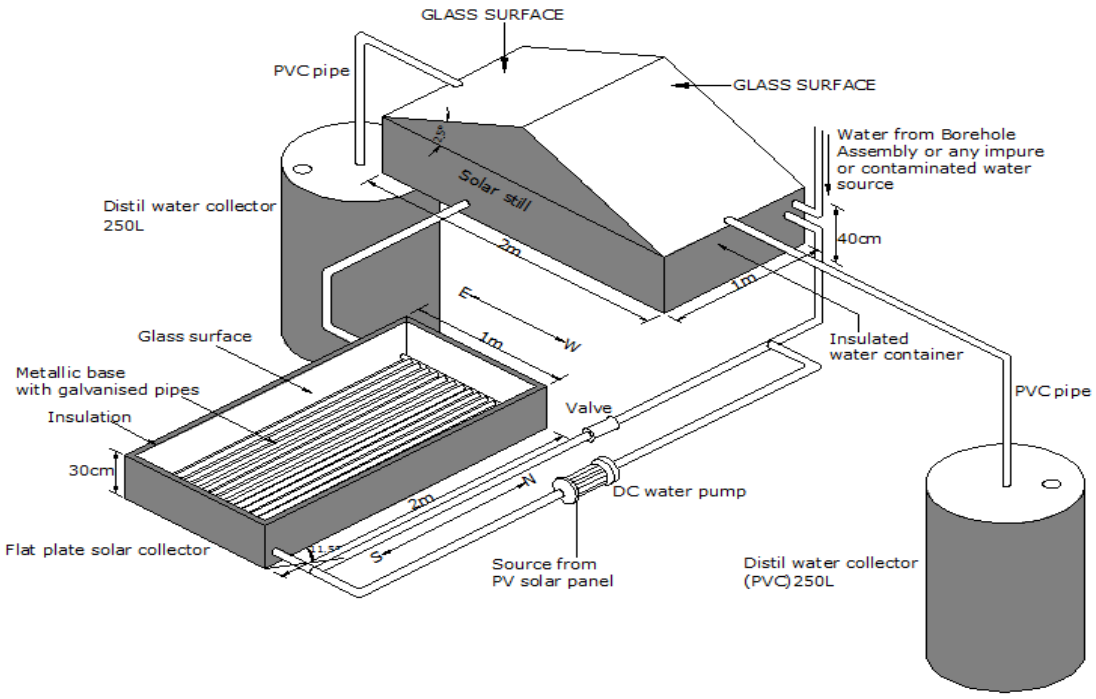

Figure 1a: Isometric Sketch of key components (solar Still and Flat Plat Solar Collector)

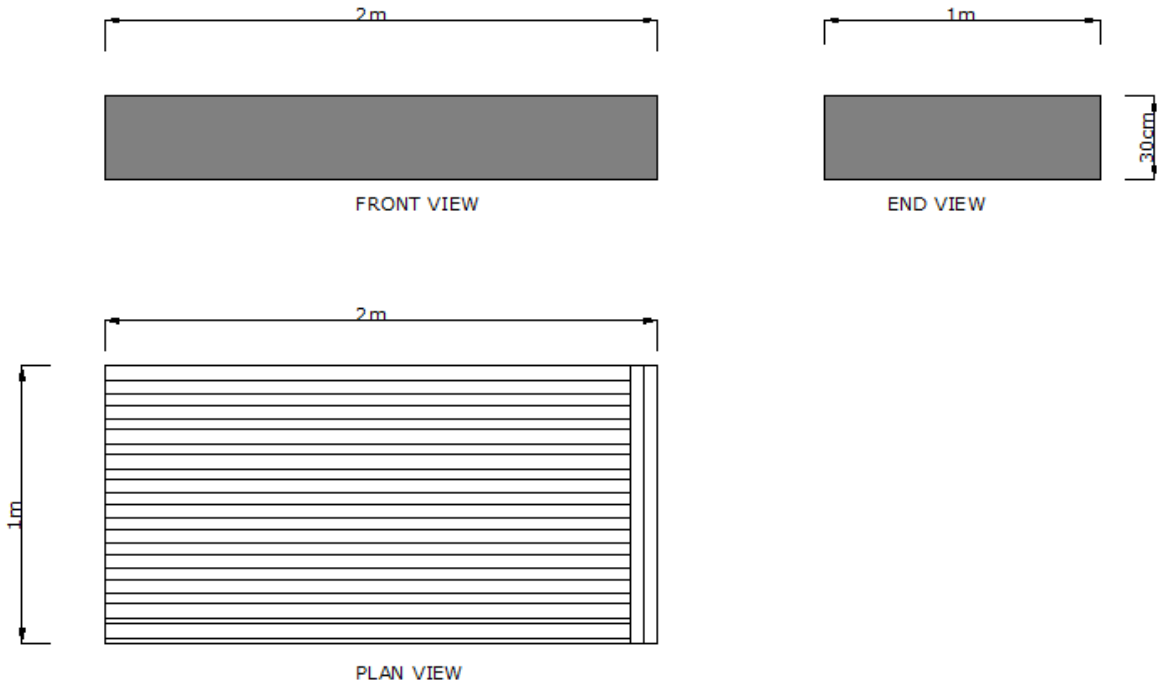

Figure 1b: Orthographic Projection of Solar Collector

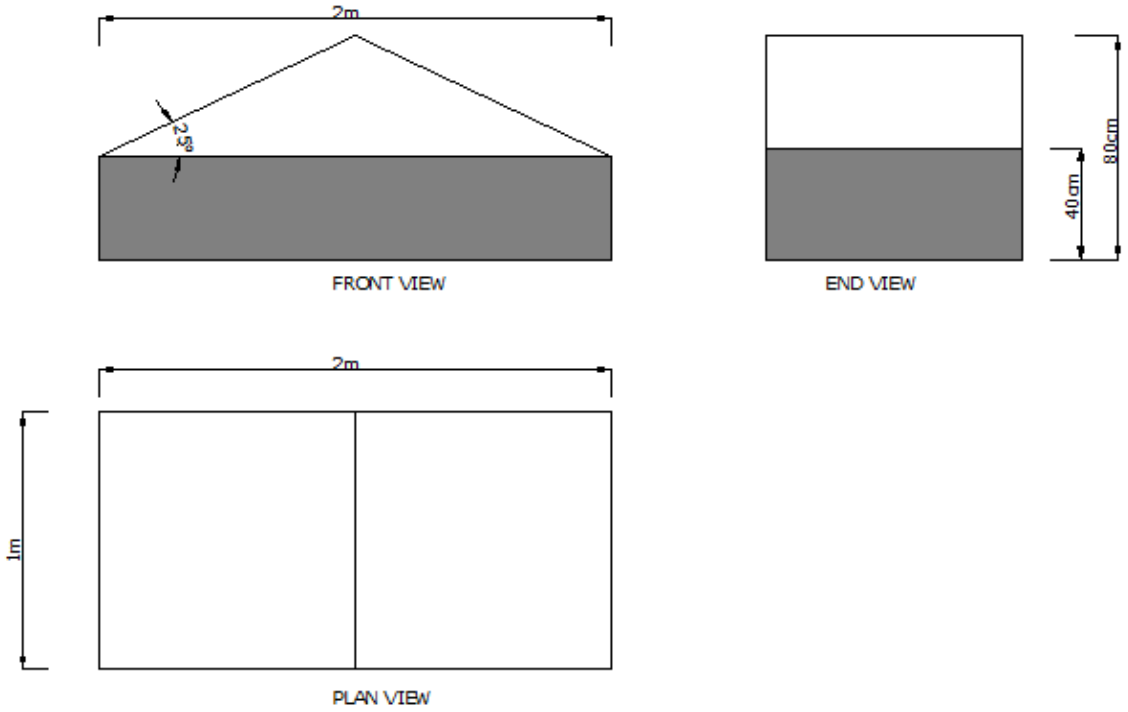

Figure 1c: Orthographic Projection of Solar Still

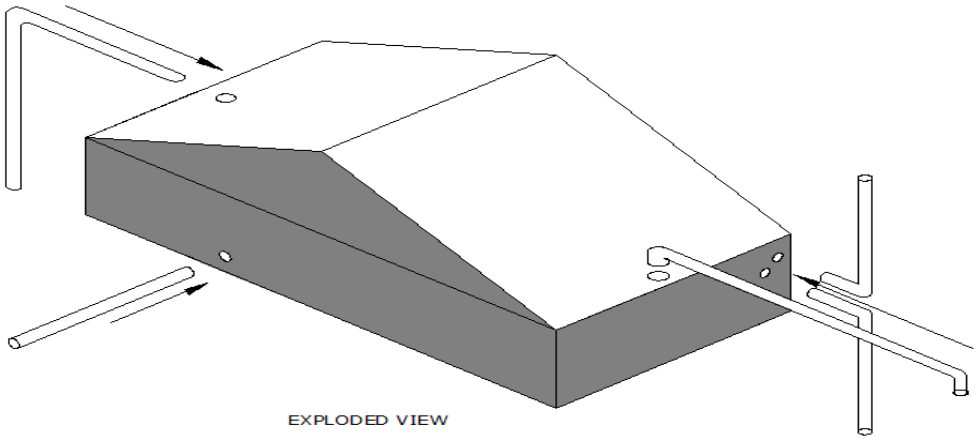

Figure 1e: Exploded Diagram for Solar Still

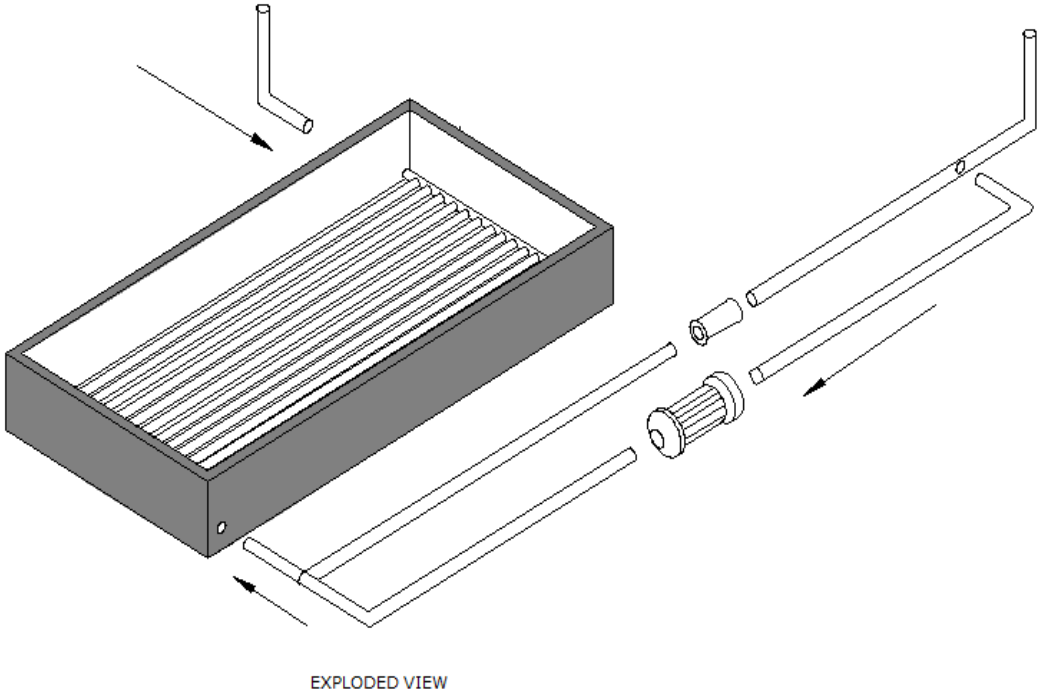

Figure 1f: Exploded Diagram for Solar Collector

5.0 Basic Operation of Solar Still

Water to be purified is poured into the still to reach a set level. The glass cover allows the solar radiation to passes through and it reaches the bottom of the still which is mostly absorbed by the base because the surface is coated with black colour material to increase the sun heat absorption. The water begins to heat up and the moisture content of the air trapped between the water surface

and the glass cover. Due to heating water gets evaporated from the basin and condenses on the inside of the cover of the glass. In this process, the impurities that present in the initial water are settled in the base itself and only Condensed water trickles in the inclined glass cover towards downward direction to collection trough and it is stored in the bottle. Every day the basin of the solar still must be cleaned to remove the settled salt contents and impurities. By removing these only, we can absorb more amount of heat energy without wastage.

6.0 Materials and Method of Fabrication

As shown in the schematic diagrams (Figure 1a to 1e), the distillation set-up consisted of four main parts:

i. A solar still without any moving parts. Solar still basin will be made up of a fiber reinforced plastic (FRP) to withstand the harsh conditions produced by water and sunlight. The advantages of FRP over other reinforcing materials such as glass fiber, carbon fiber etc are their specific strength properties, easy availability, light weight, high toughness, non-corrosive nature, low density, good thermal properties, renewability and biodegradability.
ii. A Flat-plate collector which is a metal box with a glass cover (called glazing) on top and a black-colored absorber plate on the bottom. The sides and bottom of the collector will be insulated to minimize heat loss.
iii. A DC water pump powered by solar energy from a solar panel and inverter system.
iv. The distillate water will collect in a plastic channel fixed at the lower end side of both the glass covers. The distillate collected is continuously drained through flexible pipe and stored in dedicated containers placed outside on both sides.

7.0 Measuring Instruments: Measurement of temperature:

Copper-constantan thermocouples were be used to measure water vapor and condensing cover temperature. Thermocouples used in the set-up were properly calibrated with the help of zeal thermometer (standard thermometer). The ambient air temperature will be recorded with the help of a calibrated mercury thermometer.

Measurement of solar radiation: The solar intensity was measured with the help of a calibrated solarimeter, having least count of 20 W/m^2.

Set-up: In active solar still, the flat plate collector is usually coupled with solar still in such a way that the hot water from collector plate enters into the basin of solar still under forced circulation mode. The inlet and outlet connections to the collector plate was taken from the bottom of the basin. A valve was provided in the inlet pipe to control the circulation of water through the collector plate. The collector plate absorbs the solar energy and transfers that energy to water flowing through tubes. The double slope solar still placed in east-west direction and collector plate was inclined at 11.5^o (Latitude for Kaduna) facing south to receive the maximum possible solar radiation.

8.0 Fabricated Equipment

Figures 2a to2d show the pictorial view of the fabricated equipment. Table 1 shows a summary of the materials used in the fabrication.

Table 1: Summary of the Materials Component of the Solar Still Considered

S/N	Component	Material(s)	Properties and Comments
1	Collector/Glazing (Trans- parent)	Plastic Glass	• Low water absorptance • High thermal conductivity • Transparent to short wave radiation (Transmittivity = 0.9) • Low iron content • Can withstand the effect of weather, wind,
2	Basin (Absorber)	Galvanized Iron	• High radiation absorptivity • Stable to corrosion • High thermal conductivity
3	Solar Reflector	Galvanized Iron	• Minimum corrosion problem • High thermal conductivity • High reflectivity • Cheaper and readily available
4	Cover (Casing)	Plywood/iron	• Has uniform strength • Has no cleavage • Very durable even though it is more expensive than hard wood • Stronger, Light weight and cheaper • Good insulator
5	Insulator	Fiber Glass	• Very cheap • Poor conductivity and radiation of heat • Very effective for insulation
6	Sealant	(i) Araldite (ii) Putty	• Can withstand high temperature • Good resistance to organic liquids • Joint bounded with it are difficult to break • Slow curing epoxy • Poor adhesive strength • Soften under high temperature • Cheap and readily available
7	Drain Pipe	PVC	• Stable to corrosion • Not poisonous to water • Cheap and readily available
8	Support Structure	Iron stand	• High tensile strength • Cheap and easily constructed
9	Collection trough	Rubber troughs	• Stable to corrosion • Not poisonous to water

Nigerian Journal of Renewable Energy Research
Volume 1, Number 1, pp 80-83, 2023

Figure 2a: Pictorial view of Solar Collector before cover is placed on it

Figure 2b: Pictorial view of Solar Collector after Cover is placed on it

Figure 2c: Pictorial view of Solar Still built to Specification

Figure 2d: Pictorial view of Solar Collector and Solar Still connected together

9.0 Instrumentation

Pictorial views of the instruments and equipment used for various measurements are presented below.

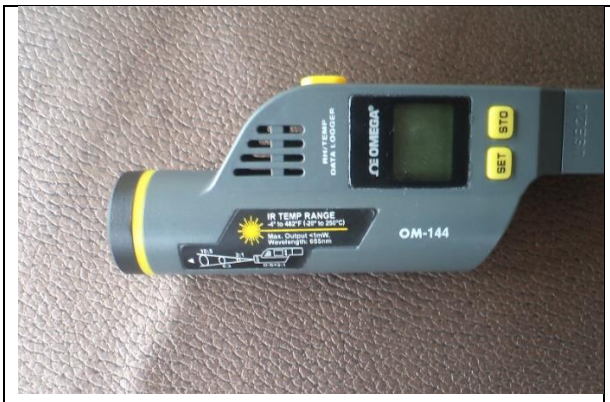

Hygrometer/Ambient Temperature Analyser

Analog and Digital thermocouple readers

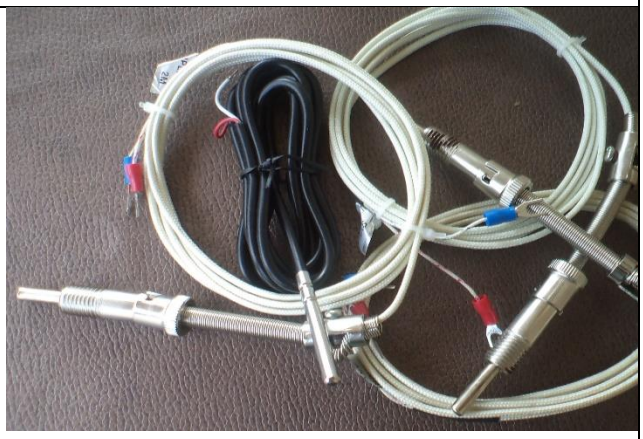

Inverter	**Thermocouple coils**
	
Water flow Sensors	**Solarimeter**

9.0 Testing the Fabricated Setup

The following parameters have been be measured every half an hour for a period of 9 hours during each runs conducted. These details are very important parameters necessary for scale up:

i. Ambient Temperatures,
ii. Water temperature from the solar collector
iii. Solar Intensity
iv. Amount of distillate for various times of the day

The data generated during the testing of the fabricated rig is presented on Tables 1 to 3 and Figures 3 to 5.

Table1: Amount of pure distilled Water collected during Interval (litres)

Time	Day1	Day2	Day3	Day4	Day5	Day6	Day7	Average
9.00-9.30	0.12	0.09	0.11	0.15	0.12	0.08	0.11	
9.30-10.00	0.22	0.18	0.16	0.21	0.21	0.22	0.19	
10.00-10.30	0.29	0.27	0.26	0.23	0.28	0.28	0.26	
10.30-11.00	0.39	0.40	0.39	0.41	0.47	0.46	0.32	
11.00-11.30	0.40	0.45	0.48	0.49	0.55	0.47	0.37	
11.30-12.00	0.46	0.55	0.55	0.64	0.67	0.58	0.56	
12.00-12.30	0.79	0.82	0.80	0.87	0.86	0.91	0.75	
12.30-1.00	0.88	0.91	0.87	0.99	0.96	0.96	0.94	
1.00-1.30	0.98	1.02	1.07	1.14	1.17	1.11	0.94	
1.30-2.00	1.21	1.22	1.18	1.25	1.32	1.31	1.15	
2.00-2.30	1.09	1.19	1.19	1.29	1.25	1.25	1.12	
2.30-3.00	0.99	1.02	1.02	0.92	1.17	1.07	0.94	
3.00-3.30	0.71	0.81	0.81	0.81	0.98	0.90	0.79	
3.30-4.00	0.50	0.60	0.59	0.61	0.73	0.57	0.55	
4.00-4.30	0.34	0.31	0.30	0.32	0.43	0.33	0.27	
4.30-5.00	0.22	0.24	0.24	0.24	0.22	0.29	0.20	
Average Ambient	33.5	30.2	32.3	30.6	29.5	30.2	31.3	**31.1**

Temperature (°C)								

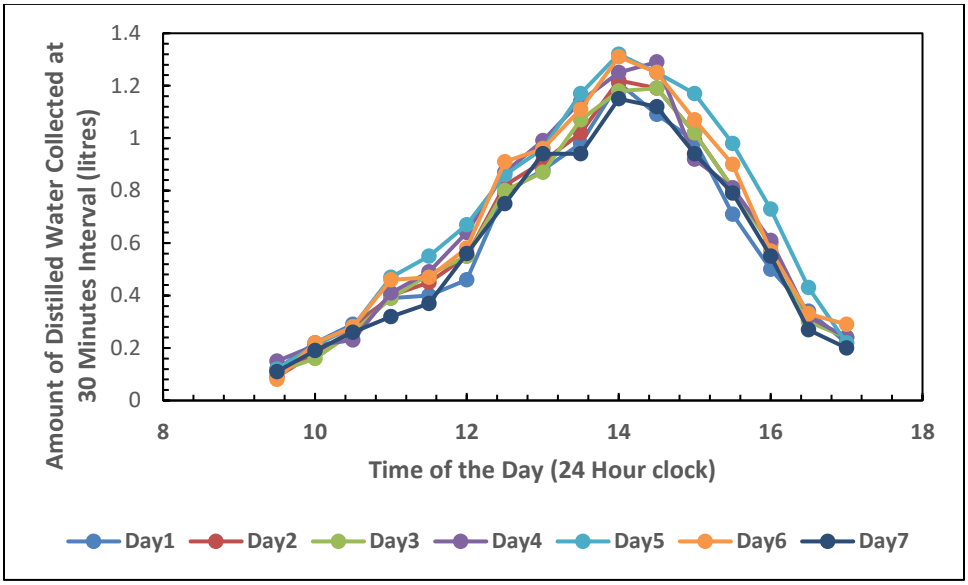

Figure 3: Amount of pure distilled Water collected during Interval (litres) for various times of the day for selected days in October, 2020

Table 2: Water temperature into still from solar collector (°C) for selected days in October, 2020

Time	Day 1	Day 2	Day 3	Day 4	Day 5	Day 6	Day 7	
9.30	32.2	31.09	32.45	35.20	31.91	31.44	32.05	
10.00	37.0	36.79	37.23	42.24	38.11	36.09	38.33	
10.30	40.0	39.62	41.68	44.15	41.05	38.92	41.98	
11.00	51.0	50.88	50.97	57.54	50.77	51.18	51.17	
11.30	57.0	56.75	57.98	64.12	56.78	57.25	58.08	
12.00	60.0	58.68	61.03	67.88	59.55	58.18	62.36	
12.30	68.4	65.90	69.57	74.93	68.33	64.88	68.78	
13.00	70.3	68.75	71.50	77.35	70.88	67.15	73.48	
13.30	78.0	78.28	79.34	86.48	77.98	79.08	79.94	
14.00	73.9	73.27	75.17	83.93	73.50	72.97	78.27	
14.30	65.0	63.57	66.11	74.06	64.55	64.27	62.68	
15.00	62.0	61.64	63.06	66.75	63.34	62.64	64.54	
15.30	58.0	57.72	58.99	65.42	5755	57.02	58.99	
16.00	47.0	45.57	47.80	53.56	47.67	44.47	47.80	
16.30	40.5	40.2	41.19	45.90	40.99	41.22	40.19	
17.00	38.0	37.36	38.65	41.24	37.94	36.16	37.05	

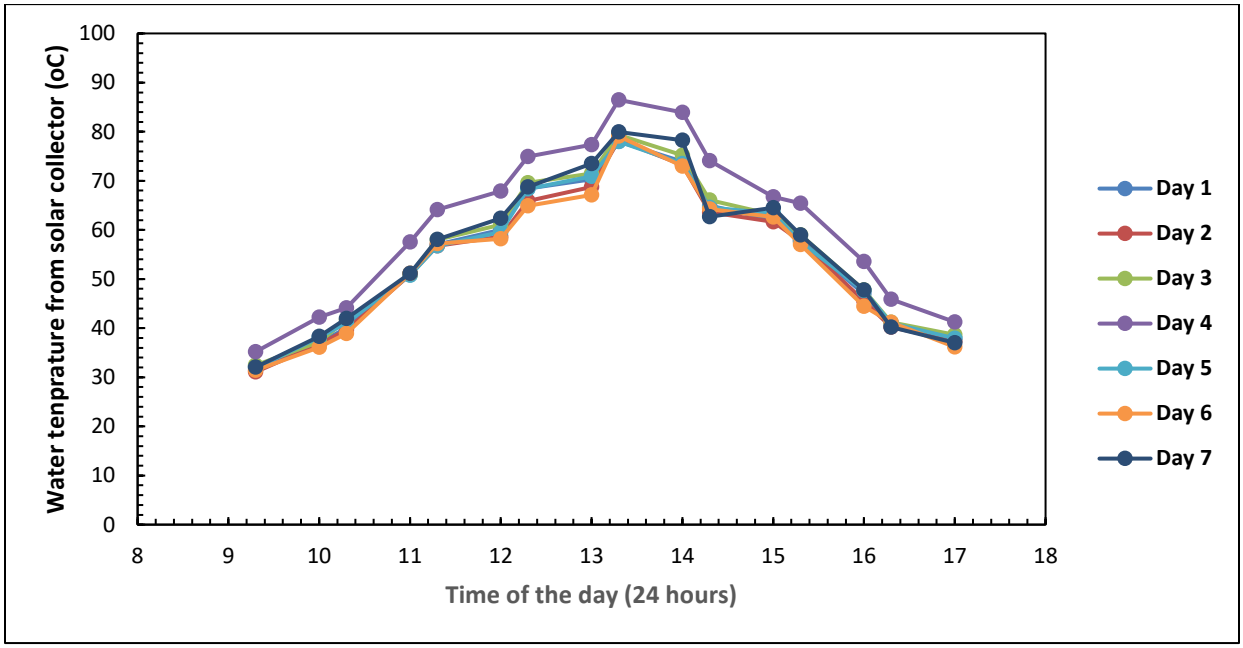

Figure 4: Water temperature into still from solar collector (°C) for various times of the day for selected days in October, 2020

Table 3: Solar Hourly Global Radiation Values (W/m^2)- for selected days in October, 2020

Time	Day1	Day2	Day3	Day4	Day5	Day6	Day7	
8.0	320.67	317.50	319.00	335.95	313.29	310.09	305.11	
8.5	360.72	354.03	357.42	374.29	352.42	348.82	350.34	
9.0	410.98	402.64	409.28	430.74	401.53	397.42	388.59	
9.5	474.76	465.59	473.76	497.45	463.84	459.09	453.07	
10	533.78	515.84	533.18	557.84	521.50	516.17	521.65	
10.5	576.87	550.37	575.87	607.66	563.60	557.83	561.02	
11	615.87	613.86	616.47	646.29	601.70	595.55	600.36	
11.5	705.86	691.68	703.86	741.05	689.63	682.57	680.04	
12	786.98	769.75	779.14	820.10	768.88	761.01	758.99	
12.5	768.98	753.98	765.24	810.50	751.29	743.60	749.52	
13	750.87	750.11	748.93	780.38	733.60	726.09	730.71	
13.5	730.98	717.48	732.17	764.78	714.17	706.86	705.47	
14	721.98	714.59	721.98	760.08	705.37	698.15	680.60	
14.5	660.97	652.38	655.22	690.98	645.77	639.16	631.91	
15	588.87	586.21	575.92	609.72	575.33	569.44	558.07	
15.5	470.48	464.36	469.54	492.02	459.66	454.95	454.98	
16	387.87	397.83	388.22	406.63	378.95	375.07	370.19	
16.5	320.65	320.48	322.29	340.40	313.28	310.07	312.30	
17	236.87	234.79	235.90	246.70	231.42	229.05	232.59	

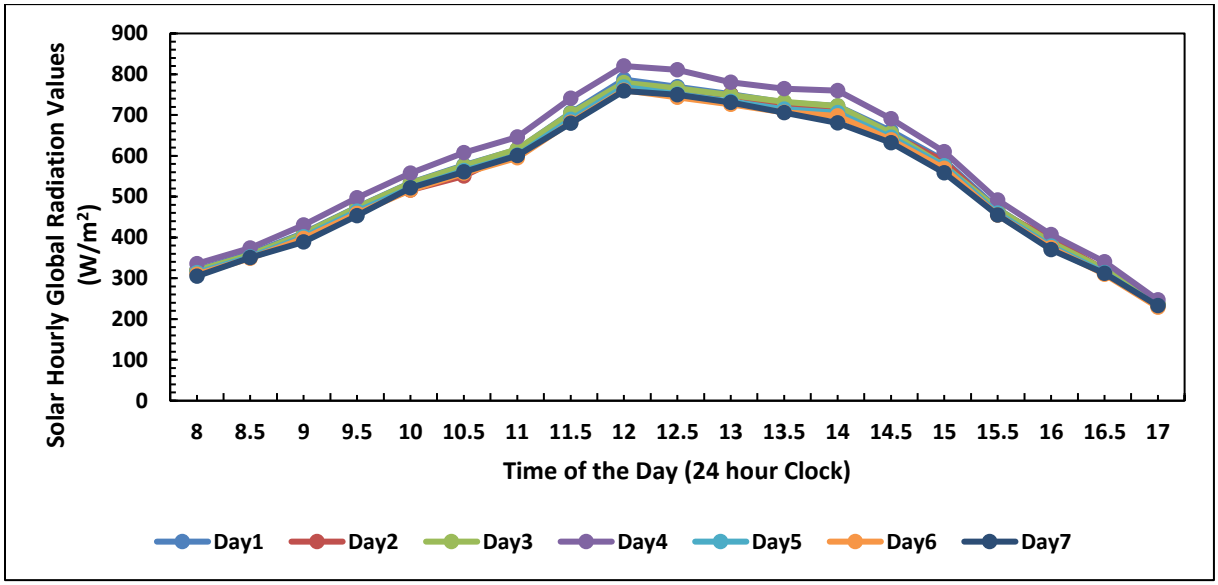

Figure 5: Solar Hourly Global Radiation Values (W/m^2) for various times of the day for selected days in October, 2020

10.0 Analysis of Data generated by the fabricated rig.

Table 1 and Figure 3 show the variation of distillate versus time for the period of seven days. Table 1 also shows the average daily ambient temperatures. Table 2 and Figure 4 show the water temperature into still from solar collector (^{o}C) while Table 3 and Figure 5 show the solar hourly global radiation values (W/m^2) for various times of the day. The Average solar intensity for the various days considered were measured using the solarimeter while the temperatures were generated using type K thermocouples.

For all the seven days considered during the testing of the rig, the ambient temperature averages 31.1 °C throughout the day for the seven days considered. From the daily measurement obtained (Figure 5), it was observed that minimum solar radiation occurs between the hours of 8:00 am and 9:00 am during which the amount of distillate obtained was also the lowest. Moreover, it was observed that even though the solar radiation was highest between the hours of 12:00 noon and 1:00 pm, and the maximum distillate yield was obtained be- tween the hours of 1:00 pm and 2:00 pm for the seven days considered.

11.0 Conclusion

Freshwater scarcity is a big issue in various communities in Nigeria especially isolated communities in rural areas. This fact and the abundance of untreated well water and water from streams and rivers in most region in the country is the main motivation to undertake this evaluation. The results generated by this fabrication justify that Single-effect solar stills are a practical solution to the purification of water in rural areas in the country.

This paper has shown that distillation of water using solar still basin is an economical method to get portable drinking water in rural areas. Salt, heavy metals, bacteria and other impurities and contaminates which are to be removed completely in this distillation process. The solar still

fabricated has been proven to be one of best technology for water purification because they do not need electricity which is unavailable in most rural areas in Nigeria.

The implications of the results from the design are for the development of a robust and dynamic single slope solar still system. With this type of design, it is easy to change the inclination angle. This has the potential and capacity to produce distilled water for domestic, industrial and commercial purposes irrespective of the geographical location. The fabricators recommend the mass fabrication of this rig for deployment in rural areas where portable drinking water is unavailable.

Acknowledgement
The author wishes to acknowledge the funds provided for this research by the Tertiary Education Trust Fund (TETFund), Nigeria, under the Institution-Based Fund (IBR) Grants. *REF: TETF/DR&D/POLY/KAD/IBR/VOLII.*

References

Abdulhaiy M. Radhwan (2004) Transient performance of a stepped solar still with built-in latent heat thermal energy storage**;** *Desalination* 171, pp 61–76

Ahsan, A. and T. Fukuhara (2009) Condensation mass transfer in unsaturated humid air inside tubular solar still. Ann. *J. Hyd. Eng*., 53: pp 97-102.

Ahsan, A. and T. Fukuhara (2010) Mass and heat transfer model of tubular solar still. *Solar Energy*, 84: 1147-1156.

Abu- Hijleh, B.A.K. and Rababa'h, H.M. (2003) Experimental Study of Solar Still with Sponge Cubes in Basin, *J. Energy Conversion and Management*, 44, pp 1411-1418.

Dinesh Kumar, Patel Himanshu and Zameer Ahmad (2013) Performance Analysis of Single Slope Solar Still; *International Journal of Emerging Technology and Advanced Engineering*, 3 (3)

Dunkle, R.V. (1961) Solar Water Distillation: The Roof Type Still and Multiple Effect Diffusion Still, International Developments in Heat Transfer, ASME (1961), *Proc. of Intl. Heat Trans. Conf., University of Colorado*, pp. 895-902.

El-Sebaii, A.A., A.A. Al-Ghamdi, F.S. Al-Hazmi, S. Faidah Adel (2009) Thermal performance of a single basin solar still with PCM as a storage medium; *Applied Energy*, 86, pp. 1187-1195

International Occupational Safety and Health Information Centre. Metals. *In Basics of Chemical Safety*, Chapter 7. Geneva: International Labour Organization.

Kabeel A E, S.A. El-Agouz (2011) Review of researches and developments on solar stills. *Desalination*, 276: pp 1–12.

Khalifa A. J.N, N, Al-Jubouri AS, Abed M.K. (1999) An experimental study on modified simple solar stills. *Energy Conversion and Management*; 40(18), pp 35–47.

Kwatra, H.S. (1996). Performance of a solar still: Predicted effect of enhanced evaporation area in yield and evaporation temperature, *Solar Energy* 56(3), pp 261-266.

Mink G., Aboabboude M.M. and Karmazsin E. (1998), *Solar Energy*, Volume 62, Issue 4, April 1998, pp 309-317

Nafey, A.S. M. Abdelkader, A. Abdelmotalip, A.A. Mabrouk (2001) Solar still productivity enhancement; *Energy Conversion and Management*, 42, pp 1401-1408

Patil B.L., Dr. J.A. Hole, Sagar Wankhede (2017) Parameters Affecting Productivity of Solar Still and Improvement Techniques: A Detailed Review; *International Journal of Engineering Technology, Management and Applied Sciences*, 5 (2)

Sethi, A.K. and V.K. Dwivedi (2013) Design, Fabrication, and Performance Evaluation of Double Slope Active Solar Still under Forced Circulation Mode; *Int. J. of Thermal & Environmental Engineering*; Volume 6, No. 1 pp 27-34

Somanchi, N.S.,.Sri Lalitha Swathi Sagi, Thotakura Ashish Kumar, .Sai Phanindra Dinesh Kakarlamudi and Ajay Parik, Modelling and Analysis of Single Slope Solar Still at Different Water Depth; *Aquatic Procedia*, Volume 4, 2015, Pages 1477-1482

Stephen, G., et al. (2012) *Low-Cost Solar Desalination Device*. Thesis Summary, Boston: North-eastern University

Tripathi, R., and Tiwari, G. N. (2005), Effect of Water Depth on Internal Heat and Mass Transfer for Active Solar Distillation; *Desalination,* 173, pp. 73–88

Nigerian Journal of Renewable Energy Research
Volume 1, Number 1, pp 100-106, 2023
 ISSN _____

Instructions for Authors

The Nigerian Journal of Renewable Energy Research (NJRER) is an open-access publication that facilitates prompt dissemination of papers across the full spectrum of renewable energy. Manuscripts that align with the rigorous scientific standards and are of notable significance are welcomed. On average, papers are published approximately 6 months post their approval.

PRE-SUBMISSION CHECKLIST

Before submitting, please use this list to ensure your paper meets all the necessary criteria. For comprehensive details, refer to the relevant sections in this Author's Guide. Ensure you have:

- Nominated one author as the main point of contact, including:
- Email address
- Complete postal details
- Uploaded all essential files:
  - The paper itself, with keywords included.
  - Arrange your paper with a single column layout per page.
  - All figures (with corresponding captions).
  - Tables (with titles, descriptions, footnotes).
  - Check that references to figures and tables within the text correspond with provided files.
  - Clearly highlight if any illustrations need to be colour printed.
  - Graphical abstracts or highlights (if relevant).
  - Any supplementary files.
- Additional Checks:
  - Run a spell-check and grammar-check.
  - Ensure all references in your list are also mentioned in your text and the other way around.
  - Acquire permissions for copyrighted content, even from online sources.
  - Include a statement about competing interests (even if none exist).
  - Familiarise yourself with the journal's policies mentioned in this guide.
  - Provide referee recommendations and their contact details, as per the journal's prerequisites.

Digital submission of papers is preferable. Make sure the content, tables, and illustrations are in a single Microsoft Word document (Arial font is preferred).

Send your papers as an email attachment to the Editorial Office at: editor_njrer@tetfundkadpolycoex.org.ng. Within a week, the primary author will receive a manuscript number.

The introductory letter should detail the main author's full contact information. This should accompany the file (named after the first author's surname) sent as an email attachment to the Editor. Authors can also propose two to four potential reviewers for their manuscript, although NJRER might nominate others.

Submissions to *The Nigerian Journal of Renewable Energy Research* are accepted solely as email attachments.

TYPES OF MANUSCRIPTS

The *Nigerian Journal of Renewable Energy Research (JRER)* considers:

1. **Original Articles**: Describing novel, thoroughly verified findings. These should be as succinct as necessary for clarity.
2. **Short Communications**: Suitable for concise research results, new theories, novel methods or equipment. They don't need to follow the layout of full-length papers and range from 6 to 12 manuscript pages.
3. **Reviews**: Synopses covering contemporary topics are appreciated. Reviews should not exceed 12 to 18 manuscript pages and undergo a peer-review process.

Procedure: Submit original articles via editor_njrer@tetfundkadpolycoex.org.ng. For review articles, send an outline and your CV to the Editor in Chief for consideration.

Paper Length: Typically, original articles range between 4,000 to 6,000 words (excluding captions and references), while review articles can be up to 10,000 words. Please mention the word count during submission.

Review Process: Every manuscript undergoes a review by the editor, Editorial Board members, or expert external reviewers. Our aim is to revert with feedback within 3 weeks. The editorial team will reassess manuscripts that are approved but need revisions. JRER's objective is to publish manuscripts within 8 weeks of submission.

MANUSCRIPT STRUCTURE FOR REGULAR ARTICLES

Manuscripts should be typed with double-spacing and pages numbered beginning from the title page.

- **Title**: A concise description of the paper's content.
- **Title Page**: Should contain full names and affiliations of all authors, and the contact details of the corresponding author.
- **Abstract**: A self-explanatory summary between 100 to 200 words, highlighting the scope, significant data, and major conclusions.
- **Keywords**: Provide 3 to 10 keywords for indexing purposes.
- **Abbreviations**: List uncommon abbreviations. General abbreviations like ATP or DNA don't need to be expanded.
- **Introduction**: A clear outline of the problem, related literature, and the proposed approach.
- **Materials and Methods**: Detailed enough for reproducibility, with references to established methods.
- **Results**: Presented clearly and in past tense.
- **Discussion**: Interpretation of the findings in light of existing knowledge.
- **Acknowledgments**: Keep it brief.

Tables and figures should be concise, understandable without referencing the main text, and be on separate pages. Graphics should be high-resolution and created using appropriate software before embedding in the Word document.

REFERENCES

Adhere to the 7th Edition - APA Style (American Psychological Association) for referencing. Ensure the proper format, which includes author name(s), publication year, article title, journal title (italicised), volume (italicised), issue number, page range, and DOI or URL. The first line of each reference should align left, with subsequent lines indented.

Example:

Ruxton, C. (2016). Tea: Hydration and other health benefits. *Primary Health Care*, *26*(8), 34-42. https://doi.org/10.7748/phc.2016.e1162

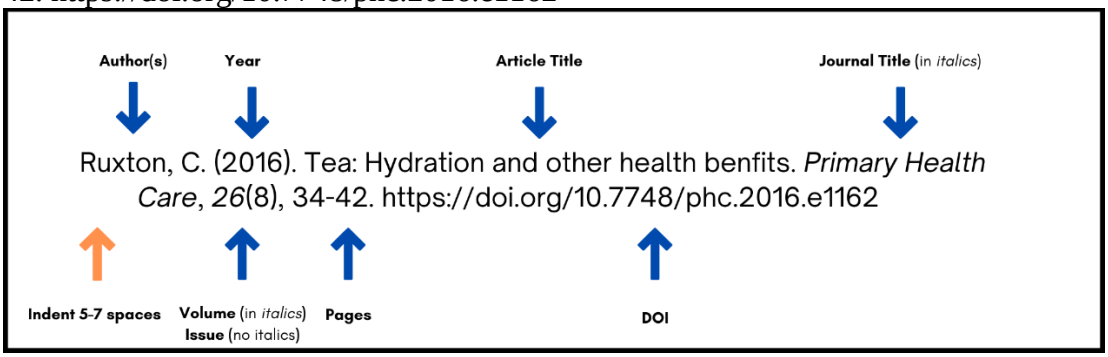

Material Type	In-Text Example	Reference List Example
Journal Article: Single author	"Black tea is the second most consumed beverage in the world after water" (Ruxton, 2016, p. 34). **OR** Ruxton (2016) suggests "Unsweetened tea can be part of a recommended diet" (p. 40). **Include page numbers for direct quotes.**	Ruxton, C. (2016). Tea: Hydration and other health benefits. *Primary Health Care*, *26*(8), 34-42. https://doi.org/10.7748/phc.2016.e1162 **Where a DOI is available it must be included at the end of the reference, in the format https://doi.org/10.xxxx**
Journal Article: 2 authors	... connection and optimism (Aspy & Proeve, 2017), but others contend ... **OR** Aspy and Proeve (2017) have found ...	Aspy, D. J., & Proeve, M. (2017). Mindfulness and loving-kindness meditation: Effects on connectedness to humanity and to the natural world. *Psychological Reports*, *120*(1), 102-117. https://doi.org/10.1177/0033294116685867

	Cite both authors each time the reference occurs.	
Journal Article: 3 to 20 authors	(Wilmott et al., 2018) OR Wilmott et al. (2018) noted that… **Cite only the surname of the first author followed by et al. and the year.**	Wilmott, C., Fraser, E., & Lammes, S. (2018). 'I am he. I am he. Siri rules: work and play with the Apple Watch', *European Journal of Cultural Studies, 21*(1), 78-95836-839. **Provide the names of all authors in the reference list.**
Journal Article: 21 or more authors	Research indicated that "lost sense of smell is a factor" (Khan et al., 2017, p. 344). **OR** Khan et al. (2019) used criteria which included "reduced or lost sense of smell" (p. 344). **Cite only the surname of the first author followed by et al. and the year. Include page numbers for direct quotes.**	Khan, A., Huynh, T. M. T., Vandeplas, G., Joish, V. N., Mannent, L. P., Tomassen P., van Zele, T., Cardell, L.O., Arebro, J., Olze, H., Forster-Ruhrmann, U., Kowalski, M. L., Olszewska-Ziaber, A., Fokkens, W., van Drunen, C., Mullol, J., Alobid, I., Hellings, P.W., Hox, V., …Bachert, C. (2019). The GALEN rhinosinusitis cohort: Chronic rhinosinusitis with nasal polyps affects health-related quality of life. *Rhinology, 57*(5), 343-351. https://doi.org/10.4193/Rhin19.158 **Provide the names of the first 19 authors, insert an ellipsis […] (but no ampersand [&]), then add the final author's name.**
Journal Article from most Library databases: No DOI	Nairne and Wilkinson (2018) assert that "our relationship with ourselves is essential to how we each show up professionally" (p. 106). **OR** "Our relationship with ourselves is	Nairne, D. C., & Wilkinson, H. (2018). What's love got to do with it? *Vermont Connection*, *39*(1), 106-112. **An article retrieved from most Library databases that does not have a DOI can be presented as though it were a print article.**

	essential to how we each show up professionally" (Nairne & Wilkinson, 2018, p. 106).	
Journal Article from the Cochrane Database of Systematic Reviews	The review included 78 trials employing a variety of intervention approaches (Hodder et al., 2019). **OR** Hodder et al. (2019) identified 78 relevant trials that employed a variety of intervention approaches.	Hodder, R. K., O'Brien, K. M., Stacey, F. G., Tzelepis, F., Wyse, R. J., Bartlem, K. M., Sutherland, R., James, E. L., Barnes, C., & Wolfenden, L. (2019). Interventions for increasing fruit and vegetable consumption in children aged five years and under. *Cochrane Database of Systematic Reviews*. https://doi.org/10.1002/14651858.CD008552.pub6 **Articles in the Cochrane Database of Systematic Reviews can only be retrieved from this database, therefore the name of the database (in italics) is included as the source of the article.**
Online Journal Article: No DOI (With an Article Number)	Marion et al. (2018) explore whether evil characters in film share ... **OR** ... including stereotypical depictions of evil characters in film (Marion et al., 2018).	Marion, T., Reese, V., & Wagner, R. F. (2018). Dermatologic features in good film characters who turn evil: The transformation. *Dermatology Online Journal*, *24*(9), Article 4. https://escholarship.org/uc/item/1666h4z5 **For an online journal article with no DOI (other than those retrieved from a Library database), provide the direct URL for the article.** **For journal issues with article numbers (rather than consecutive pagination) replace with page numbers with the word 'Article' followed by the article number or eLocator.**
Print Journal Article: No DOI assigned	… Aussie Rules is the people's game (Duncan, 2016)… **OR** Duncan (2016) states that a sense of belonging…	Duncan, S. (2016). Voices from the grandstands: The attitudes of Australian football fans towards the concept of creating, developing and binding communities. *Sporting Traditions*, *33*(2), 19-40. **Note: Where a print journal article has a DOI you must include it, even though you did not access the electronic version.**
Online Journal Article: No page numbers	... in all outcomes (Christensen et al., 2019). **OR**	stensen, G., Dafoe, A., Miguel, E., Moore, D. A., & Rose, A. K. (2019). A study of the impact of data sharing on article citations using journal policies as a natural experiment. *PLoS ONE*, *14*(2), Article e0225883. https://doi.org/10.1371/journal.pone.0225883

	Christensen et al. (2019) examine ... **For direct quotes of online material without pagination, name the sections and paragraph number:** The authors' "objective was to identify control journals that did not require data posting" (Christensen et al., 2019, Broad Analysis section, para. 4).	
Secondary Sources: When you are referring to the ideas or words of an author who has been cited in another work. Also called 'secondary citation'. ***Only recommended where the original work cannot be obtained.***	Constituting a "global movement toward a more naturalistic approach for childbirth" (Goldbas, 2012, as cited in Sullivan & McGuiness, 2015, p. 20). **OR** Goldbas's overview (2012, as cited in Sullivan & McGuiness, 2015) indicates… **Provide names of both authors. Where the year is known for the original work, include it as well as the year of the publication you read.**	Sullivan, D. H., & McGuiness, C. (2015). Natural labor pain management. *International Journal of Childbirth Education*, *30*(2), 20-25. https://scholarworks.waldenu.edu/sn_pubs/51/ **Provide the full reference for the journal article that you actually read.**

Proofs and Copies:
Digital proofs will be forwarded to the main author as a PDF attachment via email. These page proofs are deemed the conclusive rendition of the manuscript. Save for typographical or small administrative oversights, no alterations will be made to the manuscript during this phase. Given that NJRER will be freely accessible online to engage a broad readership, authors will enjoy complimentary electronic access to their article's full content (in PDF format). Authors can effortlessly download the PDF, enabling them to produce countless prints of their papers.

Copyright:
Submitting a manuscript insinuates: that the detailed work has not been previously published (barring being in abstract form or part of a published talk or dissertation); it's not being reviewed for publication elsewhere; and, should the manuscript gain acceptance for publication, authors concur to the immediate transfer of copyright to the publishing entity.

Fees and Costs:
Authors are obliged to cover a handling fee of either $100 or N30,000.00. However, publishing an article in the **Nigerian Journal of Renewable Energy Research** is not dependent on the author's capacity to settle these fees. Similarly, a commitment to handle the fee doesn't assure the manuscript's acceptance for publication. Under certain conditions, authors might petition the editorial team to consider a reduction or exemption of some handling charges in advance.